THE EFFECT OF SURFACE ROUGHNESS ON SKIN FRICTION AND TURBULENCE IN TWO DIMENSIONAL FLOW

Thesis by

Ralph D. Baker

In Partial Fulfillment of the Requirements for the Degree of

Doctor of Philosophy

California Institute of Technology

Pasadena, California

1938

CONTENTS

PART I

PART II

List of Figures

List of Figures (continued)

List of Figures (continued)

List of Tables

THE EFFECT OF SURFACE ROUGHNESS ON SKIN FRICTION AND TURBULENCE IN TWO DIMENSIONAL FLOW

Summary

This investigation is divided into two parts. Part I deals with the effect of roughness and pressure drop and skin friction, and Part II covers the effect of surface roughness and the turbulent velocity fluctuations, and the correlation between these fluctuations in the direction of the mean flow and those normal to the channel walls.

The roughness for both investigations was the same, and consisted of corrugated paper glued to the inside walls of a channel of 4.9 cm. wide by 85 cm. (inside dimensions). The roughness was changed by removing every other one of the corrugations, as illustrated in Fig. 6.

Pressure and velocity distribution measurements were made at various stations and the results compared to Karman's equation, $\frac{u}{v_*} = A_r + B \log y/k$ for rough walls, where u is the velocity in the channel, v_* is the friction velocity $= \sqrt{\tau_0/\rho}$, y = distance from wall, ν = the kinematic viscosity, k = the roughness height.

Karman's analysis showed B to be a universal constant independent of the wall roughness. Some investigators have given slightly different values to this constant. Their results were carried out in pipes or channels of near square cross section. These results appear to fall within 3% of those of Nikuradse as far as the value of B is concerned. However, a value of B a little less than 5.75 would fit the points better.

These experiments were undertaken to add some information to this subject with flow in deep narrow channels and with other types of rough surfaces which had not been investigated.

The turbulence measurements were determined with a hot-wire anemometer using a vibrating wire to calibrate it with. These results show that the correlation coefficient $\frac{u'v'}{(u')^2}$ increases with speed for smooth walls and varies materially with the type of roughness with no definite systematic trend as to this change.

THE EFFECT OF SURFACE ROUGHNESS ON SKIN FRICTION AND TURBULENCE IN TWO DIMENSIONAL FLOW

By Ralph D. Baker

PART I

Skin Friction and Pressure Drop

Introduction

In showing the results of this investigation the author wishes to present them in two parts. First, that portion relating to pressure drop and skin friction, and second, the material which deals with velocity fluctuations in turbulent flow.

Fluid resistance has been a problem for discussion and research since the first days when the "craftsmanship of the artisan builder began to crystallize into the art and science of engineering." Early scientists developed the mathematical relationships governing the laws of frictional resistance for what is now termed "laminar" flow. This type of flow, which occurs at very low velocities, is characterized by the steady, even flow of the fluid particles in congruent rectilinear paths, without perceptible molecular interchange. Only a small portion of the problems of fluid flow are in this class.

Increasing the velocity changes the character of the flow into a definite "turbulent" state, in which a thorough mixing of the particles occurs. Any colored fluid introduced into a flow of this type is quickly diffused throughout the whole fluid. The individual particles appear to have a very irregular and inordinate motion as they

are tossed about in the fluid. This type of flow constitutes, by far, the major fluid problems in Hydraulics and Aeronautics.

Not until Ludwig Prandtl's idea of the "boundary layer" was much progress made in formulating the laws governing turbulent motion. Later notable contributions have been made by Theodore von Karman, a student of Prandtl's, with his "similarity law," and statistical theory of turbulence (1)* and by G. I. Taylor (2) with his statistical theory of Isotropic Turbulence.

Previous Work

In the study of the effect of surface roughness on fluid flow Nikuradse (3) has performed some very extensive experiments, using different sizes of sand grains placed on the inside surface of pipes. He used the diameter of the sand grains as a measure of the roughness, and the ratio $\frac{k}{r}$ was designated as the "relative roughness," where k = height of the roughness, or diameter of the sand grains, and r = radius of pipe.

Schlichting (4), (published after this work was begun) has recently made an extended investigation of the effect of roughness, using various kinds of rough surfaces. From Schlichting's experiments it is seen that the friction coefficient does not only depend upon the height of the roughness, but also on the spacing, which, of course, should be expected. However, most any height and spacing may be reduced to an equivalent sand grain roughness.

These results confirm the theory that for a particular rough surface the pipe friction coefficient at high Reynolds Number is independent of Reynolds Number, and that its value is determined by the relative roughness.

*Note:- Numbers in () refer to bibliography at the end of this paper.

From Karman's analysis the velocity distribution in the fully developed region for smooth walls in pipes is given by $u = v_* (A + B \log \frac{v_* y}{\nu})$

Where:

u = velocity at a point in the pipe.

$v_* = \sqrt{\tau_0/\rho}$ called the friction velocity.

A = a constant depending on the roughness of the wall.

B = a universal constant independent of the wall roughness

τ_0 = shearing stress at the wall.

y = the distance from the wall to the point where the velocity is measured.

ρ = mass density of the fluid.

ν = the kinematic viscosity of the fluid.

log = logarithm to base 10.

For smooth walls the value of A is given as 5.5 and of B, as 5.75. Using these values the equation then becomes $(\frac{u}{v_*} = 5.5 + 5.75 \log (\frac{v_* y}{\nu})$ (smooth) which fits the experimental values for $\log (\frac{v_* y}{\nu}) > 100$.

In hydraulics the friction coefficient f is defined as $h = f \frac{L}{d} \frac{\bar{u}^2}{2g}$ where h denotes the head loss in height, L, the length, d, the diameter of the pipe, $\bar{u}$, the mean velocity, and g, the acceleration of gravity, 32.17. Following Karman's deductions Nikuradse and Prandtl gave the following formula for f,

$$\frac{1}{f^{\frac{1}{2}}} = 2 \log (Rf^{\frac{1}{2}}) - 0.8 \text{ (smooth)}$$

where $R = \frac{\bar{u}d}{\nu}$ = Reynolds Number, and d = the diameter of the pipe.

The problem of the effect or influence of surface roughness on the friction coefficient is somewhat complex. Numerous experiments have been performed in pipes and channels with rough walls, notable of which are those of Nikuradze and Schlichting. In pipes with geometri-

cal similar surface conditions, but different diameters the friction coefficient varies with Reynolds Number and the "relative roughness." The relative roughness is the ratio of a length which is characteristic of the rough surface, say the height of the projections, and the radius of the pipe. If the characteristic length of the rough surface be denoted by k, and the pipe radius by r, then $f = f\,(R, k/r)$.

Experiments seem to indicate that at high Reynolds Number and large relative roughness, f is independent of the viscosity and also independent of Reynolds Number. Nikuradse's experiments show that for surfaces made rough with sand grains the velocity distribution is given by the equation

$$u = v_* (A_r + B \log \frac{y}{k}) \quad \text{(rough)}$$

where:-

$$Ar = A_r \quad (\frac{v_* k}{\nu}) \quad \text{(rough)}$$

B = 5.75 the same as for smooth walls.

From Karman's relationships

$$f = (2 \log \frac{r}{k} + a_r)^2 \quad \text{(rough)}$$

where: $a_r = a_r \, (\frac{v_* k}{\nu}) \quad \text{(rough)}$

For geometrical similar types of roughness Ar and a_r are independent of k and Reynolds Number, at large values of k and R. But for different types of roughness Ar and a_r will vary with k, depending upon the characteristic length chosen to represent k. However, at large values of Reynolds Number the velocity distribution and the friction coefficient appear to be independent of R.

The function $(\frac{v_* k}{\nu})$ may be thought of as a dimensionless roughness characteristic of the Reynolds type.

For the Nikuradse experiments with sand roughness, the value for A_r is given as 8.48, and for a_r is 1.74. Experiments by Hopf (5) and Fromm (6) on different types of roughness gave values of a_r from 0.96 to 1.48. Values of A_r given by Schlichting's experiments range from 2.28 to 13.8.

Present Work

Channel and Motor

This investigation was carried out in a small wind tunnel at the California Institute of Technology, shown schematically in Fig. 1. The channel was the same one used by Wattendorf (14) in his investigation of curved flow. However, another straight section was added, making the length of the straight portion double the length of the old part. The channel had a breadth of about 4.9 cm and a depth of 85 cm, giving a ratio of depth to breadth of 17.35. The large ratio was used in order to avoid so far as possible the disturbing effect of the top and bottom walls, simulating more or less two dimensional flow.

The bell-shaped intake was built with a honeycomb in the entrance to straighten out the eddies entering from the room. The straight portion consisted of 3/8" plywood covered on both sides with metal. It was 530 cm long, with the measuring stations located as shown in Fig. 1.

The curved section was the same as the old tunnel, but was of no importance for this investigation.

The exit cone consisted of a transition portion from rectangular to circular cross-section, and a propeller section 55 cm in diameter. A 10, H. P. D. C. motor at the exit end furnished the necessary power for the air velocity through the channel. The speed was controlled by

FIG. 1
Sketch Of Wind Tunnel
for
Roughness Measurements

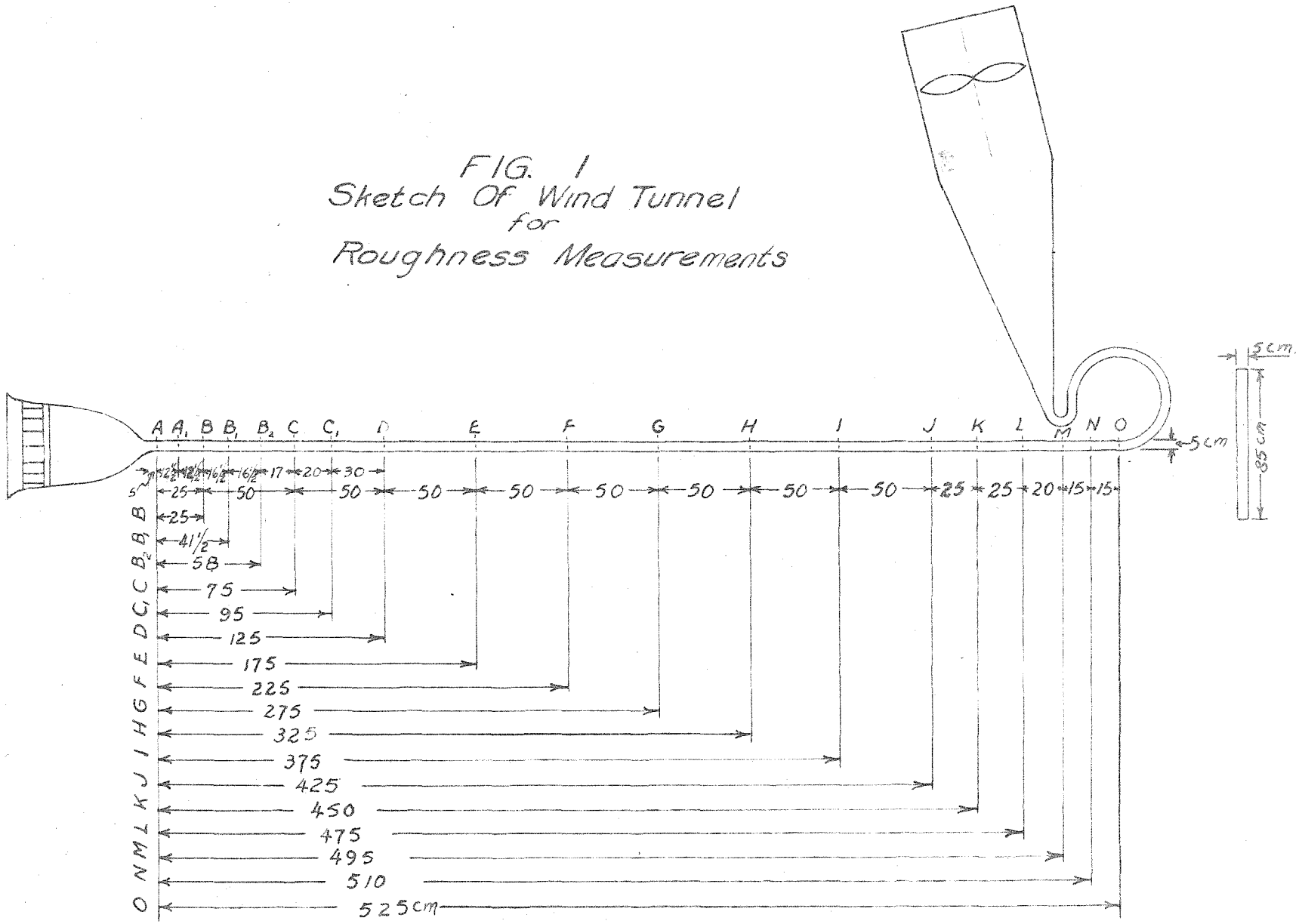

a portable rheostat on wheels, at the operator's table near the point of measurements.

Pitot Tubes and Manometers

The tube used for measuring total head consisted of a small copper tube 2.3 mm outside diameter with about 1.5 mm inside diameter. The sketch in Fig. 2 indicates the approximate dimensions. Static pressure was obtained with a tube of the same size having the upstream end closed with solder and rounded off to give a good streamlined nose. At a section 8 mm from the nose four small holes at 90° from each other were drilled normal to the axis of the tube. This static tube was calibrated in the center of the channel against a wall orifice in the smooth portion of the tunnel. A special double micrometer screw was used to move the tubes across the channel. Each micrometer had a travel of 25 mm and could be read to 0.01 mm. Fig. 4 illustrates this instrument. It was so made that it could be bolted to the outside wall of the channel at each station for making measurements. This instrument was also used to determine the exact width of the channel at each station.

The manometer, Fig. 3, consisted of a vertical screw thread and liquid reservoir mounted on a brass base. A rubber tube connected the reservoir with an inclined glass tube mounted on the vertical screw. A hair line in front of the glass tube was used to accurately tell when the liquid height was in balance with the pressure. By means of a small hand wheel the height of the glass tube could be adjusted to balance the pressure. The height could be read accurately on a counter to 0.01 mm. Two of these instruments were used in making the pressure

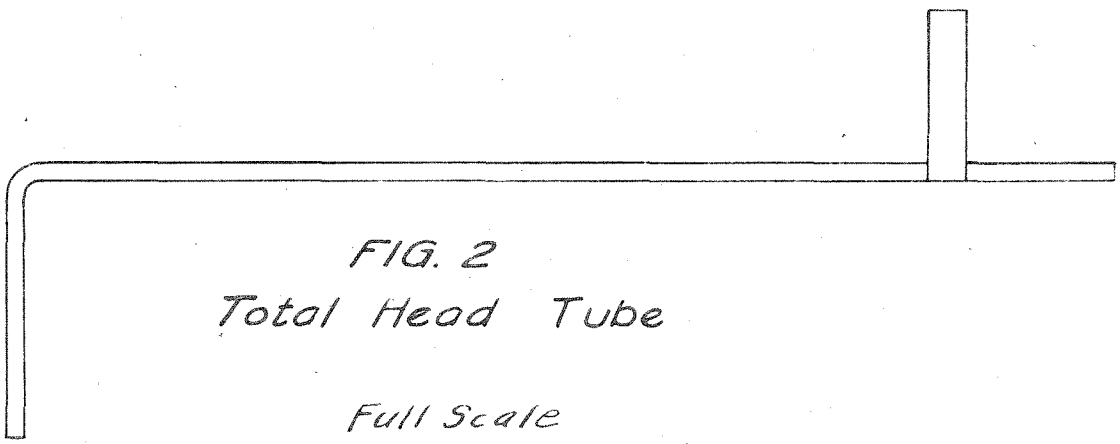

FIG. 2
Total Head Tube

Full Scale

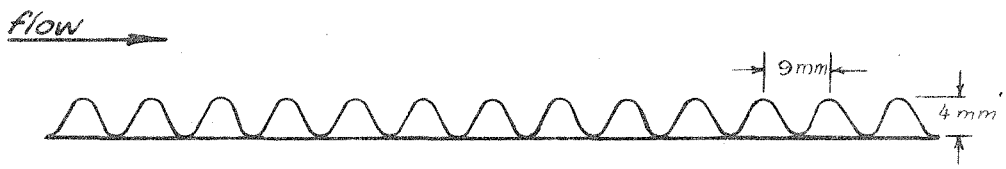

FIG. 3
Cross Section of Corrugated Paper
Roughness R-1

Full Scale

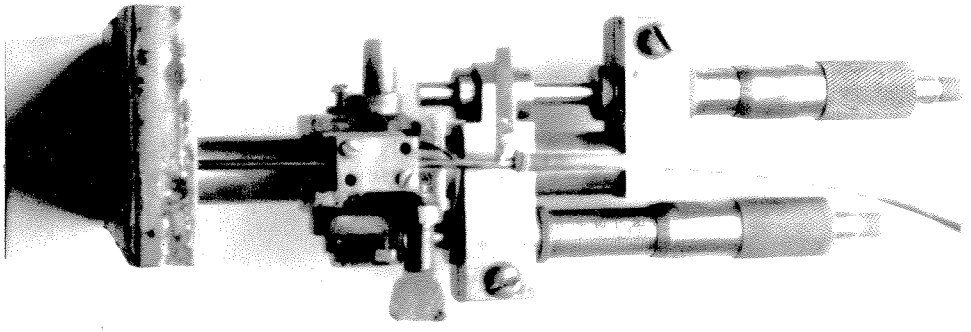

Fig. 4

Double Micrometer Instrument
for
Velocity and Hot Wire Surveys
Across the Channel

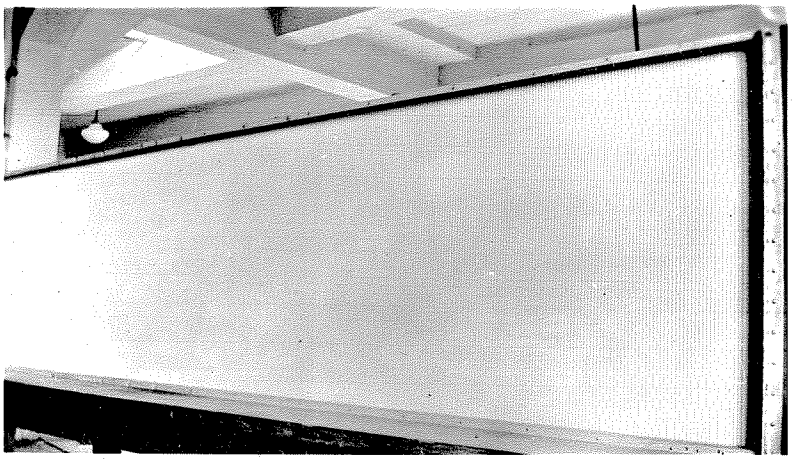

Fig. 5

View of Channel With
One Side Removed
Roughness R-1

drop measurements and velocity traverses. One was used to measure the reference pressure, the other to measure the difference between the total head at a station and the static pressure at the reference station. Alcohol was used as the liquid in the manometers.

Testing Procedure and Measurements

Seven different roughnesses were investigated, smooth walls being listed as one of the degrees of roughness. The different types of roughness are designated as R-1, R-2, R-3, R-4, R-5, R-6, and R-7, the latter being smooth walls.

The first degree of roughness was obtained by removing the two walls of the straight portion of the channel and glueing to the inside surface of each a layer of corrugated paper. Fig. 5 shows a photograph of the straight part of the channel with one side removed. A cross-section of the corrugated paper as used for the first roughness is shown in the sketch, Fig. 3.

Successive roughnesses were obtained by using a razor blade and cutting out every other one of the peaks in the original paper. In Fig. 6 is shown how these types of roughness were obtained. Figs. 7 and 8 show views of the second and third roughness respectively. Roughness R-5 had all the corrugations removed from the base paper, leaving only a layer of roughened paper to which the corrugations had been glued. In Fig. 6 the appearance of this surface is shown between the ridges.

The width, b, of the channel in this instance was 56.7 mm.

For roughness, R-6, the same wall surface was maintained as for R-5, but the width of the channel was decreased to 49.0 mm, which was about the width of the channel at the crest of the corrugations before they were

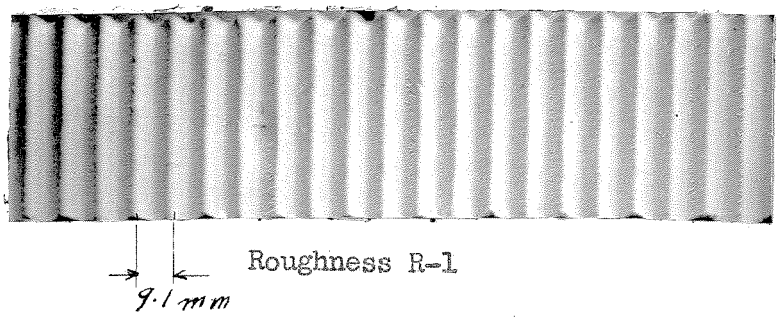

Roughness R-1

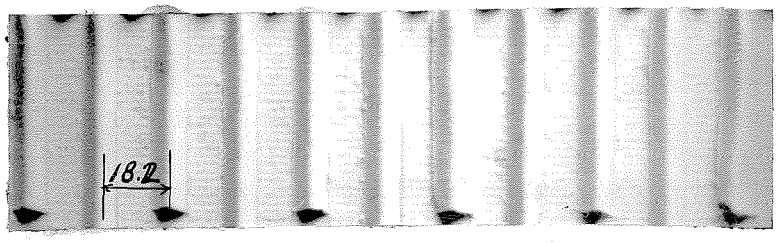

Roughness R-2

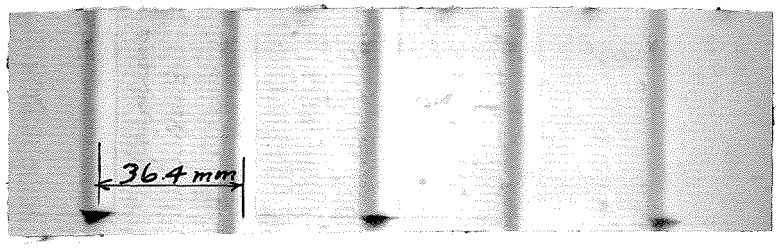

Roughness R-3

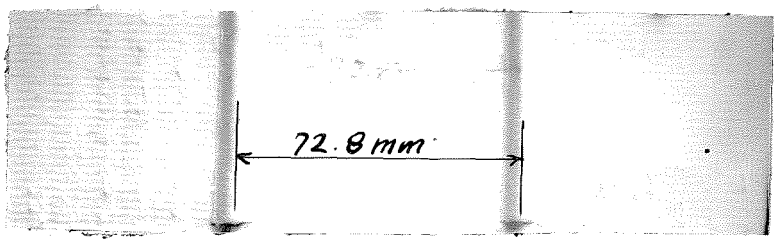

Roughness R-4

Fig. 6

Showing Types of Roughness

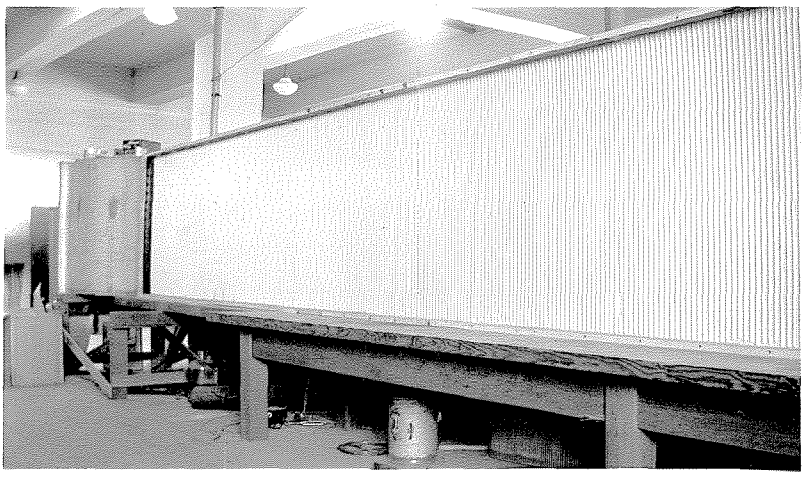

Fig. 7

Channel With One Side Removed

Roughness R-2

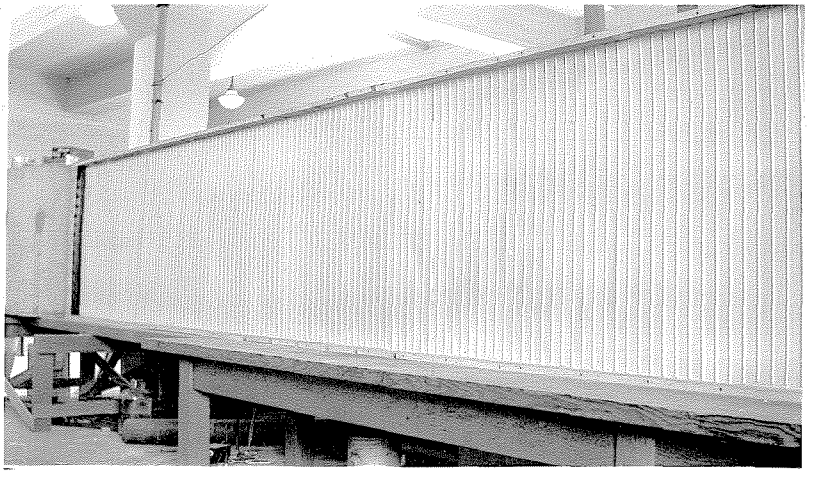

Fig. 8

Channel With One Side Removed

Roughness R-3

removed . In roughnesses 1 to 4 inclusive, the width of the channel was taken as the distance between the crests of the corrugations on opposite walls. Measurements of pressure and velocity distribution were also taken across the channel at the crest of the corrugations. In cases R-3 and R-4, measurements were also taken at points longitudinally between the crests at Station K. For this purpose a slot was made in the channel wall, and a third micrometer screw was added to the pitot tube instrument to give a motion of 50 mm parallel to the wind tunnel. A photograph of this arrangement is shown in Fig. 9.

Measurements were made of the pressure at each of the stations as located on the sketch in Fig. 1 for each type of roughness. In the entrance section the stations were closely spaced in order to show the development of the boundary layer for the different roughnesses, and to indicate the change in the velocity distribution in the transition region between the laminar and fully developed turbulent regions.

Velocity traverses were made at each station from A to D inclusive for each roughness except R-3 and R-4, and at stations G and K for all roughnesses.

In making the measurements, the exact width of the channel was determined at each station. A "speed run" was then made at station K, this station being the reference for velocity. Station N was used as the static pressure reference. The speed run consisted of placing the total head tube in the center of the channel, connecting it to one side of the manometer. The other side of the manometer was connected to the reference pressure at Station N. This arrangement gave a dynamic pressure, q_{kn}, with total pressure head at station K and static pressure P_n

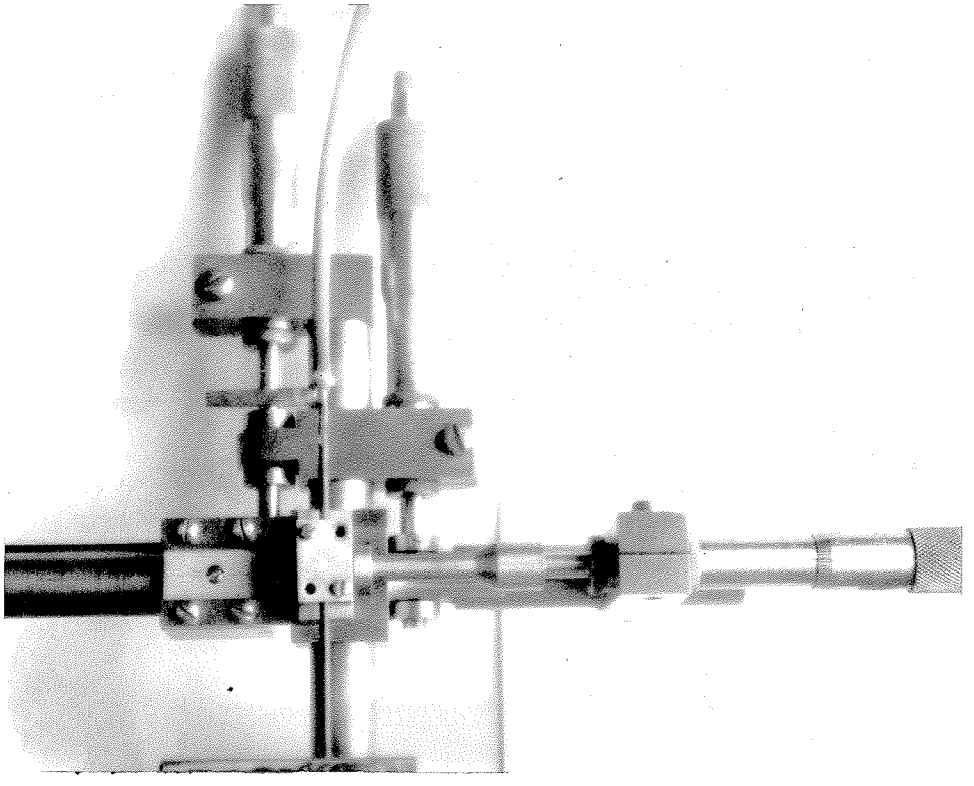

Fig. 9

Double Micrometer Instrument

With Third Micrometer Attached

For Longitudinal Motion.

at station N. With station N, also connected to a second manometer, values of q_{kn} were determined at several values of P_n. Another run was then made placing the static pressure tube in the center of station K, and connecting to the first manometer so as to read (P_n-P_k), the difference between the pressure at N, and the pressure at K. In order to determine the dynamic pressure q_k at K, we have $q_{kn} = H_k - P_n$ and $q_k = H_k - P_k$. Subtracting these two equations we have $q_k = q_{kn}+(P_n-P_k)$ and (P_n-P_k) is a negative quantity.

Where H_k is the total pressure head at station K, and the other terms have the same significance as defined above. The velocity was then determined by the relationship $q_k = \frac{1}{2}\rho\frac{U^2}{\gamma}$

Where ρ denotes the mass density of the air,

γ, the specific gravity of alcohol and

u, the velocity.

With q_k measured in mm of alcohol and in $\frac{kg - sec^2}{m^4}$, the velocity is obtained in meters per second. The velocity at other stations was obtained in this manner. In obtaining a velocity traverse it was assumed that the static pressure was constant across the channel. This was not strictly true for R-3 and R-4. In these two cases the wall pressure was 2 to 4% larger in absolute value than at the center of the channel. For other roughnesses the variation of pressure from center to wall was less than $\frac{1}{2}$ of 1%.

At $\frac{y}{r} = 0.35$ the pressure variation for R-3 was about 0.5%, while for R-4 it was necessary to go to $\frac{y}{r} = 0.65$ to obtain only 0.5% variation in the static pressure. Here y is the distance from the wall to the point of measurement, and r is half the channel width. Because of

this pressure variation across the channel the velocity profiles for roughnesses R-3 and R-4 have not been included with the rest of the curves. In view of this condition the values of f and R in fig. 14 have been based upon the maximum velocity in the center of the channel instead of the mean velocity.

For roughnesses R-1, R-2, R-5, R-6, and R-7 the values of f and Reynolds Number based on the mean velocity have been calculated in Table III but have not been plotted. Although for these experiments R-1 to R-4 inclusive the absolute height of the roughnesses remained constant a different friction coefficient was obtained by varying the spacing of the corrugations. For R-5 and R-6 the height of the roughness was changed from the former group but remained constant for these two conditions, and the roughness was changed by changing the width of the channel. To make a comparison with Nikuradse's experiments one may calculate an equivalent sand grain roughness, k_s. If m = hydraulic radius, his experiments show the relationship

$$\frac{1}{\sqrt{f}} = 2 \log \frac{2m}{k_s} + 1.74 \qquad (1)$$

For these experiments we will have

$$\frac{1}{\sqrt{f}} = 2 \log \frac{2m}{k} + a_r \qquad (2)$$

Combining equations (1) and (2) the result is

$$2 \log \frac{k_s}{k} = 1.74 - a_r$$

where a_r is determined from equation (2). In the case of R-5 and R-6 the height of the roughness was not measurable and equation (2) may be put into the form

$$\frac{1}{\sqrt{f}} = 2 \log 2m + d$$

where $d = a_r - 2 \log k$. Combining this with equation (1) we obtain the relationship

$$\log k_s = \frac{1.74 - d}{2}$$

The values of the equivalent sand grain roughness are given in Table II.

Discussion of Curves and Results

The plot of $\frac{u}{v_*}$-vs-log $\frac{y}{k}$ in fig. 15 for R-5 and R-6 was obtained by assuming k = 4.35 mm, the same as for R-1 and R-2.

Using the equivalent sand grain roughnesses obtained in this manner a plot of $\frac{u}{v_*}$-vs-log $\frac{y}{k_s}$ for four roughnesses is shown in figure 16. This figure indicates that these results fall within 3 per cent of the curve representing Nikuradse's experiments, and indicates the universality of the constant 5.75 which is independent of the condition of the surface, as shown by Karman's theoretical analysis.

The points on this curve represent two entirely different types of roughness, and the value u/v_* depends a great deal on how, b, is measured in the equation for τ_o. Especially is this true with the corrugated paper with large spacing, since it is difficult to determine what value should be used for the channel width.

Figs. 10 to 13 inclusive show the plots of the pressure in the channel against the different stations for the various types of roughness. From these curves the pressure drop $\frac{dp}{dx}$ was determined. The forward portion of the channel was used to determine $\frac{dp}{dx}$, because there was less wall deflection in this part. The measured pressure at each station was corrected for variation in channel width due to

irregularities in the channel and that due to deflection, with speed change. It was found that at high speeds the walls of the channel would move in at the center due to the low pressure existing in the channel. Extra bracing was placed on the walls to lessen this deflection. The correction was applied to the pressure at the station as follows: First the width of the channel at the station was measured and then the deflection at various speeds was determined. It was found that this was a straight line variation when plotted against the static reference pressure, Pn, so zero speed and high speed served to determine this deflection rate at each station. If, P_X represents the pressure measured at a particular station, then the true pressure is $P_X + \Delta P_X$, where $\Delta P_X = \frac{2q_X \Delta b_X}{b_o}$ (see appendix)

q_X = dynamic pressure at station.

Δb_X = difference between standard width and width when deflected.

b_o = standard width of channel.

To show the importance of the deflection of the channel, suppose it is desired to have the variation of f_m within 1%, then $\frac{\Delta P_X}{P_1 - P_2} < 0.01$. From Bernoulis' theorem we have $\Delta P_X = -\rho u \Delta u$ and from the continuity equation ub = const, therefore

$$u \Delta b + b \Delta u = 0 \text{ and } \Delta u = -\frac{u}{b}\Delta b$$

Hence $$\Delta P_X = \rho u^2 \frac{\Delta b}{b} = 2q \frac{\Delta b}{b}$$

$$P_1 - P_2 = \frac{dp}{dx} L \text{ but } f_m = \frac{dp}{d_X}\frac{4m}{q}$$

then $$P_1 - P_2 = \frac{qLf_m}{4m}$$

For Roughness R-5, $f_m = 0.0288$ = friction coefficient

$L = 200$ cm

$m = 2.32$ cm = hydraulic radius

$b = 4.9$ cm

then

$$\frac{\Delta P_x}{P_1 - P_2} = \frac{8 \times 2.32}{200 \times .0288} \times \frac{\Delta b}{4.9} < 0.01$$

$$0.66\, \Delta b < 0.01$$

or $\Delta b < \frac{1}{66}$ cm $\approx \frac{1}{6.6}$ mm.

The width of the channel could be determined accurately to 0.05 mm. For the smooth walls the variation of, b, would have to be kept within about $\frac{1}{13}$ mm in order to insure f_m to 1% accuracy.

Two typical profiles of the velocity distribution at different speeds for R-2 and smooth walls are shown in Figs. 17 and 18. The mean velocity in the channel was determined by obtaining the aera under the curve and dividing by the abscissa. The area was determined by means of a planimeter.

These curves serve to illustrate clearly the change in the velocity profile for change in roughness.

Figs. 19 to 21 represent a plot of $\frac{u}{u_m}$ -vs-$(1-\frac{y}{r})$ and they illustrate the effect of roughness on the velocity profile at different speeds. As the relative roughness increases, the curves show that ratio of the mean velocity to the maximum velocity is decreased also. Scale effect of each type of roughness is shown in the curves of Figs. 22 to 24. Smooth walls seem to exhibit the greatest scale effect and the largest relative roughness the least. These velocity profiles represent conditions at station "K". Even with smooth walls the effect of scale is very small on the velocity profile.

In order to compare the development of the boundary layer for each relative roughness, traverses were made at the first 7 or 8 stations from the entrance. These curves are shown in Figs. 25 to 30 and indicate fully developed flow at a shorter distance from the entrance as the relative roughness increases.

The plot $\frac{U_m - u}{\sqrt{\tau_0/\rho}}$ - vs - $1-\frac{y}{r}$ for four different velocities is shown in Figs. 31 to 35 for the various types of surface roughness, and also for smooth walls. $\sqrt{\tau_0/\rho} = V_*$

The sine wave at the right wall for R-1 and R-2 shows the relative magnitude of the surface roughness compared to half the channel width. On each sheet of this group of curves is plotted the curve corresponding to the equation $\frac{U_m - u}{\sqrt{\tau_0/\rho}} = -\frac{1}{\text{Kappa}}\left[\log_e \left(\frac{y}{r}\right)\right]$ where kappa is Karman's universal constant and its value is taken as 0.40.

The deviation from this equation appears to be more at larger relative roughness. The experimental curves would be in better agreement if the value of Kappa were increased slightly for each increase in roughness.

The parallelism of the curves in the wide central region clearly illustrates the broad features of the flow pattern as brought out by Karman's universal velocity deficiency law

$$\frac{U_m - u}{V_*} = \frac{1}{\text{Kappa}}\left[\log_e\left\{1-(1-\frac{y}{r})^{\frac{1}{2}}\right\} + (1-\frac{y}{r})^{\frac{1}{2}}\right] \qquad (3)$$

which reduces to

$$\frac{u}{V_*} = \frac{U_m}{V_*} + \frac{1}{\text{Kappa}} \log_e \frac{y}{r} \text{ for small values of } y/r$$

where Kappa is a universal constant.

In the equation for f as given on page 4 the factor 2 corresponds to the value 0.403 for Kappa.

There appears to be some spread for the different types of roughness, part of which may be due to the determination of τ_o. As mentioned earlier in this paper $\tau_o = \frac{b}{2} \frac{dp}{dx}$, and, b, is the distance measured between the crests of the corrugations. When the corrugations are spaced differently along the walls it appears as though there should be an effective width which would take into account the increased area not covered by the corrugations.

Fig. 13a is a plot of $\frac{\tau_o}{\rho}$ -vs-$(U_m)^2$ showing that for each type of roughness the ratio of $\frac{\tau_o/\rho}{(U_m)^2}$ is constant for different speeds.

Roughness R-5 and R-6 are very close together and show the result of varying the roughness by changing the width of the channel, even though it was only a change of 7.6 mm.

The effect on the velocity profile of a traverse across the channel at the crest and at the valley of the corrugations is shown in Figs. 36 and 37 for Roughness R-1 and R-2.

These curves indicate that for spacings of corrugations up to 18.2 mm, for this height of roughness there is little effect on the velocity profile, whether it is made at the crest or at the valley of the corrugations. However, the spacing for R-3 which was 36.4 mm, showed marked effect, and this may be illustrated in Fig. 38 by the change in the static pressure across the channel at various longitudinal positions.

Conclusions

It appears that within the accuracy of these experiments, that the friction factor for this type of rough surface may be computed from Nikuradse's equation for any relative roughness, providing that the equivalent sand grain roughness is known for that particular surface.

Even though this work and Schlichting's work shows the validity of the logarithmic velocity distribution law for varied types of roughness, still more experiments should be performed in larger pipes and various rectangular conduits, with the thought in mind of a more precise determination of the numerical value of the Karman constant, kappa. Both the friction law and the velocity destribution law have the form $\frac{\quad}{\quad} = A + B \log \frac{\quad}{\quad}$ the A coefficient varies over a wide range with the condition of the surface.

The extent and character of the wide variation of this coefficient should be investigated further.

The B coefficient appears to be constant, directly dependent on the value of kappa.

The friction coefficient increased with increase in the spacing of the corrugations until R-4, when it decreased to a value between R-2 and R-3. Fig. 14 illustrates this very clearly. The spacing of the corrugations in the order from high friction coefficient to low value are as follows:

R-3 - 36.4 mm.
R-4 - 72.8 mm.
R-2 - 18.2 mm.
R-1 - 9.1 mm.

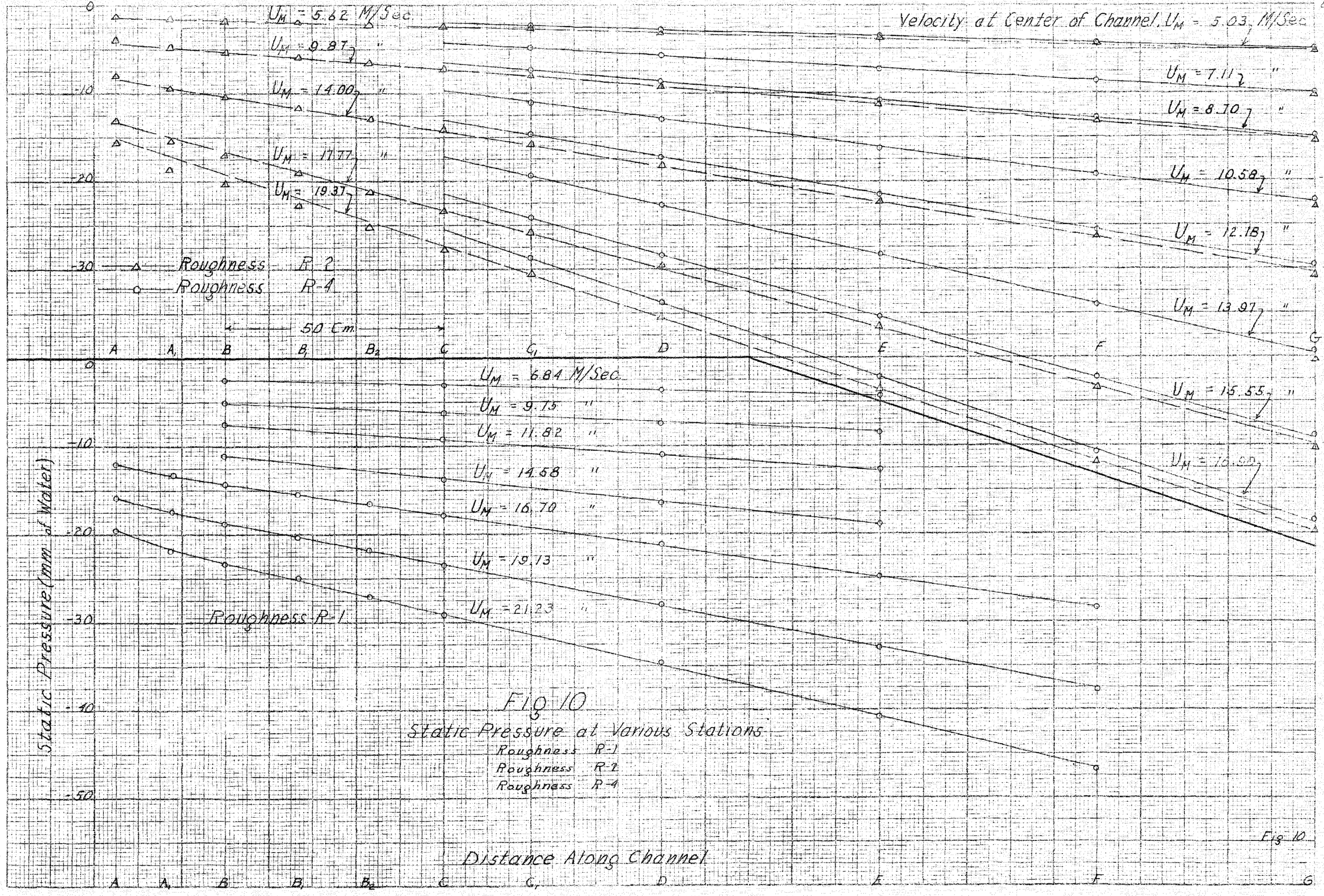

Fig 10

Static Pressure at Various Stations

Roughness R-1

Roughness R-2

Roughness R-4

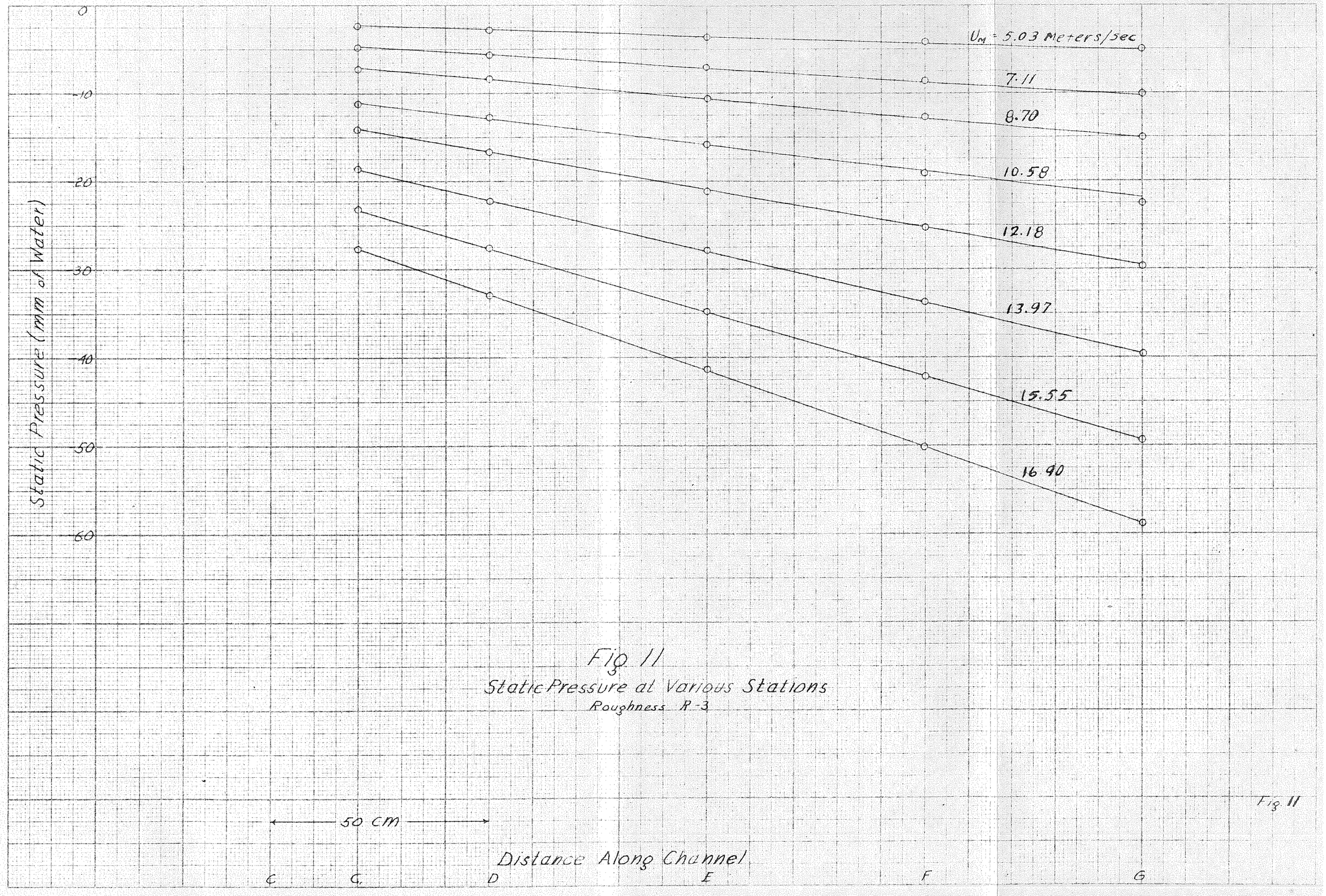

Fig 11

Static Pressure at Various Stations

Roughness R-3

Fig 11

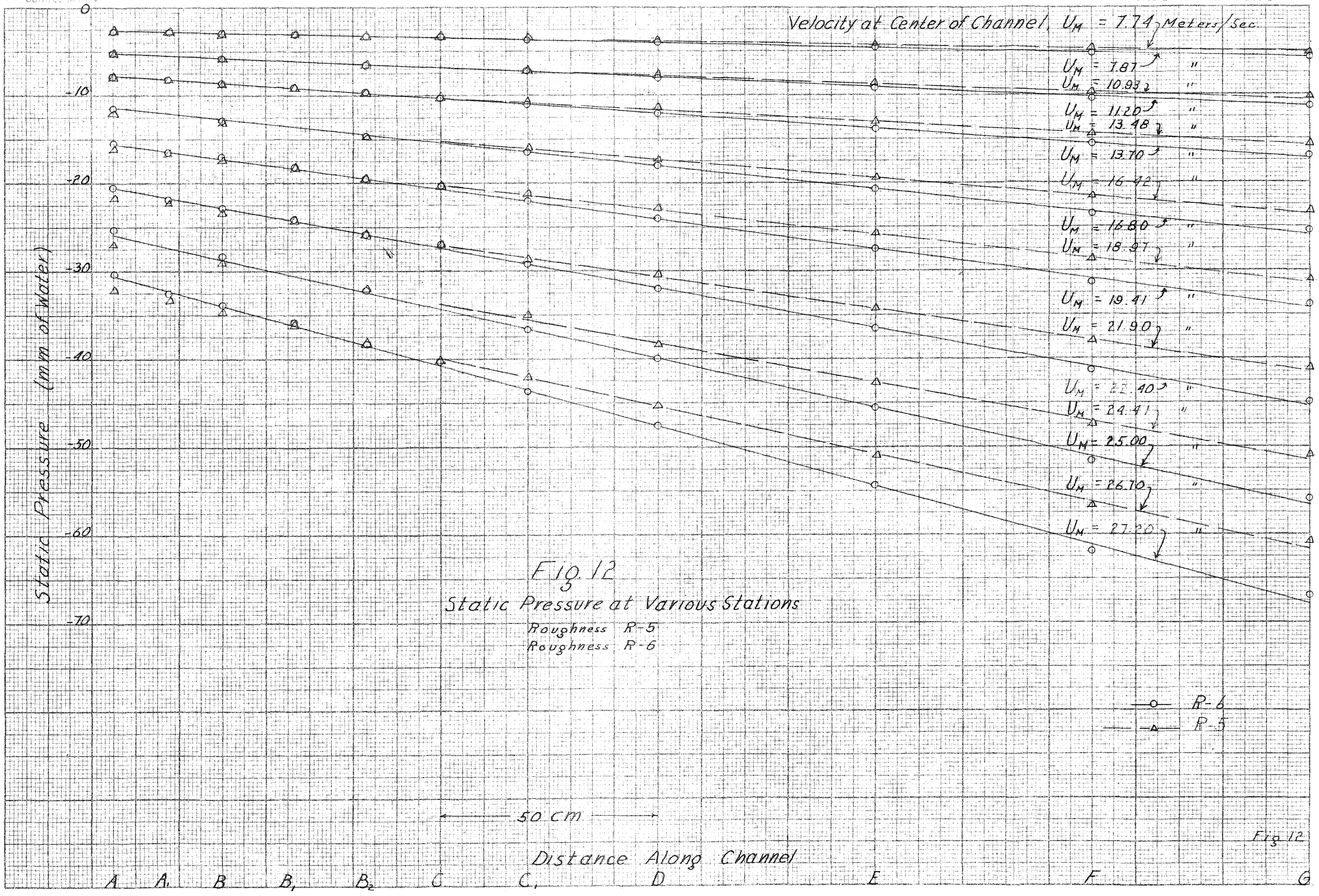

Fig. 12

Static Pressure at Various Stations

Roughness R-5

Roughness R-6

Fig. 12

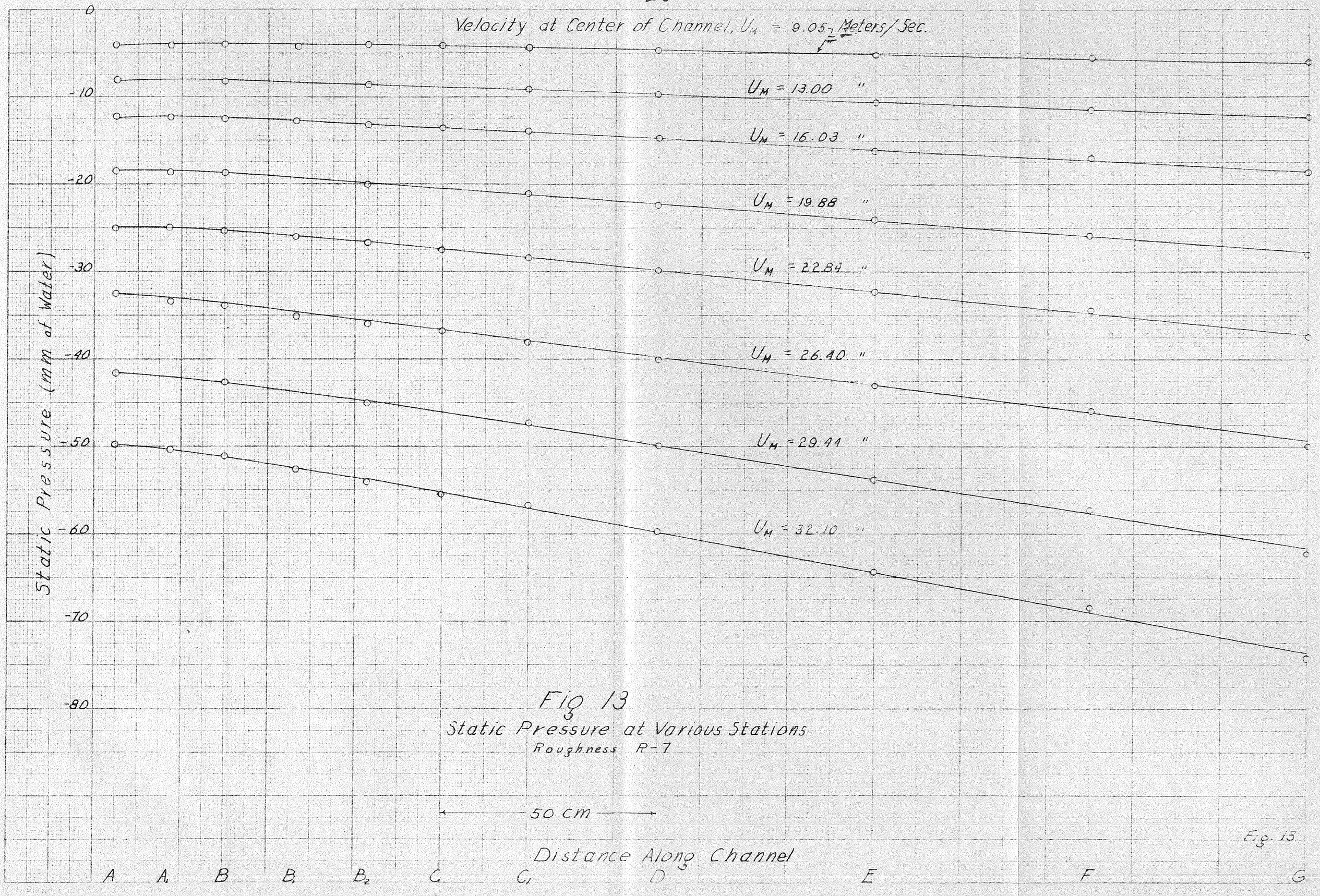

Fig 13

Static Pressure at Various Stations

Roughness R-7

Fig. 13.

27

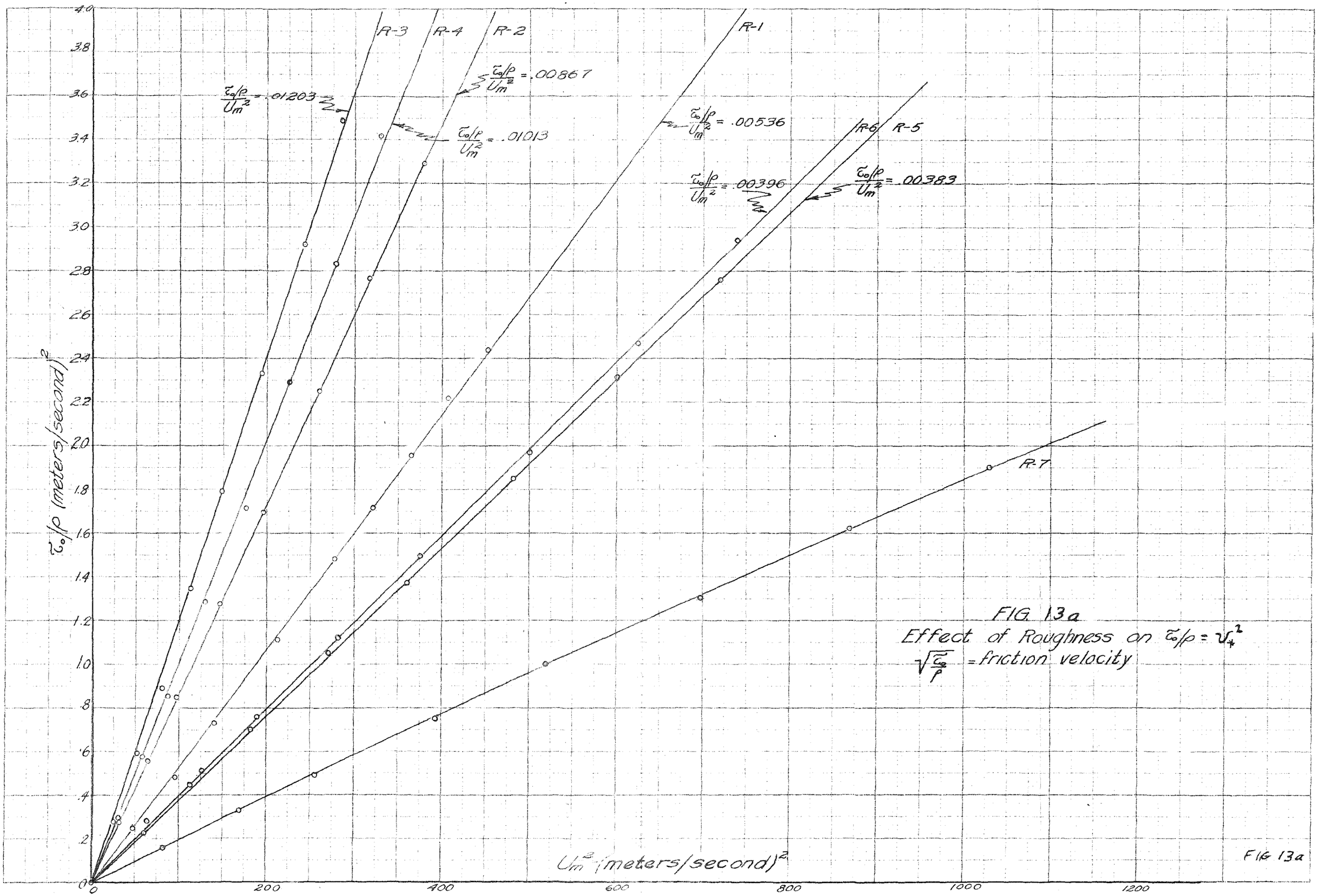

FIG 13a
Effect of Roughness on $\tau_o/\rho = v_*^2$
$\sqrt{\frac{\tau_o}{\rho}}$ = friction velocity

FIG 13a

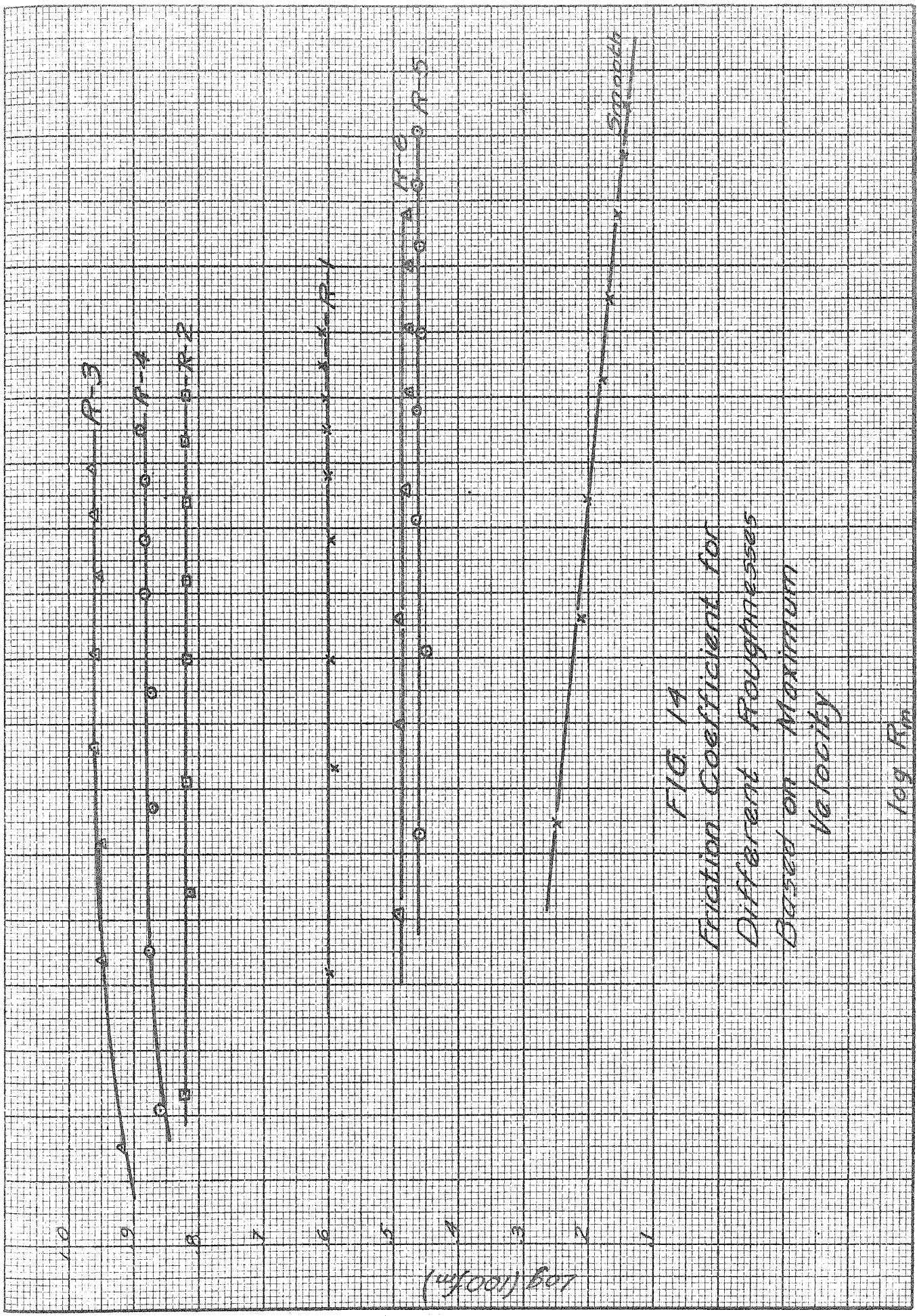

FIG 14
Friction Coefficient for
Different Roughnesses
Based on Maximum
Velocity

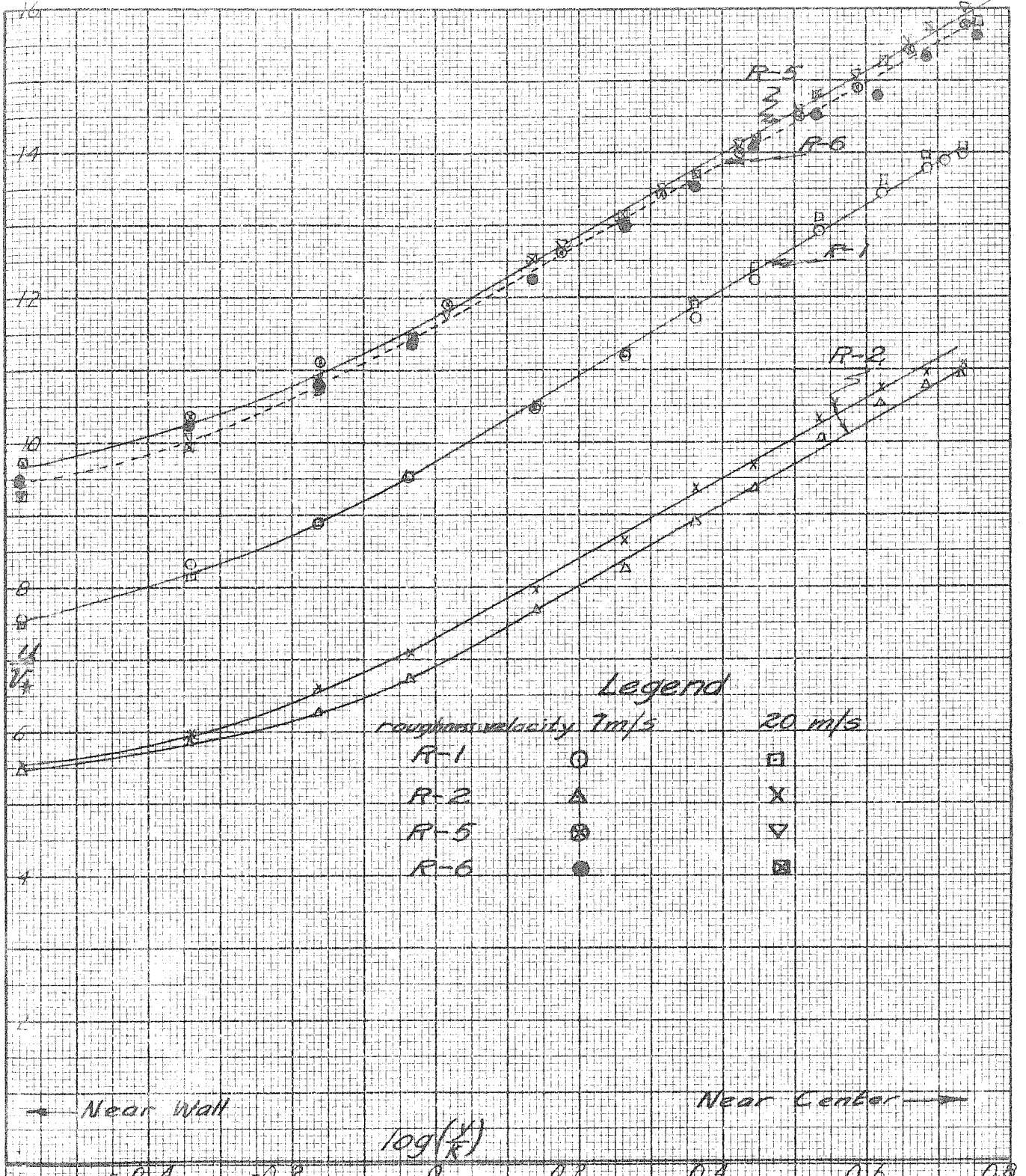

FIG 15
Dimensionless Velocity Distribution
for
Four Roughnesses

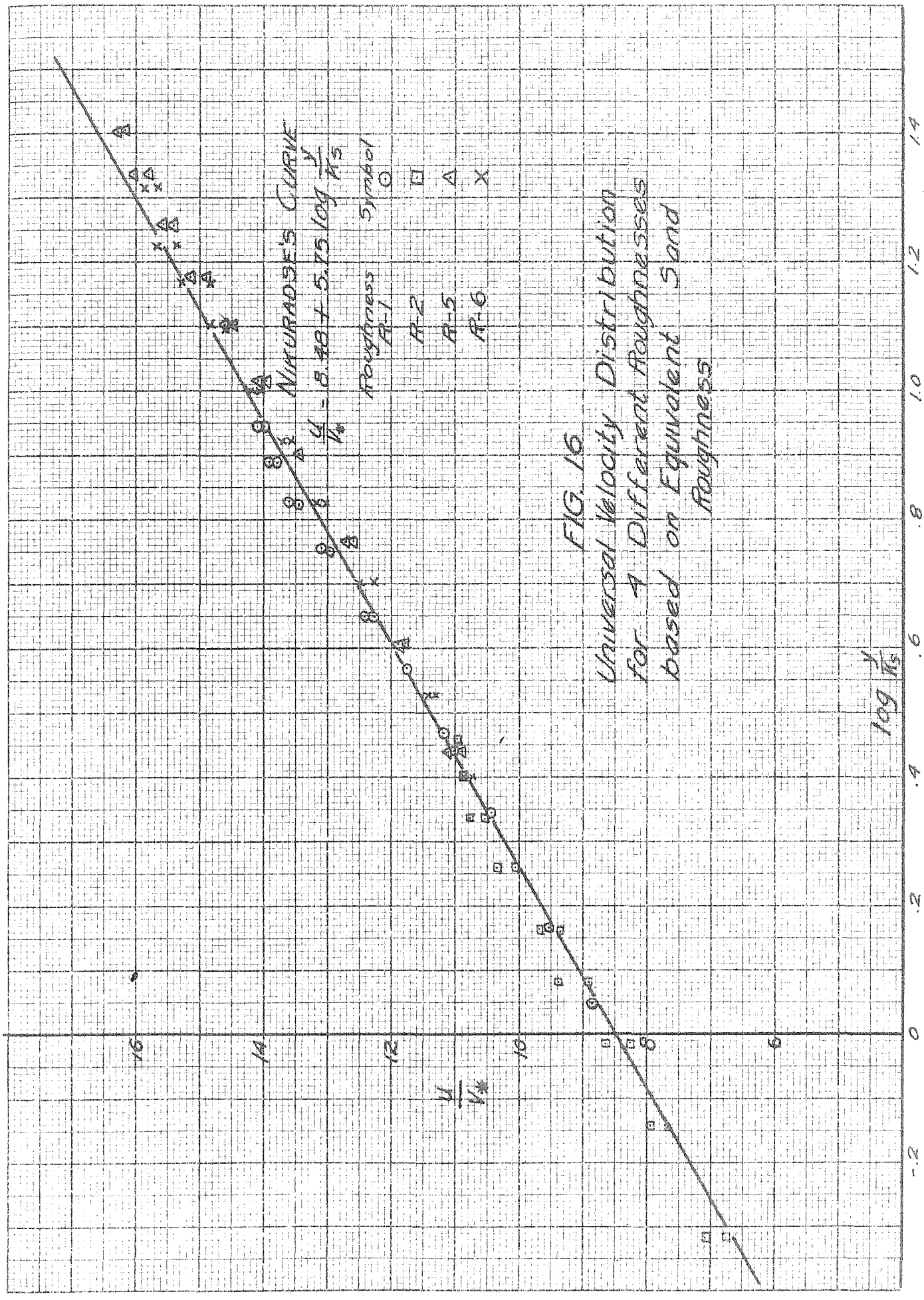

FIG. 16
Universal Velocity Distribution
for 4 Different Roughnesses
based on Equivalent Sand
Roughness

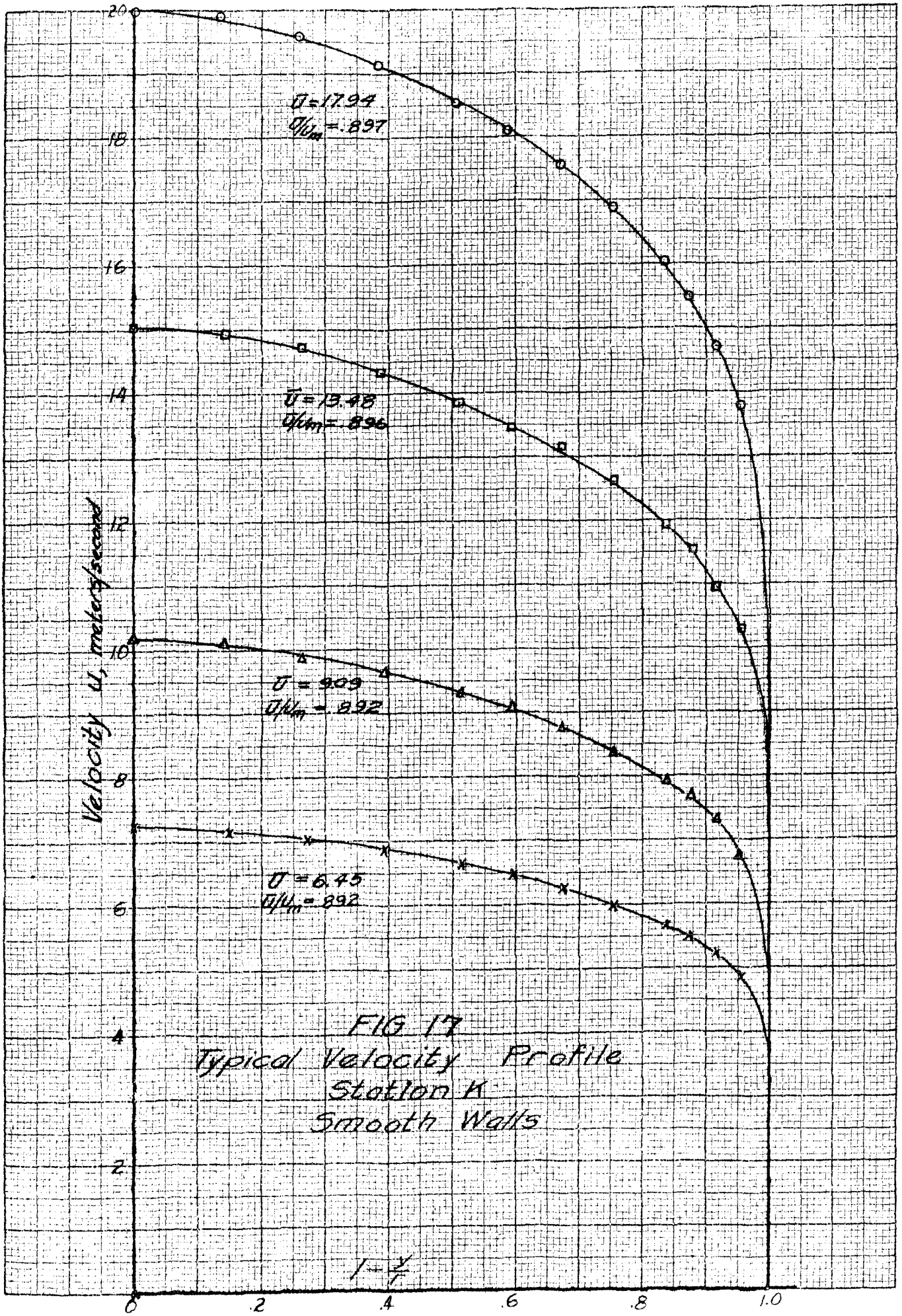

FIG 17
Typical Velocity Profile
Station K
Smooth Walls

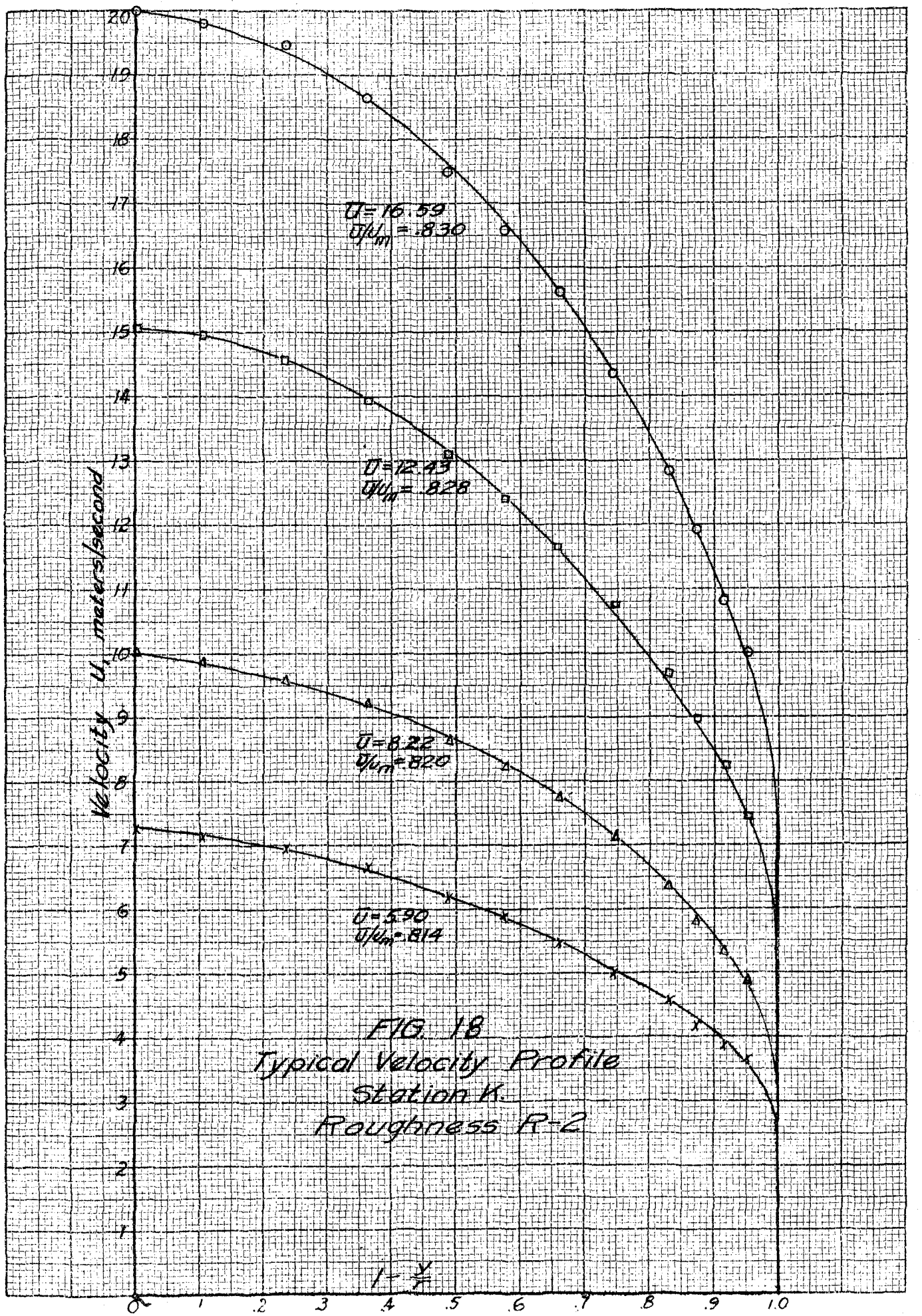

FIG. 18
Typical Velocity Profile
Station K.
Roughness R-2

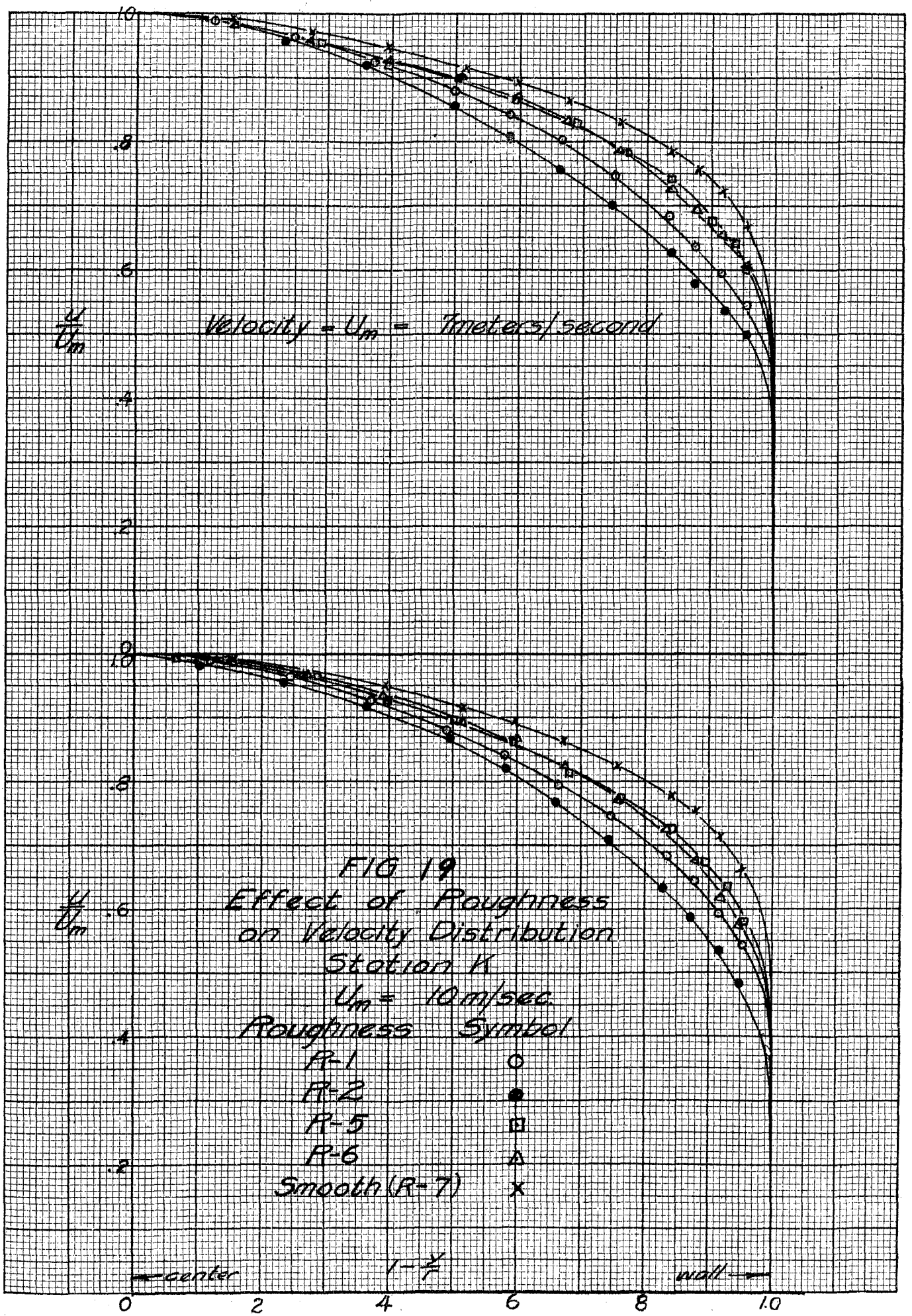

FIG 19
Effect of Roughness
on Velocity Distribution
Station K
U_m = 10 m/sec.

Roughness	Symbol
R-1	○
R-2	●
R-5	□
R-6	△
Smooth (R-7)	×

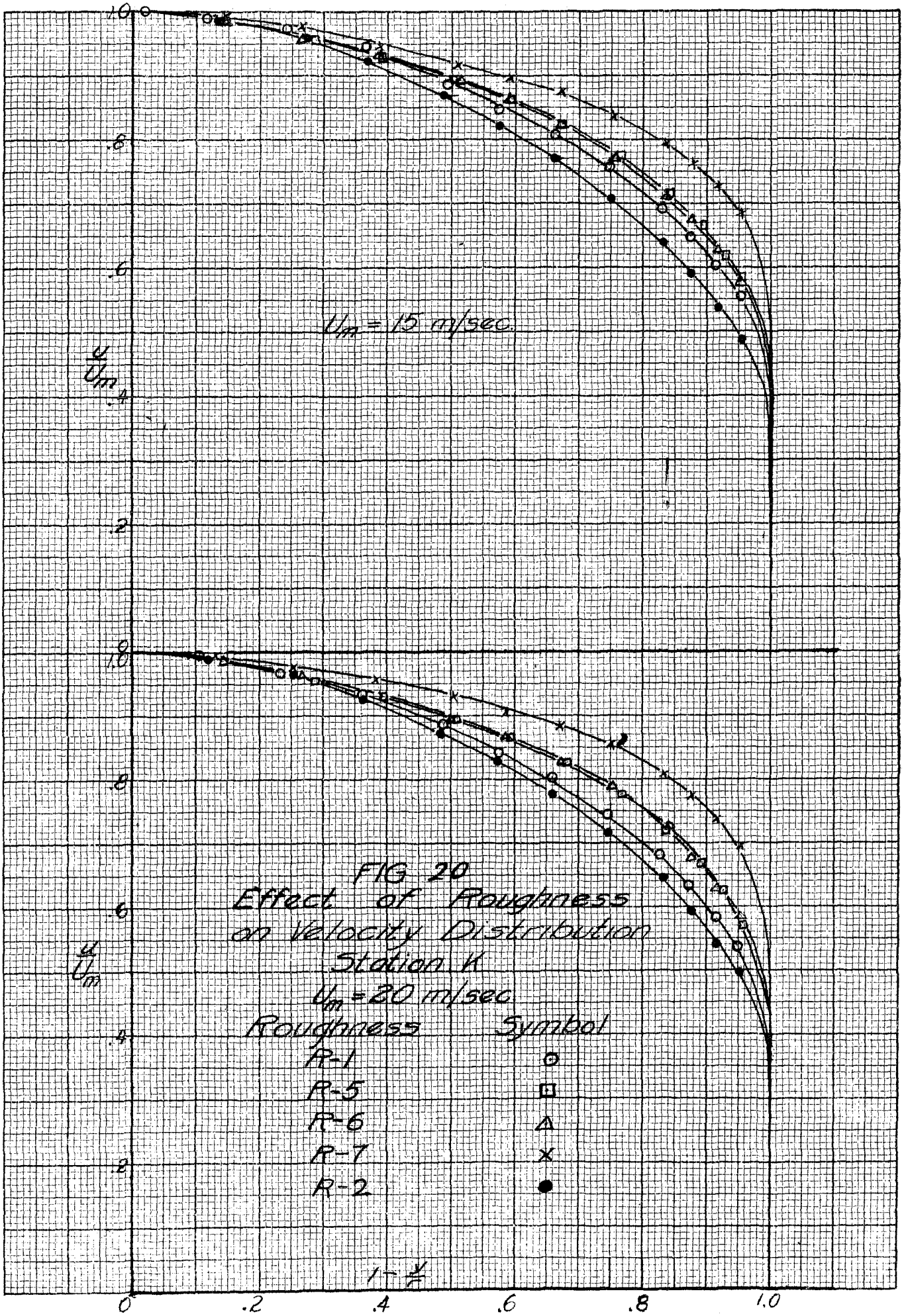

FIG 20
Effect of Roughness on Velocity Distribution
Station K

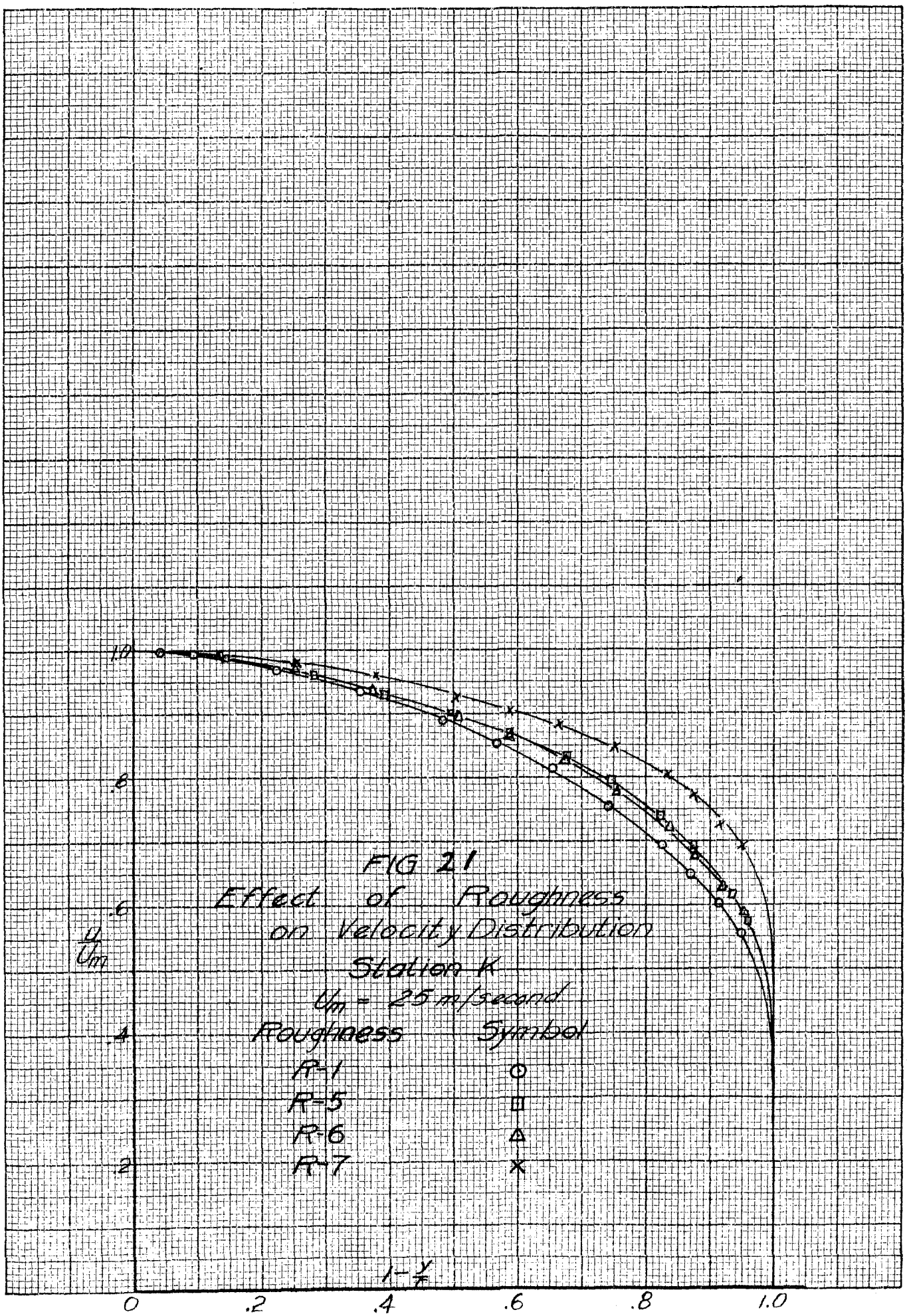

FIG 21

Effect of Roughness on Velocity Distribution Station K

U_m = 25 m/second

Roughness	Symbol
R-1	○
R-5	□
R-6	△
R-7	×

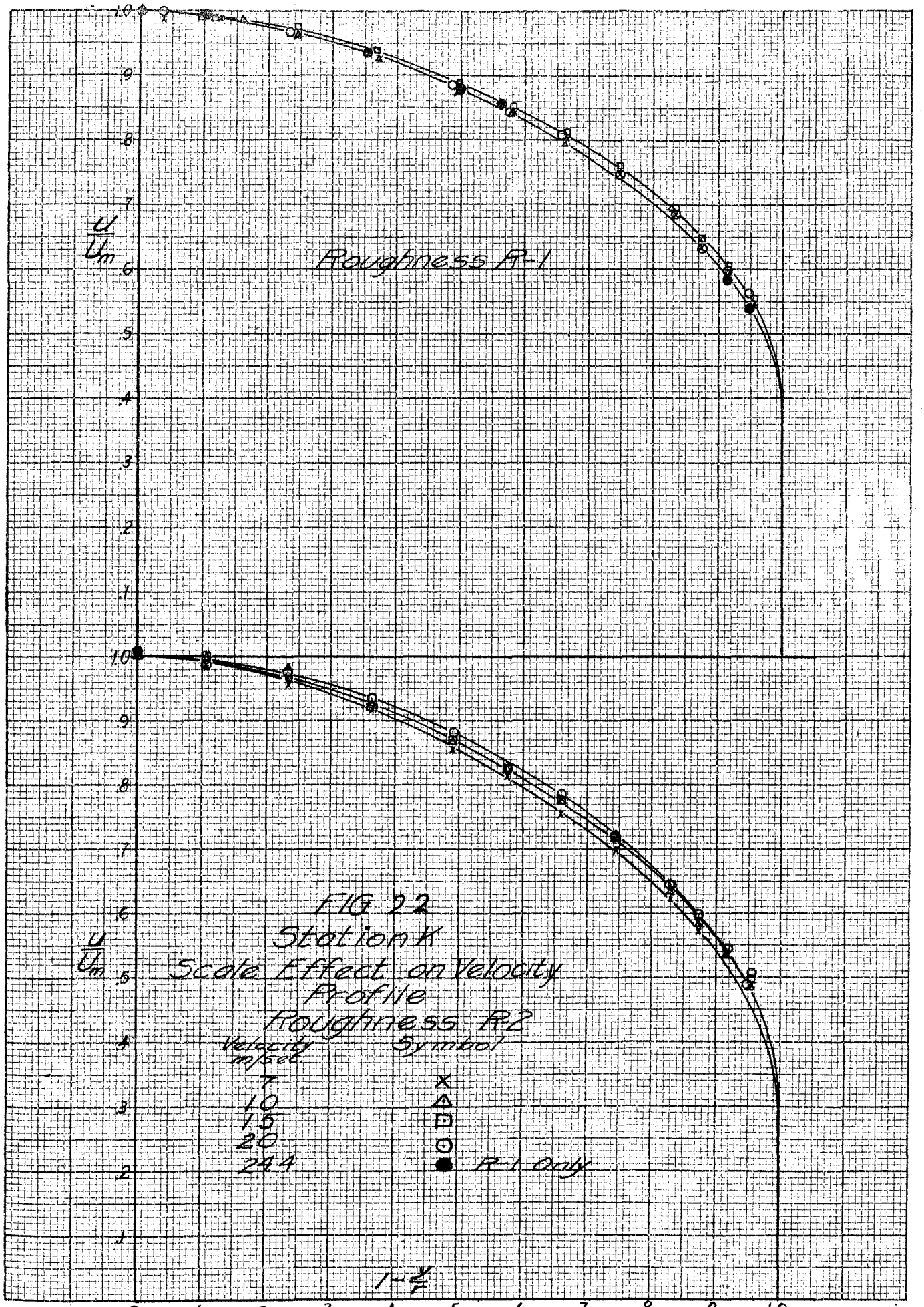

FIG 22
Station K
Scale Effect on Velocity Profile
Roughness R-2

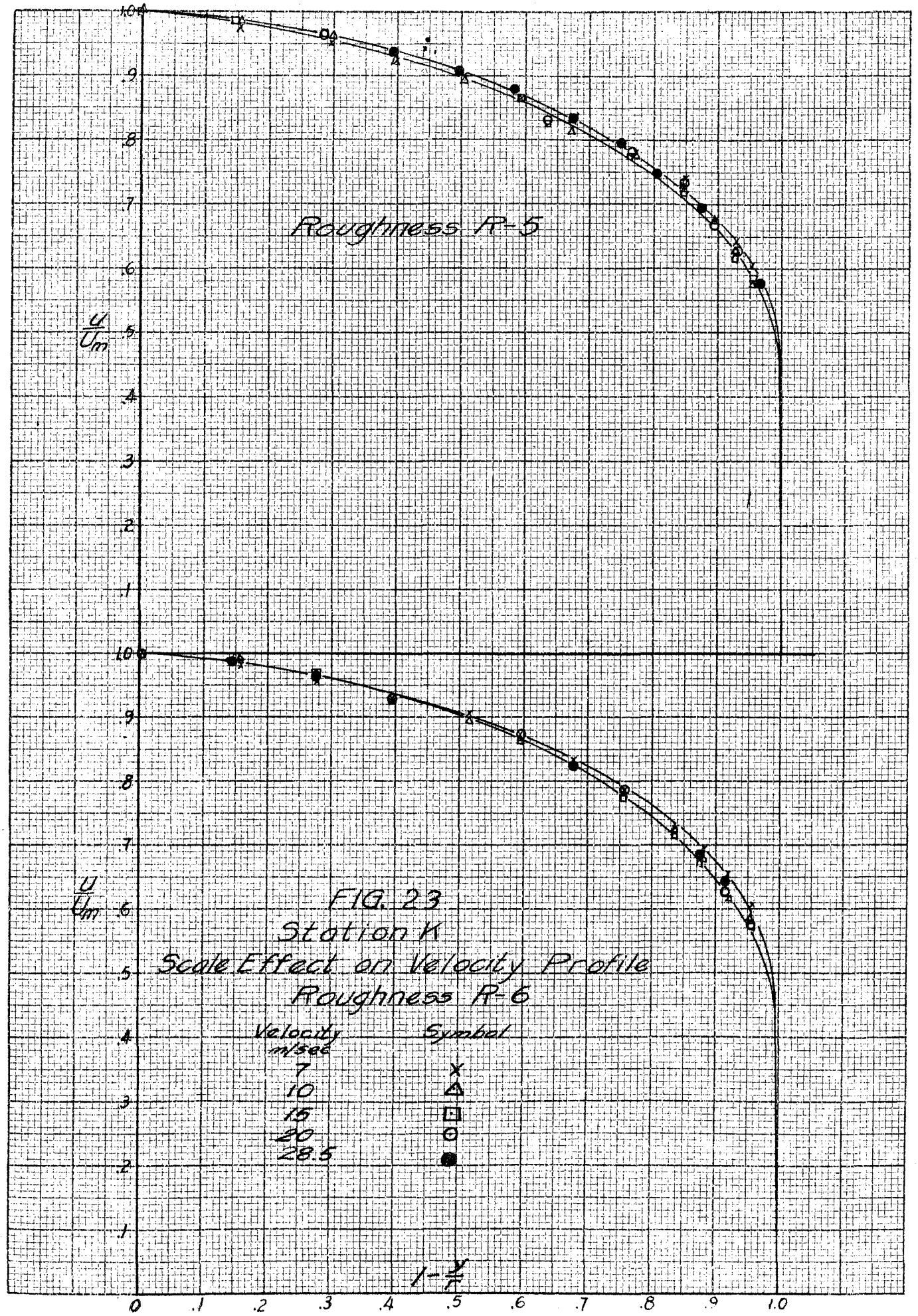

FIG. 23
Station K
Scale Effect on Velocity Profile
Roughness R-6

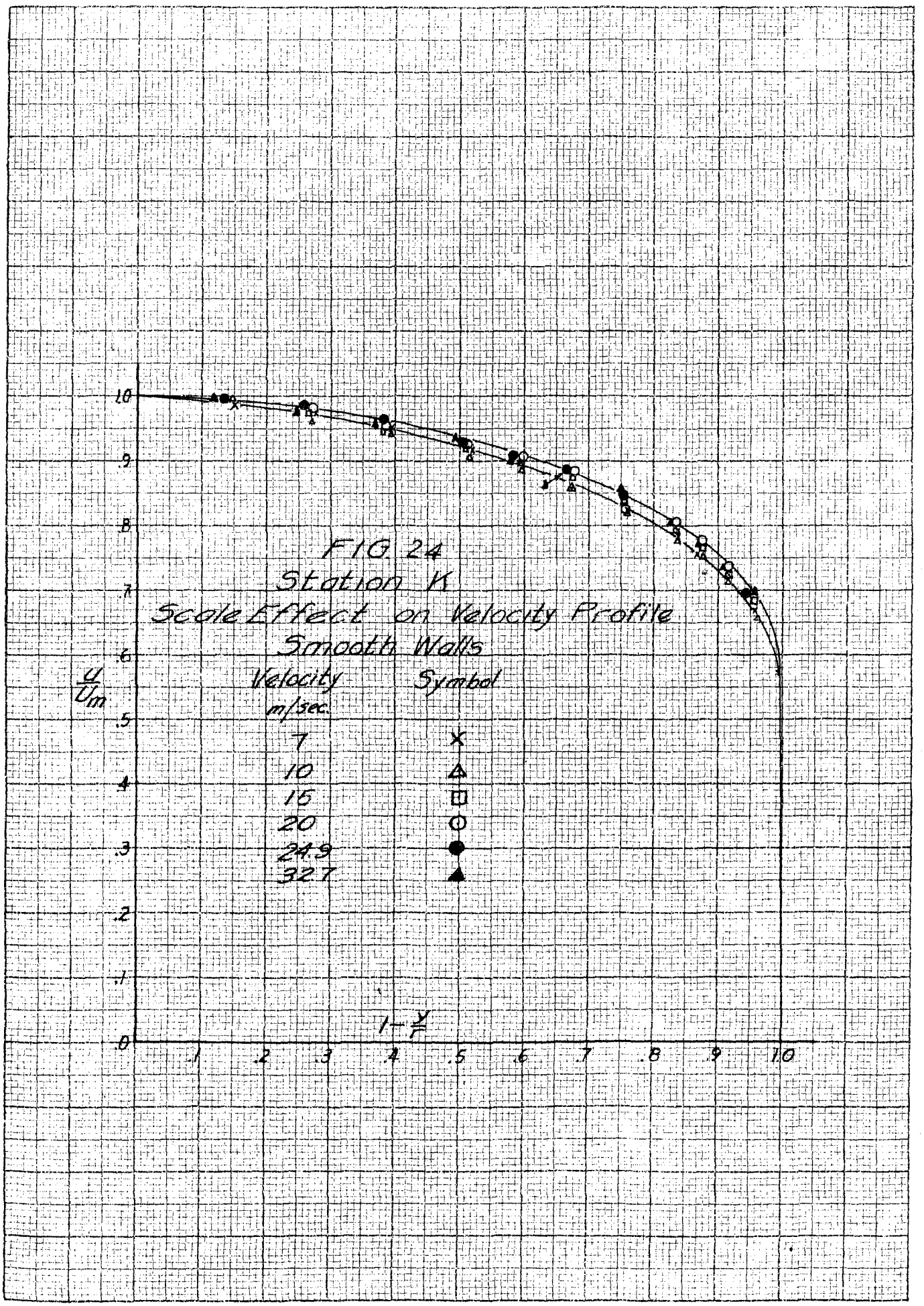

FIG 24
Station K
Scale Effect on Velocity Profile
Smooth Walls

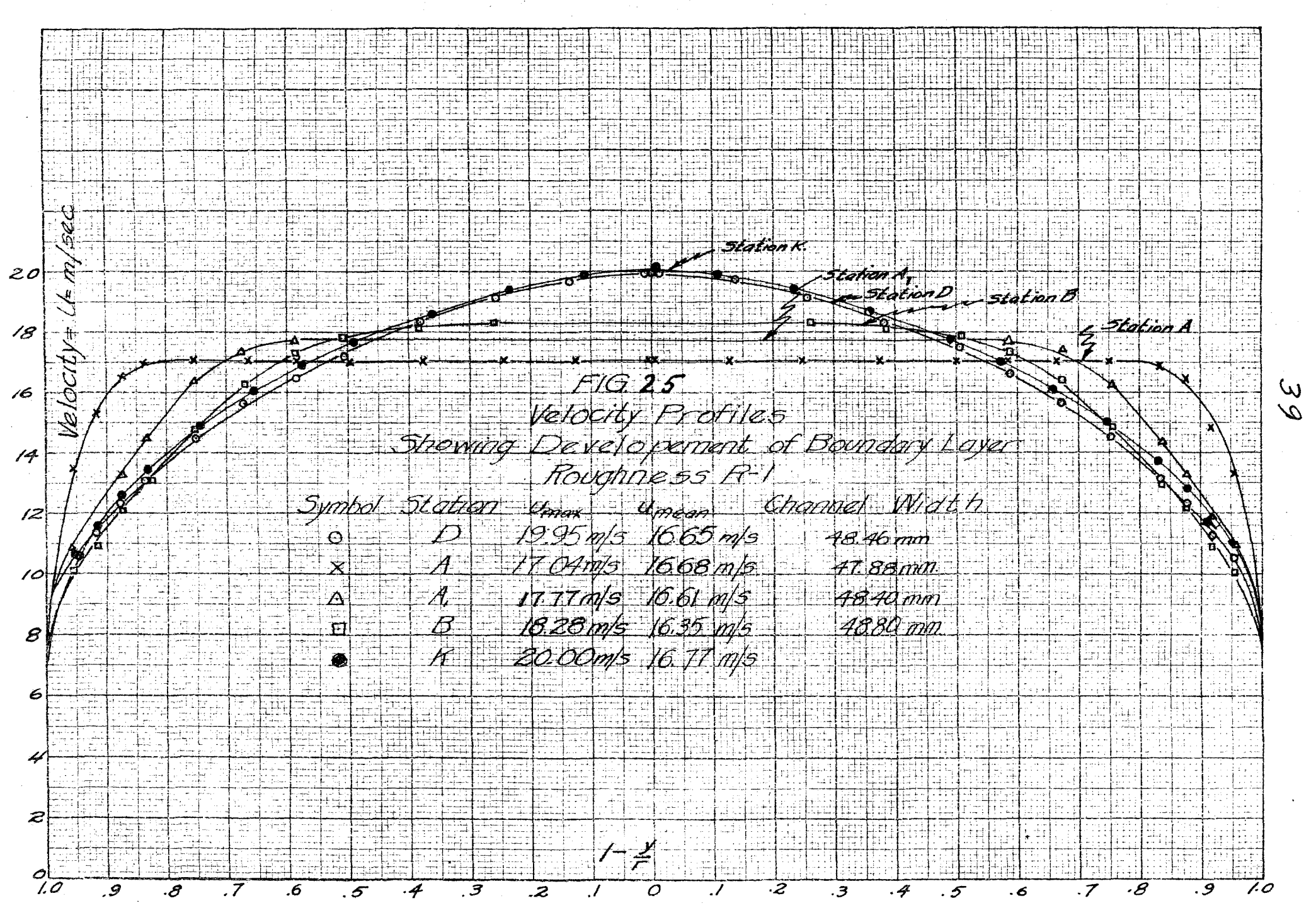

FIG. 25

Velocity Profiles

Showing Development of Boundary Layer

Roughness R-1

Symbol	Station	U_{max}	U_{mean}	Channel Width
○	D	19.95 m/s	16.65 m/s	48.46 mm
×	A	17.04 m/s	16.68 m/s	47.88 mm
△	A_1	17.77 m/s	16.61 m/s	48.40 mm
□	B	18.28 m/s	16.35 m/s	48.80 mm
●	K	20.00 m/s	16.77 m/s	

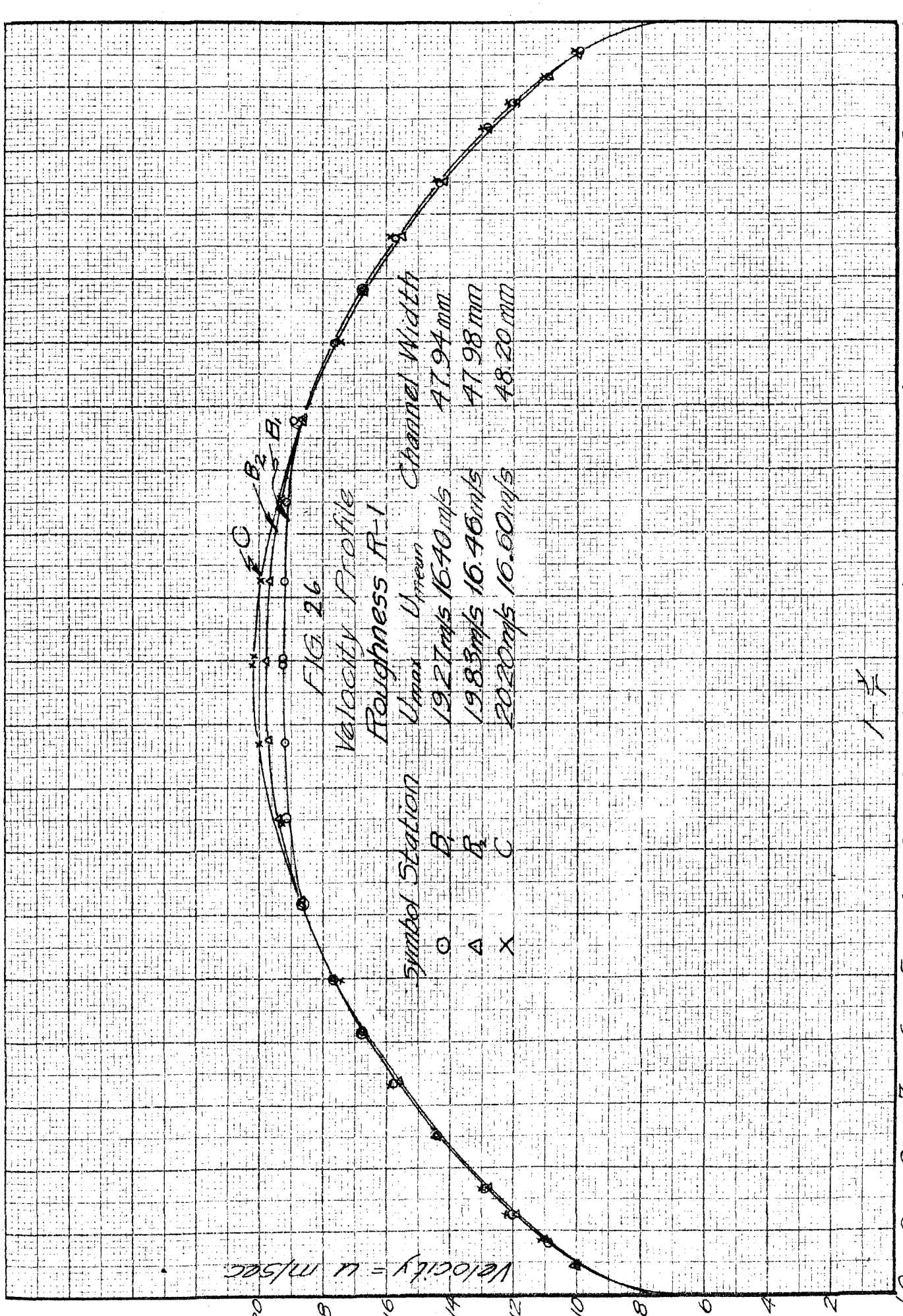

FIG 26

Velocity Profile

Roughness R-1

Symbol	Station	U_{max}	U_{mean}	Channel Width
○	B_1	19.27m/s	16.40 m/s	47.94 mm
△	B_2	19.83m/s	16.46 m/s	47.98 mm
X	C	20.20m/s	16.60 m/s	48.20 mm

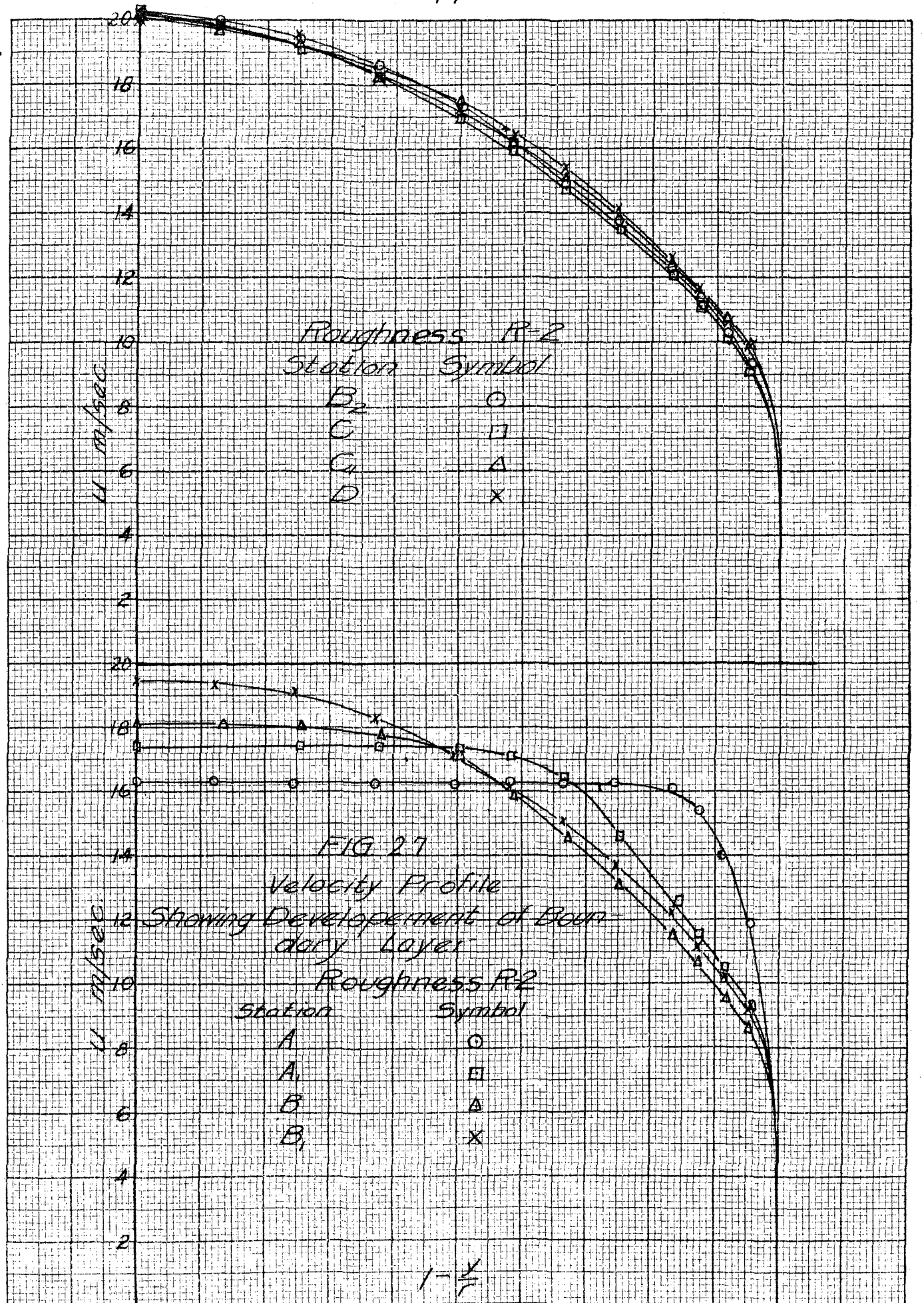

FIG 27
Velocity Profile
Showing Development of Boundary Layer

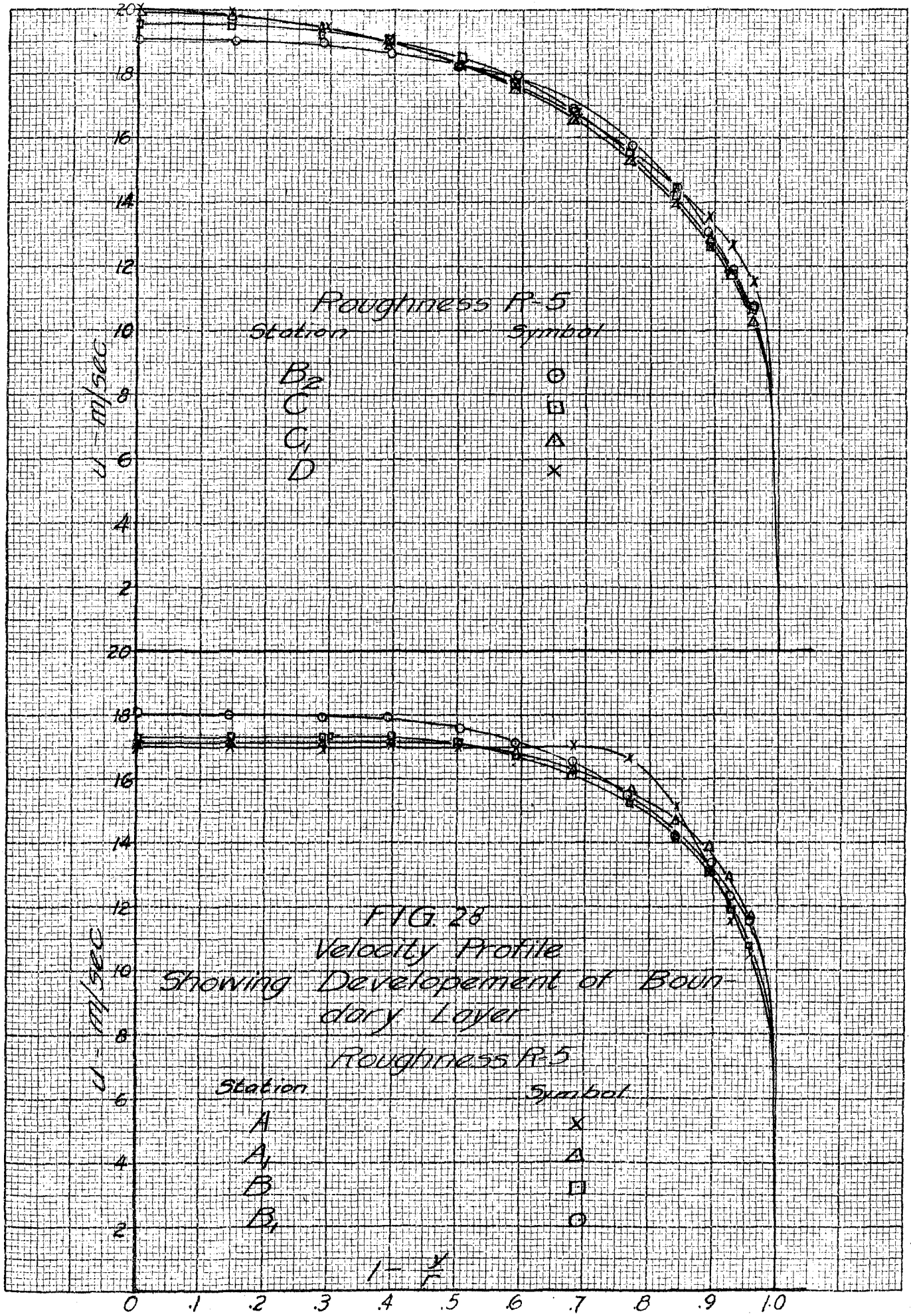

FIG. 28
Velocity Profile
Showing Development of Boundary Layer

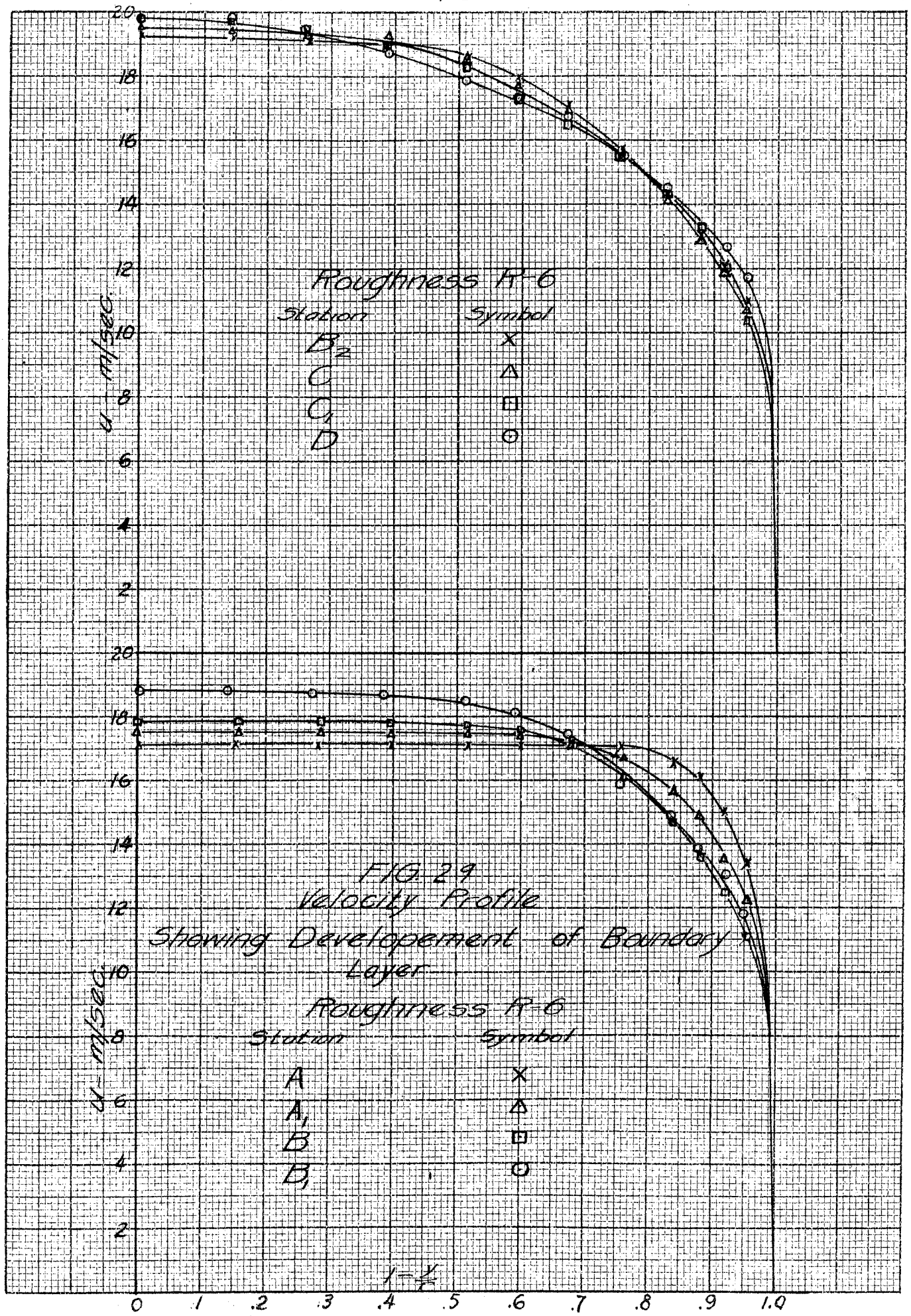

FIG. 29
Velocity Profile
Showing Development of Boundary Layer

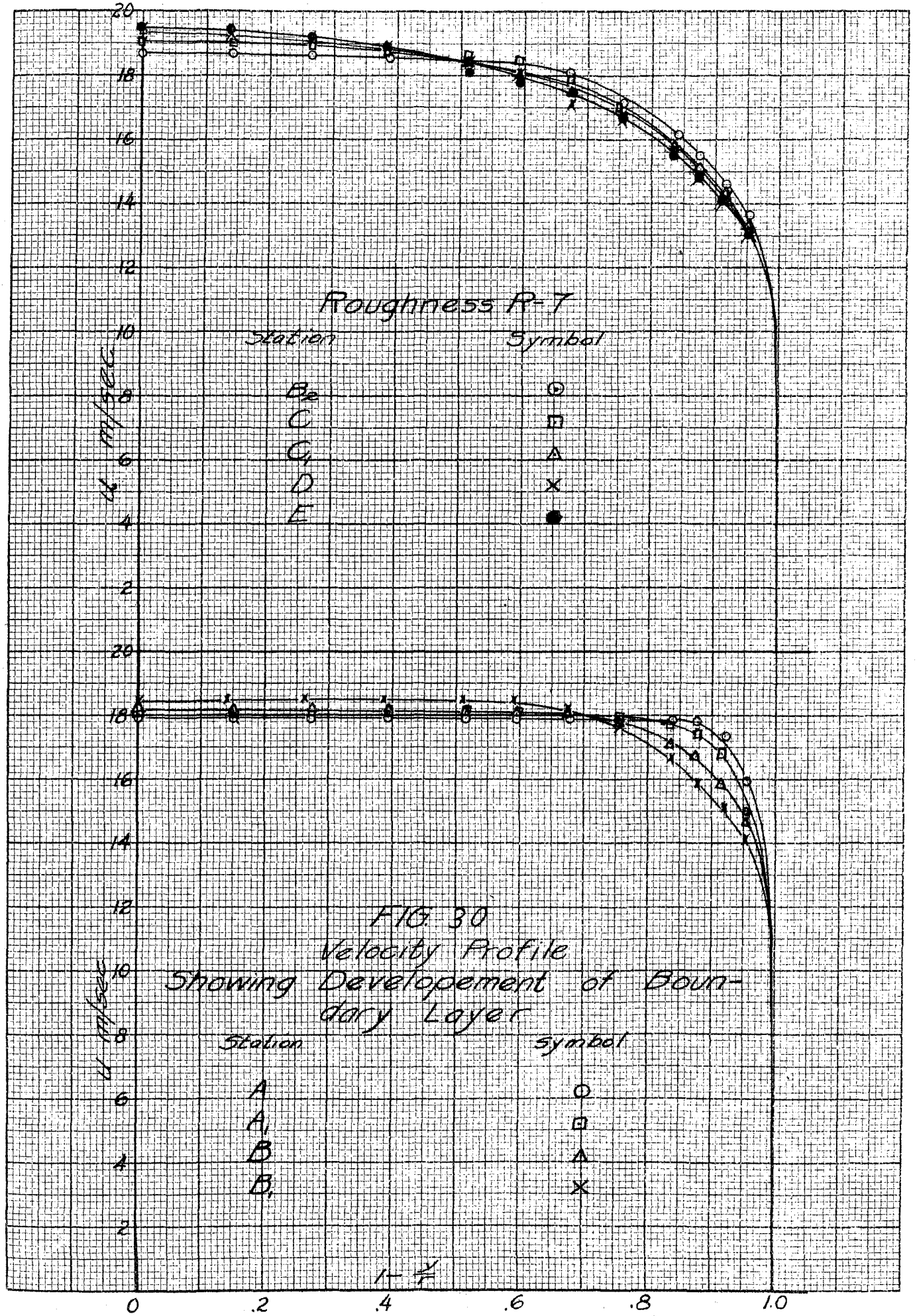

FIG 30
Velocity Profile
Showing Developement of Boundary Layer

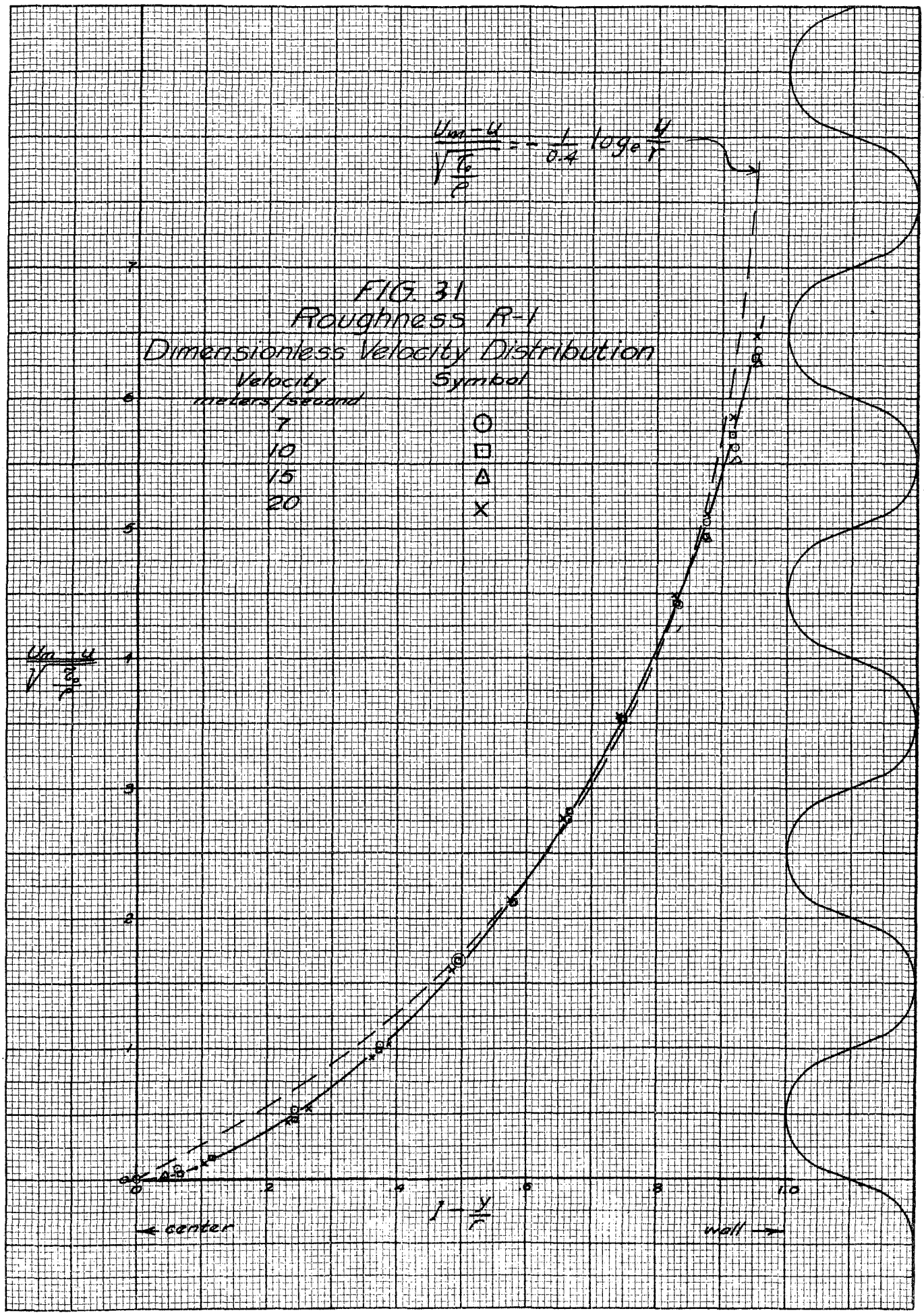
$\frac{U_m - u}{\sqrt{\frac{\tau_0}{\rho}}} = -\frac{1}{0.4} \log_e \frac{y}{r}$
FIG. 31
Roughness R-1
Dimensionless Velocity Distribution
Velocity meters/second
Symbol
7
10
15
20
$\frac{U_m - u}{\sqrt{\frac{\tau_0}{\rho}}}$
$\frac{y}{r}$
center
wall

$$\frac{U_m - u}{\sqrt{\frac{\tau_0}{\rho}}} = -\frac{1}{0.4} \log_e \frac{y}{r}$$

FIG. 32

Roughness R-2

Dimensionless Velocity Distribution

Velocity meters/second	Symbol
7	○
10	□
15	△
20	×

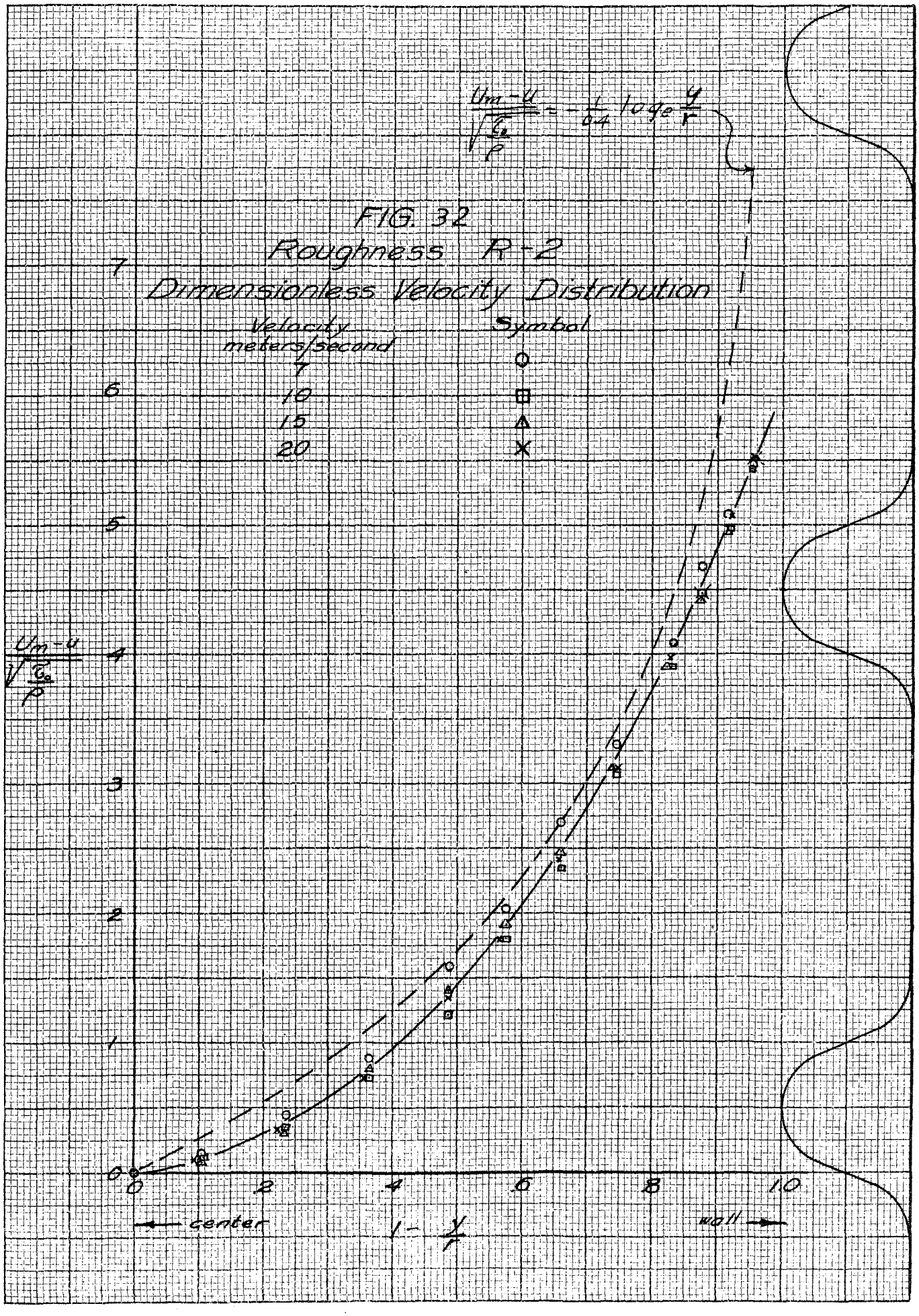

$$\frac{U_m - u}{\sqrt{\frac{\tau_0}{\rho}}} = -\frac{1}{0.40} \log_e \left(\frac{y}{r}\right)$$

FIG 33
Roughness R – 5
Dimensionless Velocity Distribution

Velocity meters/second	Symbol
7	○
10	□
15	△
20	×

$\frac{U_m - u}{\sqrt{\frac{\tau_0}{\rho}}}$

0 1 2 3 4 5 6 7

0 2 4 6 8 10

← center

$1 - \frac{y}{r}$

wall →

$$\frac{U_m - u}{\sqrt{\frac{\tau_0}{\rho}}} = -\frac{1}{0.40} \log_e \frac{y}{r}$$

FIG. 34

Roughness R-6

Dimensionless Velocity Distribution

Velocity meters/second	Symbol
7	○
10	□
15	△
20	×

$\frac{U_m - u}{\sqrt{\frac{\tau_0}{\rho}}}$

0 1 2 3 4 5 6 7

0 .2 .4 .6 .8 1.0

← center $1 - \frac{y}{r}$ wall →

$$\frac{U_m - u}{\sqrt{\frac{\tau_0}{\rho}}} = -\frac{1}{0.40} \log_e \frac{y}{r}$$

FIG 35
Roughness R-7 (Smooth)
Dimensionless Velocity Distribution

Velocity meters/second	Symbol
7	○
10	□
13	△
20	×

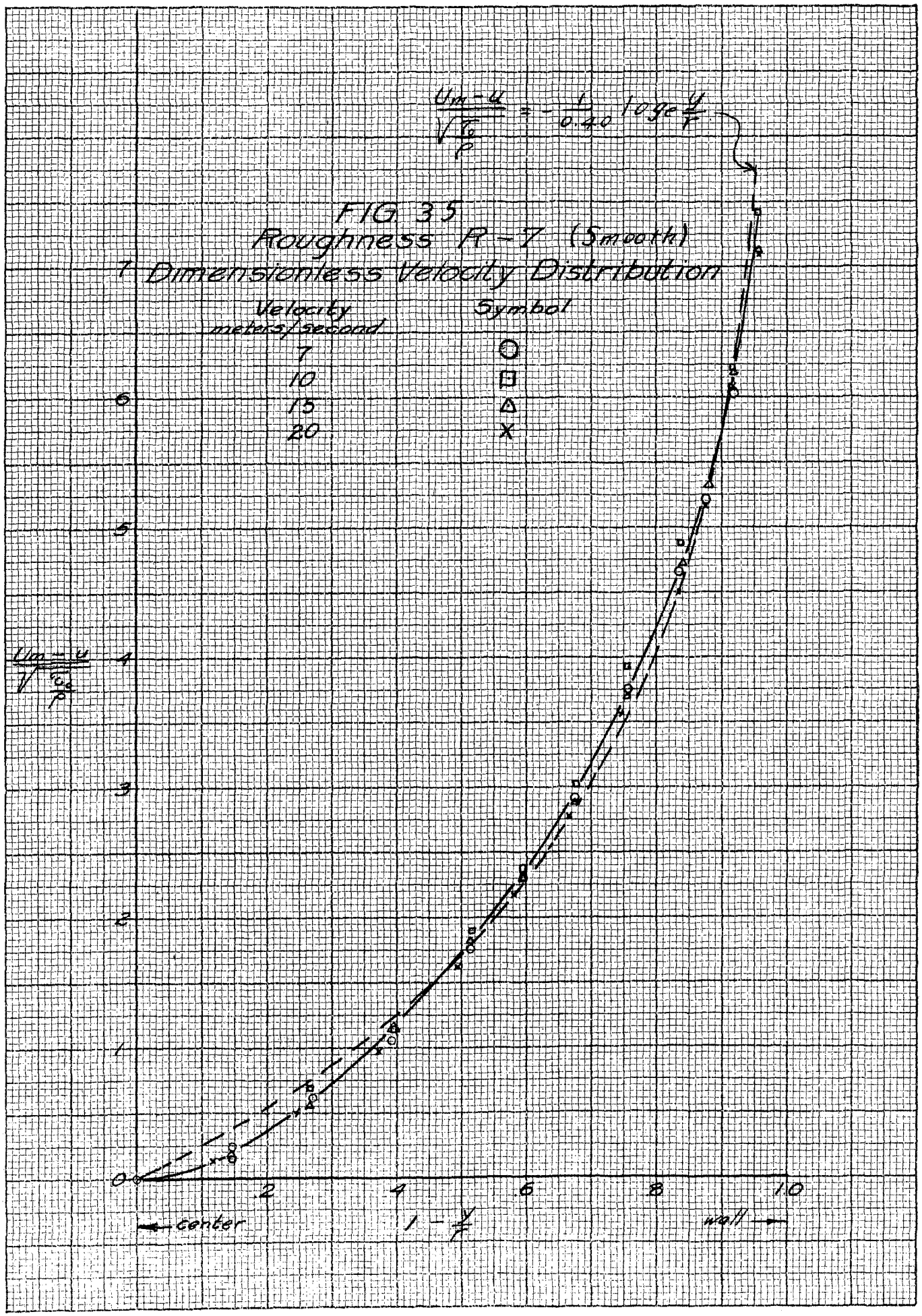

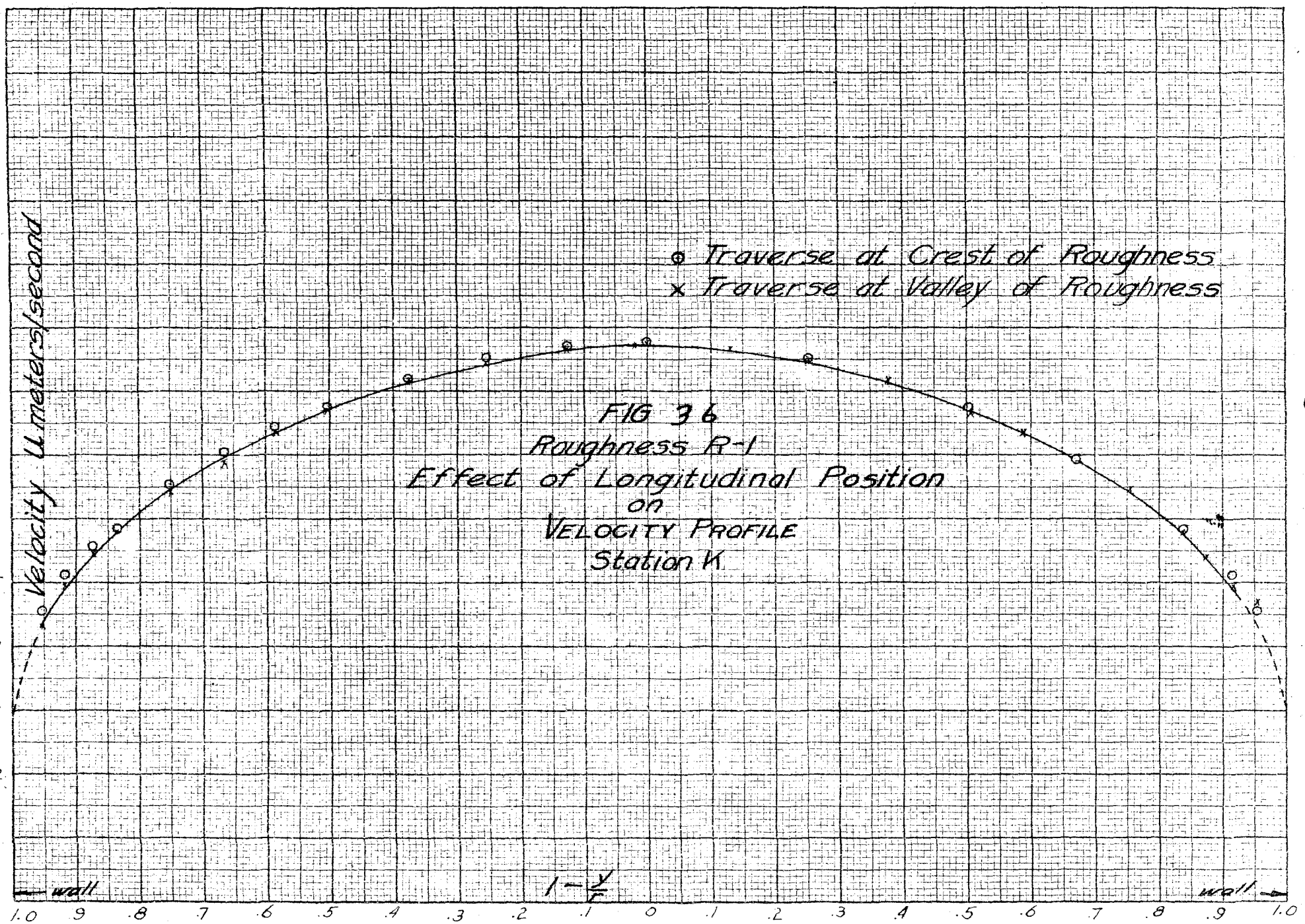

FIG 36
Roughness R-1
Effect of Longitudinal Position
on
VELOCITY PROFILE
Station K

FIG 37
Roughness R-2
Effect of Longitudinal Position
on
Velocity Profile

× Traverse at Crest
□ Traverse 4 mm Behind Crest
△ Traverse 8.7 mm Behind Crest

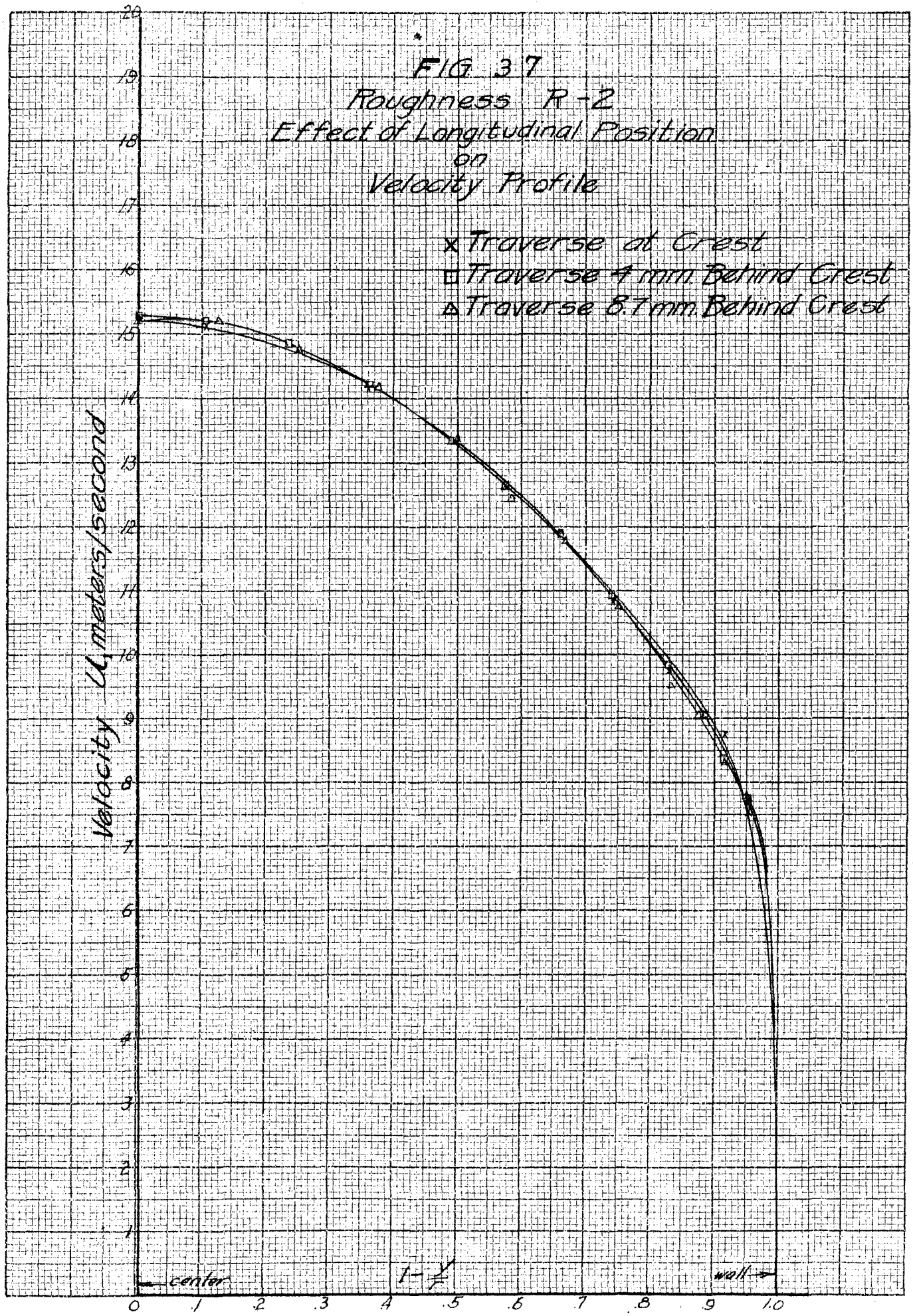

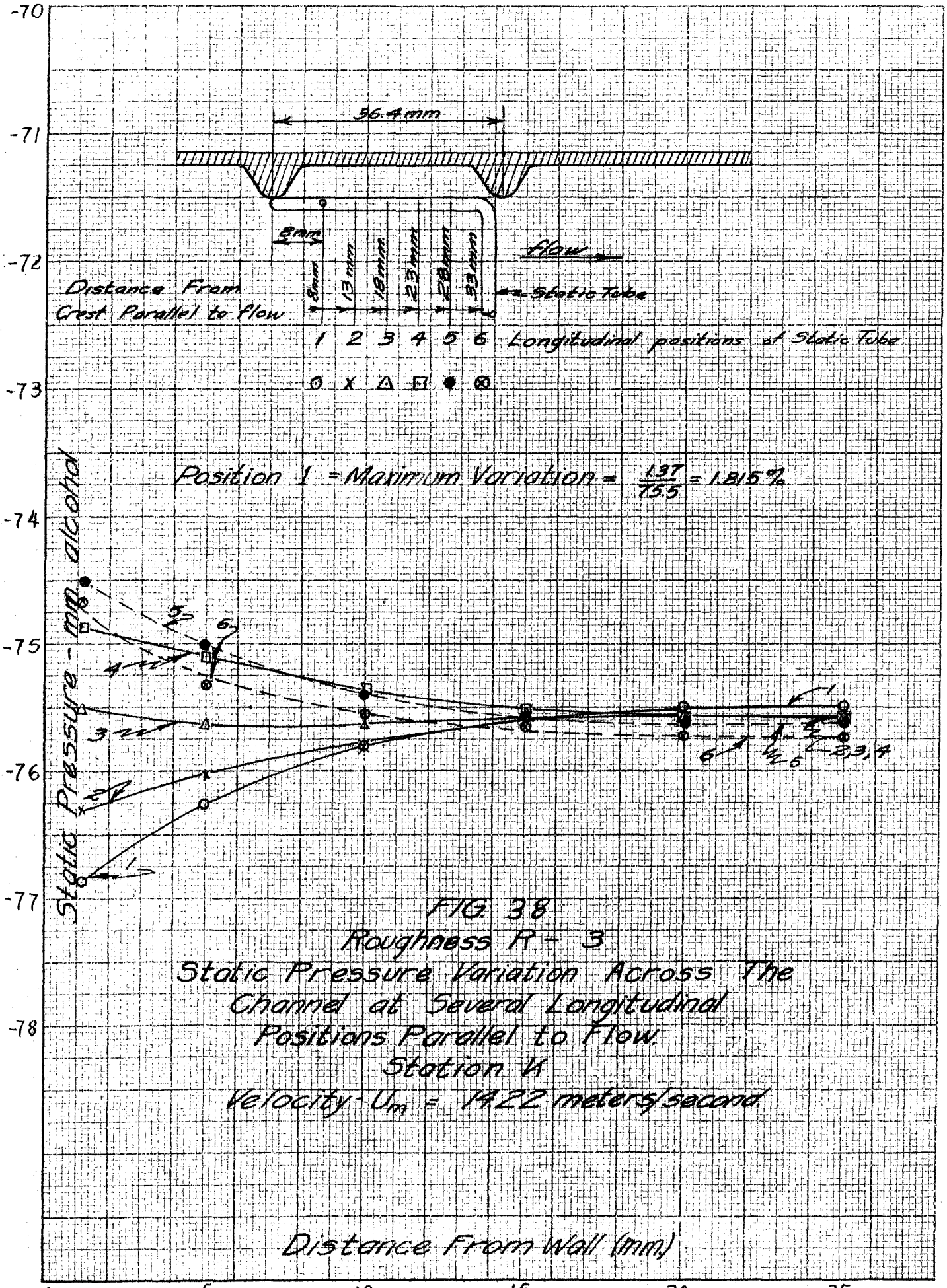

FIG 38

Roughness R - 3

Static Pressure Variation Across The Channel at Several Longitudinal Positions Parallel to Flow.

Station H

Velocity - U_m = 14.22 meters/second

TABLE I

Static Pressure * Measurements at Various Stations
U_m = Maximum velocity at center of channel, meters per sec.

U_m m/sec	Static Pressure at Various Stations (mm of water) A	B	B_2	C	C_1	D	E	F	G
				Roughness R-1					
6.84		2.45		3.16		3.78	4.20		
9.75		4.96		6.31		7.84	8.53		
11.82		7.39		9.34		11.12	12.71		
14.58		10.97		13.86		16.52	18.90		
16.70	12.00	14.28	16.57	17.92		21.20	24.95	28.61	32.81
17.97	13.91	16.61	19.20	20.78		24.63	28.98	33.23	38.13
19.13	15.85	18.84	21.82	23.60		27.98	32.90	37.87	43.60
20.20	17.74	21.10	24.45	26.30		31.23	36.90	42.40	48.70
21.23	19.58	23.34	27.00	29.20		34.54	40.80	46.89	53.70

*Note:- All pressures are measured below atmosphere and are therefore negative.
Air density, ρ, = 0.1200 $(Kg\text{-}sec^2)/m^4$
Kinematic viscosity, ν, = 0.154 cm^2/sec.

Roughness R-2

5.62	1.25	1.72	2.20	2.40	2.63	3.05	3.77	4.47	5.20
9.87	3.95	5.29	6.62	7.27	7.95	9.20	11.31	13.34	15.52
14.00	7.96	10.40	13.03	14.34	15.85	18.21	22.28	26.50	30.80
17.77	13.11	17.03	21.27	23.40	25.75	29.72	36.50	43.45	50.23
19.37	15.58	20.20	25.32	27.83	30.57	35.40	43.50	51.80	59.80

Air density = 0.1190 $Kg\text{-}sec^2/m^4$
Kinematic viscosity = 0.156 cm^2/sec.

TABLE I (continued)

Static Pressure Measurements at Various Stations

U_m m/sec	Static Pressure at Various Stations (mm of water) C_1	D	E	F	G
			Roughness R-3		
5.03	2.41	2.86	3.57	4.26	5.00
7.11	4.80	5.66	7.06	8.53	10.04
8.70	7.23	8.54	10.68	12.74	15.00
10.58	11.27	12.70	15.90	19.13	22.40
12.18	14.21	16.78	21.10	25.37	29.83
13.97	18.71	22.25	27.95	33.72	39.57
15.55	23.25	27.70	34.75	42.03	49.30
16.90	27.79	33.00	41.44	50.20	58.90

Air density = 0.1190 Kg-sec^2/m^4
Kinematic viscosity = 0.155 cm^2/sec.

			Roughness R-4		
5.45	2.45	2.92	3.66	4.35	4.99
7.68	4.91	5.86	7.28	8.67	9.97
9.34	7.43	8.69	10.81	12.94	14.93
11.40	11.12	12.96	16.15	19.33	22.28
13.31	14.70	17.23	21.48	25.62	29.60
15.00	19.44	22.74	28.49	34.10	39.35
16.70	24.15	28.32	35.35	42.30	48.90
18.19	28.83	33.80	42.25	50.70	58.50

Air density = 0.1188 Kg-sec^2/m^4.
Kinematic viscosity = 0.156 cm^2/sec.

TABLE I (continued)

Static Pressure Measurements at Various Stations

U_m m/sec	Static Pressure at Various Stations (mm of water) A	B	B_2	C	C_1	D	E	F	G
				Roughness R-5					
7.74	2.75	2.90	3.21	3.43	3.55	3.85	4.32	4.83	5.16
10.93	5.48	5.84	6.53		7.13	7.71	8.69	9.65	10.34
13.48	8.20	8.82	9.85	10.26	10.68	11.56	13.02	14.47	15.58
16.42	12.22	13.17	14.65		15.99	17.27	19.46	21.63	23.18
18.97	16.18	17.55	19.54	20.40	21.31	22.95	25.85	28.69	30.85
21.90	21.70	23.37	25.93	27.06	28.23	30.42	34.28	38.14	40.90
24.41	27.05	29.06	32.35		35.04	37.90	42.70	47.50	50.85
26.70	32.34	34.80	38.60	40.30	42.00	45.25	51.00	56.75	60.75

Air density = 0.1175 Kg-sec^2/m^4.
Kinematic viscosity = 0.159 cm^2/sec.

Roughness R-6

7.87	2.65	2.91	3.29	3.38	3.62	3.95	4.63	5.25	5.64
11.20	5.12	5.69	6.50		7.34	8.02	9.20	10.44	11.29
13.70	7.68	8.58	9.75	10.25	11.04	12.03	13.87	15.64	16.98
16.80	11.55	12.90	14.62		16.52	18.04	20.71	23.48	25.42
19.41	15.35	17.14	19.52	20.60	22.08	24.10	27.52	31.20	33.80
22.40	20.46	22.78	25.90	27.26	29.27	32.05	36.55	41.32	44.90
24.99	25.30	28.39	32.20		36.67	39.90	45.55	51.55	55.90
27.20	30.27	33.90	38.40	40.45	43.65	47.60	54.40	61.65	66.85

Air density = 0.1157 Kg-sec^2/m^4.
Kinematic viscosity = 0.164 cm^2/sec.

TABLE I (continued)

Static Pressure Measurement at Various Stations

U_m	Static Pressure at Various Stations (mm of water)								
m/sec	A	B	B_2	C	C_1	D	E	F	G
	Roughness R-7 (Smooth Walls)								
9.05	3.96	4.09	4.11	4.33	4.50	4.74	5.19	5.56	6.12
13.00	8.06	8.23	8.56		9.22	9.75	10.57	11.35	12.40
16.03	12.15	12.39	13.12	13.60	13.98	14.81	16.04	17.07	18.67
19.88	18.58	18.70	20.00		21.20	22.35	24.14	25.88	28.05
22.84	25.03	25.27	26.84	27.55	28.41	29.94	32.30	34.40	37.50
26.40	32.50	33.90	36.00	36.84	37.95	40.10	43.10	45.80	49.90
29.44	41.60	42.55	45.10		47.44	49.97	53.80	57.30	62.20
32.10	49.80	51.10	54.00	55.40	56.90	59.80	64.40	68.50	74.40

Air density = 0.1175 Kg-sec^2/m^4.
Kinematic viscosity = 0.159 cm^2/sec.

TABLE II

Equivalent Sand grain Roughness

Type of Roughness	100 f	d	k_s cm
R-5	3.85	3.65	0.111
R-6	4.13	3.58	0.120
R-1	5.66	2.87	0.272
R-2	9.68	1.90	0.831

TABLE III

Friction Coefficient

U_m m/sec	$\bar{U}$ m/sec	dp/dx kg/m^3	τ_o/ρ (m/sec)^2	v_* m/sec	v_*/U_m x10^2	f_mx10^2	R_mx10^{-3}	fx10^2	Rx10^{-3}
				Roughness R-1					
6.84	5.75	1.20	0.247	0.497	7.26	3.99	40.8	5.64	34.3
9.75	8.20	2.40	0.484	0.695	7.13	3.92	58.2	5.54	49.0
11.82	9.95	3.55	0.731	0.854	7.22	3.95	70.7	5.58	59.5
14.58	12.26	5.40	1.112	1.055	7.23	3.95	87.2	5.58	73.4
16.70	14.05	7.35	1.477	1.225	7.33	4.00	98.2	5.66	82.6
17.97	15.12	8.50	1.708	1.306	7.27	4.00	105.5	5.66	88.7
19.13	16.08	9.75	1.958	1.400	7.32	4.04	112.5	5.71	94.6
20.20	17.00	10.05	2.220	1.490	7.37	4.10	118.8	5.80	99.8
21.23	17,86	12.15	2.440	1.562	7.35	4.09	125.0	5.78	105.0

ρ = 0.1193 kg-sec^2/m^4 ν = 0.155 cm^2/sec
$\bar{U}/U_m$ = 0.841

				Roughness R-2					
5.62	4.64	1.372	0.277	0.526	9.36	6.71	32.7	9.82	27.0
8.04	6.64	2.760	0.556	0.745	9.28	6.50	46.7	9.51	38.6
9.87	8.15	4.210	0.849	0.921	9.33	6.57	56.9	9.62	47.0
12.10	9.99	6.28	1.266	1.125	9.30	6.55	70.4	9.58	58.2
14.00	11.56	8.40	1.693	1.301	9.30	6.53	81.5	9.55	67.3
16.06	13.27	11.16	2.253	1.490	9.28	6.59	93.5	9.64	77.3
17.77	14.68	13.75	2.772	1.665	9.36	6.63	103.5	9.70	85.5
19.37	16.00	16.30	3.287	1.812	9.35	6.62	112.8	9.68	93.2

ρ = 0.1190 kg-sec^2/m^4 ν = 0.156 cm^2/sec
$\bar{U}/U_m$ = 0.826 b = 4.8 cm m = 2.27 cm

TABLE III (continued)

Friction Coefficient

U_m m/sec	dp/dx kg/m^3	τ_o/ρ (m/sec)^2	V_* m/sec	V_*/U_m x10^2	f_mx10^2	R_mx10^{-3}
			Roughness R-3			
5.03	1.37	0.277	0.528	10.50	8.27	29.5
7.11	2.94	0.593	0.769	10.81	8.87	41.6
8.70	4.42	0.891	0.943	10.83	8.91	51.0
10.58	6.69	1.350	1.162	10.98	9.15	62.0
12.18	8.86	1.788	1.337	10.98	9.11	71.3
13.97	11.53	2.325	1.525	10.92	9.03	81.8
15.55	14.50	2.921	1.708	10.98	9.16	91.1
16.90	17.30	3.490	1.867	11.05	9.21	99.1

ρ = 0.1190 kg-sec^2/m^4 ν = 0.155 cm^2/sec
b = 4.8 cm m = 2.27 cm

			Roughness R-4			
5.45	1.400	0.283	0.532	9.75	7.24	31.8
7.68	2.875	0.580	0.761	9.90	7.48	44.7
9.34	4.225	0.853	0.923	9.88	7.42	54.3
11.40	6.350	1.284	1.134	9.95	7.50	66.4
13.31	8.450	1.707	1.305	9.91	7.63	77.4
15.00	11.35	2.290	1.513	10.08	7.70	87.2
16.70	14.00	2.825	1.680	10.06	7.71	97.1
18.19	16.90	3.415	1.847	10.15	7.86	105.7

ρ = 0.1188 kg-sec^2/m^4 ν = 0.156 cm^2/sec
b = 4.8 cm m = 2.27 cm

TABLE III (continued)

Friction Coefficient

U_m m/sec	$\bar{u}$ m/sec	dp/dx kg/m^3	τ_o/ρ (m/sec)^2	v_* m/sec	v_*/U_m x10^2	f_mx10^2	R_mx10^{-3}	fx10^2	Rx10^{-3}
				Roughness R-5					
7.74	6.70	0.95	0.229	0.479	6.19	2.87	51.8	3.83	44.8
10.93	9.45	1.85	0.445	0.666	6.09	2.79	73.1	3.72	63.2
13.48	11.66	2.90	0.699	0.835	6.19	2.90	90.0	3.87	77.9
16.42	14.20	4.35	1.050	1.025	6.24	2.92	110.0	3.89	95.1
18.97	16.40	5.78	1.368	1.170	6.17	2.86	126.7	3.81	109.6
21.90	18.94	7.65	1.847	1.359	6.20	2.88	148.0	3.84	128.0
24.41	21.11	9.60	2.317	1.521	6.23	2.91	163.0	3.88	141.0
26.70	23.10	11.45	2.760	1.661	6.22	2.91	178.6	3.88	154.5

ρ = 0.1175 kg-sec^2/m^4 ν = 0.159 cm^2/sec
b = 5.67 cm $\bar{u}/U_m$ = 0.865 m = 2.66 cm

Roughness R-6

7.87	6.97	1.20	0.254	0.504	6.40	3.09	45.0	4.18	38.7
11.20	9.63	2.40	0.507	0.712	6.36	3.09	63.2	4.18	54.3
13.70	11.78	3.60	0.763	0.873	6.37	3.09	76.1	4.18	65.2
16.80	14.45	5.30	1.121	1.058	6.30	3.03	94.9	4.09	81.6
19.41	16.69	7.10	1.500	1.225	6.31	3.00	110.0	4.06	94.6
22.40	19.26	9.25	1.957	1.398	6.25	2.98	127.0	4.03	109.2
24.99	21.49	11.55	2.463	1.570	6.28	2.99	141.5	4.04	121.6
27.20	23.39	13.90	2.935	1.713	6.30	3.01	158.1	4.07	136.0

ρ = 0.1157 kg-sec^2/m^4 ν = 0.164 cm^2/sec
b = 4.9 cm $\bar{u}/U_m$ = 0.860 m = 2.32 cm

TABLE III (continued)

Friction Coefficient

U_m m/sec	$\bar{u}$ m/sec	dp/dx kg/m^3	τ_o/ρ (m/sec)^2	v_* m/sec	v_*/U_m x10^2	f_mx10^2	R_mx10^{-3}	fx10^2	Rx10^{-3}
			Smooth Walls R-7						
9.05	8.11	0.925	0.193	0.439	4.85	1.781	52.7	2.22	47.2
13.00	11.65	1.750	0.365	0.604	4.65	1.628	75.8	2.03	67.9
16.03	14.36	2.585	0.539	0.734	4.58	1.585	93.5	1.97	83.8
19.88	17.81	3.70	0.772	0.878	4.42	1.502	115.7	1.87	103.7
22.84	20.46	4.88	1.017	1.008	4.42	1.472	133.2	1.83	119.3
26.40	23.65	6.35	1.325	1.152	4.36	1.435	154.0	1.79	138.0
29.44	26.34	7.80	1.625	1.274	4.33	1.413	172.0	1.76	157.7
32.10	28.76	9.20	1.902	1.379	4.30	1.390	187.0	1.73	167.5

ρ = 0.1175 kg-sec^2/m^4 $\quad \nu$ = 0.159 cm^2/sec

$\bar{u}/U_m$ = 0.896 $\quad$ b = 4.9 cm $\quad$ m = 2.32 cm

U_m = Maximum velocity at center of the channel

$\bar{u}$ = mean velocity, $\frac{dp}{dx}$ = pressure drop, $\tau_o = \frac{dp}{dx}\frac{b}{2}$ = shearing stress at the wall, b = width of channel, $v_* = \sqrt{\tau_o/\rho}$ = friction velocity

ρ = mass density of air, $R = \frac{4\bar{u}m}{\nu}$ = Reynolds number based on the mean velocity, $m = \frac{\text{cross-sectional area}}{\text{perimeter}}$ = hydraulic radius,

ν = kinematic viscosity, $f = \frac{4m}{q}\frac{dp}{dx}$ = friction coefficient based on the mean velocity, $q = \frac{1}{2}\rho\bar{u}^2$. The subscript (m) for R, f, and q, refers to the values based on the maximum velocity in the center of the channel.

TABLE IV

Velocity Distribution Measurements
Station K
Roughness R-1

1-y/r	u m/sec	u/U_m	N*	1-y/r	u m/sec	u/U_m	N*
	$v_* = 0.569$				$v_* = 0.716$		
0.952	4.32	0.544	6.36	0.952	5.47	0.547	6.33
0.916	4.73	0.596	5.64	0.916	5.91	0.591	5.71
0.874	5.06	0.637	5.06	0.874	6.46	0.646	4.94
0.832	5.42	0.683	4.42	0.832	6.83	0.683	4.43
0.749	5.94	0.748	3.51	0.748	7.49	0.749	3.51
0.665	6.37	0.803	2.76	0.664	7.97	0.797	2.84
0.582	6.68	0.842	2.21	0.580	8.40	0.840	2.23
0.498	6.98	0.880	1.68	0.496	8.79	0.879	1.69
0.373	7.36	0.927	1.02	0.370	9.28	0.928	1.00
0.247	7.64	0.963	0.53	0.244	9.67	0.967	0.46
0.121	7.85	0.988	0.16	0.160	9.88	0.988	0.17
0.038	7.90	0.990	0.07	0.034	9.96	0.996	0.05
0.004	7.94	1.000	0	0	10.00	1.00	0
	$v_* = 1.071$				$v_* = 1.422$		
0.952	8.24	0.551	6.27	0.950	10.79	0.540	6.47
0.916	9.03	0.603	5.53	0.914	11.65	0.583	5.87
0.873	9.70	0.648	4.91	0.873	12.71	0.636	5.12
0.831	10.38	0.693	4.28	0.829	13.61	0.681	4.49
0.747	11.38	0.760	3.35	0.744	14.94	0.747	3.56
0.662	12.12	0.810	2.66	0.659	16.06	0.803	2.77
0.578	12.70	0.849	2.11	0.574	16.95	0.843	2.14
0.494	13.30	0.888	1.56	0.489	17.73	0.887	1.60
0.367	14.00	0.936	0.90	0.361	18.66	0.933	0.94
0.241	14.53	0.972	0.41	0.233	19.38	0.969	0.44
0.114	14.83	0.990	0.13	0.105	19.84	0.992	0.11
0	14.97	1.00	0	0	20.00	1.00	0

*$N = (U_m - u)/v_*$

TABLE IV (continued)

Velocity Distribution Measurements
Station K
Roughness R-2

1-y/r	u m/sec	u/U_m	N*
	v_* = 0.662		
0.952	3.62	0.500	5.48
0.916	3.88	0.535	5.09
0.874	4.15	0.573	4.68
0.832	4.54	0.626	4.09
0.748	5.06	0.700	3.31
0.664	5.46	0.755	2.70
0.580	5.89	0.814	2.05
0.496	6.20	0.856	1.59
0.370	6.66	0.920	0.89
0.244	6.96	0.962	0.44
0.118	7.15	0.987	0.15
0.013	7.25	1.00	0
	v_* = 1.370		
0.951	7.45	0.495	5.53
0.915	8.21	0.545	4.98
0.872	8.96	0.595	4.43
0.830	9.68	0.644	3.90
0.745	10.74	0.714	3.13
0.660	11.64	0.775	2.47
0.574	12.42	0.825	1.91
0.489	13.10	0.870	1.41
0.382	13.92	0.925	0.81
0.234	14.55	0.966	0.35
0.106	14.94	0.995	0.07
0	15.03	1.000	0

1-y/r	u m/sec	u/U_m	N*
	v_* = 0.942		
0.952	4.86	0.488	5.48
0.916	5.32	0.534	4.99
0.873	5.80	0.582	4.48
0.831	6.34	0.636	3.91
0.747	7.11	0.714	3.09
0.662	7.71	0.774	2.35
0.578	8.21	0.825	1.82
0.494	8.65	0.869	1.45
0.367	9.22	0.925	0.74
0.241	9.69	0.972	0.35
0.114	9.90	0.995	0.13
0.021	10.02	1.00	0
	v_* = 1.806		
0.950	10.02	0.502	5.53
0.914	10.82	0.542	5.09
0.870	11.94	0.597	4.46
0.828	12.82	0.642	3.98
0.742	14.36	0.718	3.12
0.656	15.61	0.781	2.43
0.568	16.69	0.834	1.83
0.482	17.50	0.874	1.38
0.354	18.66	0.933	0.74
0.224	19.47	0.973	0.30
0.094	19.79	0.988	0.12
0.013	20.00	1.00	0

*$N = (U_m - u)/v_*$

TABLE IV (continued)

Velocity Distribution Measurements
Station K
Roughness R-5

1-y/r	u m/sec	u/U_m	N*
	$v_* = 0.439$		
0.958	4.27	0.603	6.40
0.929	4.55	0.643	5.76
0.895	4.78	0.675	5.24
0.841	5.22	0.737	4.24
0.771	5.53	0.781	3.53
0.682	5.89	0.832	2.71
0.593	6.14	0.867	2.14
0.505	6.37	0.900	1.62
0.399	6.53	0.922	1.25
0.293	6.76	0.955	0.73
0.152	6.93	0.979	0.34
0	7.08	1.00	0
	$v_* = 0.930$		
0.958	8.82	0.585	6.83
0.928	9.33	0.619	6.17
0.893	10.05	0.667	5.40
0.842	10.86	0.721	4.53
0.768	11.67	0.774	3.65
0.631	12.42	0.824	2.85
0.591	13.02	0.864	2.20
0.502	13.49	0.895	1.70
0.395	13.98	0.928	1.17
0.288	14.39	0.955	0.73
0.146	14.85	0.985	0.24
0	15.07	1.00	0

1-y/r	u m/sec	u/U_m	N*
	$v_* = 0.620$		
0.958	5.81	0.580	6.79
0.929	6.33	0.632	5.95
0.895	6.76	0.675	5.26
0.841	7.29	0.728	4.40
0.771	7.78	0.776	3.61
0.682	8.13	0.811	3.05
0.593	8.63	0.861	2.24
0.505	8.98	0.896	1.68
0.399	9.28	0.926	1.19
0.293	9.63	0.961	0.63
0.152	9.90	0.988	0.19
0	10.02	1.00	0
	$v_* = 1.235$		
0.958	11.53	0.573	6.97
0.928	12.48	0.622	6.15
0.893	13.44	0.669	5.38
0.842	14.54	0.724	4.48
0.768	15.67	0.779	3.57
0.631	16.61	0.827	2.81
0.591	17.41	0.867	2.16
0.502	18.00	0.896	1.69
0.395	18.68	0.930	1.13
0.288	19.20	0.956	0.71
0.146	19.81	0.987	0.22
0	20.08	1.00	0

*$N = (U_m - u)/v_*$

TABLE IV (continued)

Velocity Distribution Measurements
Station K
Roughness R-6

1-y/r	u m/sec	u/U_m	N*
	$v_* = 0.447$		
0.954	4.25	0.609	5.88
0.920	4.57	0.655	5.19
0.880	4.84	0.693	4.61
0.839	5.06	0.725	4.14
0.759	5.48	0.785	3.23
0.679	5.80	0.831	2.54
0.598	6.06	0.868	1.98
0.518	6.30	0.903	1.47
0.398	6.48	0.928	1.08
0.277	6.67	0.956	0.67
0.157	6.85	0.981	0.28
0	6.98	1.00	0
	$v_* = 0.949$		
0.953	8.73	0.575	6.52
0.918	9.38	0.628	5.83
0.878	10.10	0.671	5.07
0.838	10.67	0.714	4.47
0.756	11.68	0.773	3.40
0.675	12.31	0.826	2.74
0.594	12.87	0.863	2.15
0.512	13.30	0.892	1.70
0.391	13.91	0.933	1.05
0.268	14.40	0.965	0.54
0.147	14.72	0.987	0.20
0	14.91	1.00	0

1-y/r	u m/sec	u/U_m	N*
	$v_* = 0.649$		
0.954	5.78	0.583	6.38
0.920	6.13	0.618	5.84
0.880	6.74	0.679	4.90
0.839	7.17	0.723	4.24
0.759	7.66	0.772	3.48
0.679	8.17	0.824	2.70
0.598	8.58	0.865	2.06
0.518	8.86	0.893	1.63
0.398	9.23	0.930	1.06
0.277	9.60	0.968	0.49
0.157	9.82	0.990	0.15
0	9.92	1.00	0
	$v_* = 1.254$		
0.953	11.62	0.585	6.62
0.918	12.50	0.629	5.81
0.878	13.46	0.677	5.14
0.837	14.31	0.720	4.46
0.755	15.67	0.789	3.37
0.673	16.48	0.826	2.72
0.592	17.18	0.865	2.16
0.510	17.81	0.896	1.65
0.388	18.58	0.935	1.03
0.265	19.19	0.966	0.55
0.143	19.62	0.987	0.20
0	19.87	1.00	0

*$N = (U_m - u)/v_*$

TABLE IV (continued)

Velocity Distribution Measurements
Station K
Smooth Walls R-7

1-y/r	u m/sec	u/U_m	N*
	$v_* = 0.335$		
0.954	4.84	0.669	7.16
0.919	5.22	0.721	6.03
0.879	5.49	0.758	5.22
0.838	5.68	0.785	4.66
0.757	5.98	0.826	3.76
0.676	6.26	0.865	2.93
0.595	6.47	0.894	2.30
0.514	6.65	0.918	1.76
0.393	6.88	0.950	1.07
0.271	7.03	0.971	0.63
0.150	7.16	0.989	0.24
0	7.24	1.00	0
	$v_* = 0.665$		
0.953	10.30	0.684	7.14
0.918	10.93	0.726	6.20
0.878	11.52	0.765	5.31
0.837	11.90	0.791	4.74
0.755	12.60	0.837	3.68
0.673	13.13	0.872	2.89
0.592	13.53	0.899	2.29
0.510	13.83	0.919	1.83
0.388	14.32	0.945	1.10
0.265	14.70	0.977	0.53
0.143	14.93	0.992	0.18
0	15.05	1.00	0

1-y/r	u m/sec	u/U_m	N*
	$v_* = 0.465$		
0.953	6.75	0.662	7.42
0.918	7.30	0.716	6.24
0.878	7.70	0.755	5.38
0.838	7.93	0.777	4.88
0.756	8.37	0.821	3.94
0.675	8.79	0.862	3.03
0.594	9.09	0.891	2.39
0.512	9.31	0.913	1.92
0.391	9.67	0.948	1.14
0.268	9.87	0.968	0.71
0.147	10.13	0.993	0.15
0	10.20	1.00	0
	$v_* = 0.875$		
0.953	13.78	0.669	7.12
0.918	14.70	0.735	6.08
0.876	15.47	0.774	5.18
0.836	16.05	0.803	4.51
0.753	16.90	0.846	3.55
0.671	17.57	0.879	2.78
0.589	18.10	0.905	2.17
0.506	18.55	0.928	1.66
0.382	19.18	0.959	0.94
0.259	19.60	0.980	0.46
0.135	19.90	0.995	0.11
0	20.00	1.00	0

*$N = (U_m - u)/v_*$

TABLE V

Dimensionless Velocity Distribution
Station K

k = 4.35 mm = height of corrugations.

v_* = 0.569 m/sec			v_* = 1.422 m/sec		v_* = 0.622 m/sec			v_* = 1.086 m/sec	
y/k	u m/sec	u/v_*	u m/sec	u/v_*	y/k	u m/sec	u/v_*	u m/sec	u/v_*
	Roughness R-1					Roughness R-2			
0.26	4.32	7.59	10.64	7.48	0.26	3.62	5.47	10.02	5.55
0.46	4.73	8.32	11.57	8.13	0.46	3.88	5.87	10.82	5.99
0.69	6.06	8.88	12.65	8.90	0.69	4.15	6.28	11.94	6.62
0.92	5.42	9.53	13.53	9.52	0.92	4.54	6.76	12.82	7.10
1.38	5.94	10.44	14.85	10.43	1.38	5.06	7.64	14.36	7.95
1.84	6.37	11.20	16.00	11.20	1.84	5.46	8.25	15.61	8.65
2.30	6.68	11.74	16.89	11.90	2.30	5.89	8.90	16.96	9.39
2.76	6.98	12.28	17.67	12.40	2.76	6.20	9.36	17.50	9.69
3.45	7.36	12.94	18.60	13.10	3.45	6.66	10.05	18.66	10.33
4.14	7.64	13.43	19.37	13.63	4.14	6.96	10.51	19.47	10.78
4.83	7.85	13.80	19.82	13.93	4.83	7.15	10.80	19.79	10.95
5.42	7.94	14.00	20.00	14.07	5.38	7.25	10.95	20.00	11.07

	Roughness R-5					Roughness R-6			
v_* = 0.439 m/sec			v_* = 1.235 m/sec		v_* = 0.477 m/sec			v_* = 1.254 m/sec	
0.26	4.27	9.73	11.53	9.33	0.26	4.25	9.50	11.62	9.26
0.46	4.55	10.36	12.48	10.10	0.46	4.57	10.22	12.50	9.97
0.69	4.78	11.12	13.44	10.87	0.69	4.84	10.82	13.46	10.73
1.01	5.22	11.89	14.54	11.78	0.92	5.06	11.32	14.31	11.40
1.49	5.53	12.60	15.67	12.70	1.38	5.48	12.26	15.67	12.50
2.07	5.89	13.42	16.61	13.45	1.84	5.80	12.97	16.48	13.13
2.64	6.14	13.98	17.41	14.10	2.30	6.06	13.56	17.18	13.69
3.22	6.37	14.50	18.00	14.57	2.76	6.30	14.10	17.81	14.20
3.91	6.53	14.87	18.68	15.13	3.45	6.48	14.50	18.58	14.80
4.60	6.76	15.40	19.20	15.55	4.14	6.67	14.82	19.19	15.30
5.52	6.93	15.78	19.81	16.04	4.83	6.85	15.32	19.62	15.73
6.51	7.08	16.13	20.08	16.25	5.38	6.98	15.61	19.87	15.84

PART II

Turbulent Velocity Fluctuations

Introduction

Irregular fluctuating motion superimposed on a mean flow is termed turbulent flow. Osborne Reynolds (13), expressed the shearing stresses for a parallel mean flow in the x-direction as

$$\tau_{xy} = -\rho\,\overline{u'v'}, \quad \tau_{xz} = -\rho\,\overline{u'w'}$$

where u', v' and w' are the fluctuations in the velocity in the direction and perpendicular to the mean flow, respectively, and ρ, is the mass density of the fluid. The bar denotes the time average of the product.

In these experiments only the root-mean-square value of the fluctuations have been determined, that is, $(\overline{u'^2})^{\frac{1}{2}}$ with the various types of roughnesses. To avoid so many exponents and subscripts the following notation will be used:

u' = root-mean-square value of the velocity fluctuations in the direction of mean flow.

v' = root-mean-square value of the velocity fluctuations perpendicular to the walls of the channel.

$\tau = -\rho\,u'v'$ = shearing stress in the direction of mean flow.

u = mean velocity of flow at any point in the channel as measured by a pilot tube.

$\frac{u'}{u}$ = per cent turbulence.

The same number and type of rough surfaces were used for the turbulence measurements as for the pressure drop experiments, as shown in Fig. 6.

This investigation was undertaken to show the effect of roughness on the relationship of, $\frac{u'v'}{(u')^2}$, at different positions in an air stream, or to show what correlation existed between the u' and v' fluctuations in turbulent flow caused by different types of rough surfaces. Also to show the magnitude of the fluctuations parallel to the air stream caused by the condition of the wall surface.

Many measurements of the velocity fluctuation in an air stream have been made, including measurements in wind tunnels, pipes, and channels and also in the free atmosphere.

Mention may be made of only a few of the investigators in this field, such as Wattendorf and Kuethe, (7), Dryden and Kuethe (8), Fage (9), and others in the experimental field, and Prandtl (10), Karman (1), G. I. Taylor (2), and Gebelein (11), in the theoretical field.

These measurements have been made in the hope of understanding more about the laws which govern fluid flow in the fully developed turbulent state. The hot wire anemometer has been used extensively for this purpose. King (12) first showed the possibilities of an instrument of this type for measuring the turbulence in an air stream.

The principle of the operation of this instrument is based on the change in resistance of an electrically heated fine platinum wire, due to the cooling effect of the fluctuating air stream. King developed an equation for the heat lost from a hot wire of this type in a steady stream of fluid:

$$i^2R = (K + Cu^{\frac{1}{2}})(T - T_o)$$

where i = current flowing in the wire, R = resistance of the wire, K = a constant allowing for free convection, C = a constant to account for forced convection, T = temperature of the wire, T_o = temperature of the moving fluid. With this equation a means of determining the velocity fluctuations can be developed as shown in reference (7) or (8).

Putting $$T - T_o = \frac{R-R_o}{R_o \alpha}$$

where R = cold resistance of the wire and α = temperature coefficient of resistance of the wire, we have on differentiating, with respect to i, u, and R, and making a few substitutions and transformations,

$$\frac{du}{u} = \frac{2}{c\sqrt{u}} \left[\frac{2i\alpha RR_o}{R-R_o} \times \frac{b}{1-Rb} + \frac{i\alpha R_o^2}{(R-R_o^2)} \times \frac{1}{1-Rb} \right] dE$$

In this equation du is the fluctuating velocity and the term b, includes terms of resistance voltage and the current in the bridge circuit.*

The term dE includes an item known as the time constant,

$$M = \frac{4.2 - s \rho a^2}{r \alpha i^2} \left(\frac{R-R_o}{R_o} \right)$$

where s = specific heat of wire, ρ = the density, r = the resistivity, and a = the area of the wire.

It will be observed that the diameter of the wire enters into the calculations to the fourth power and therefore necessitates very accurate measurement of the diameter in order to insure suitable results. Because of this condition and also the amount of necessary calculations involved in computing the results, F. D. Knoblock developed an instrument for vibrating the hot wire at a known amplitude and fre-

* See Reference (7)

quency, and making a calibration of the wire before it is put into the air stream of unknown turbulence. All of the hot wire measurements in these tests were made by first calibrating the hot wire in the vibrator tunnel, except one or two tests, where the other method was used as a check. The check tests were found satisfactory so the calibration method was used throughout.

Experimental Apparatus

The photographs in Figs. 30 and 40 show the complete apparatus used in the calibration and making the hot wire measurements. Fig. 39 shows the circular wind tunnel about 14" in diameter with the entrance at the extreme right. The vibrator power unit, cathode ray oscilliscope and beat frequency oscillator are shown on the table at the right. The telescope for observing the amplitude of the vibrations is mounted on a frame work around the tunnel entrance just above the instruments mentioned. It is shown clearly at the left in Fig. 40. This figure shows the three wire suspension for the hot wire, which is mounted in the center of the tunnel at the intersection of these three wires. Just below the tunnel entrance is shown the electro magnetic vibrator coil. Referring back to Figure 39 the hot wire set is shown on the high table with the alcohol manometer for speed determination at the left. The speed control unit is seen at the right of the tall table. A more complete description and operation of this apparatus is given in a thesis by Knoblock.

A view of the hot wire and holder is seen in Fig. 41. The spindles marked 1 and 2 are the parts that were mounted on the vibrating wire for calibration. No. 1 was used generally for the traverses

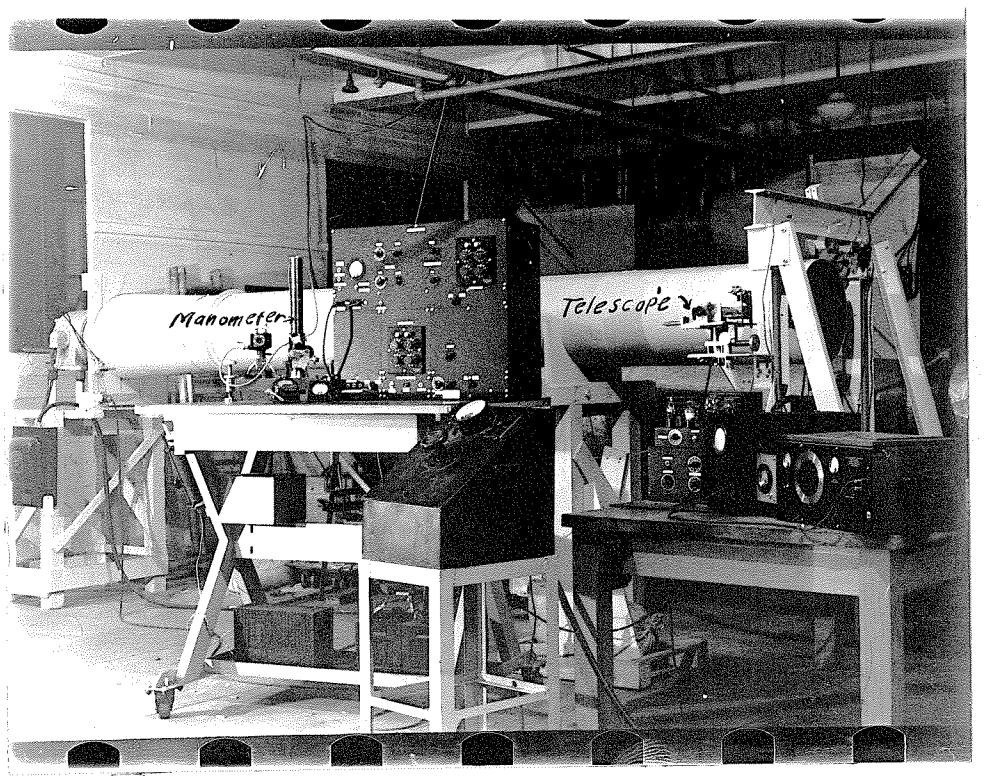

Fig. 39

Vibrator Wind Tunnel
and
Hot Wire Apparatus

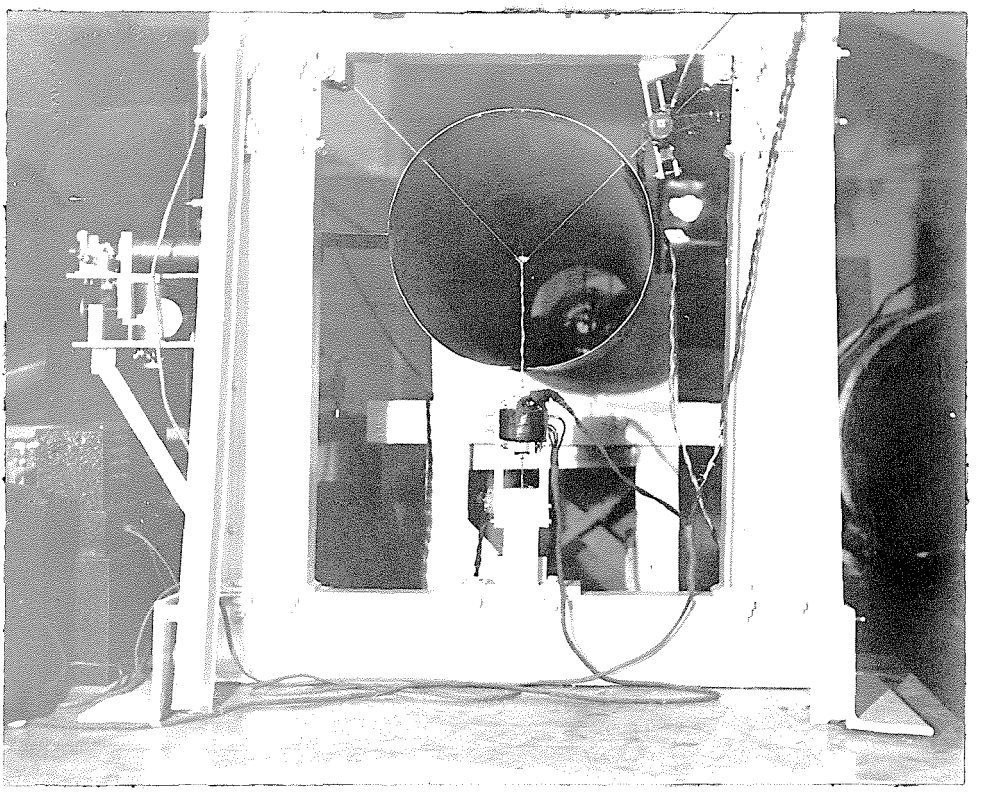

Fig. 40

Vibrator Tunnel Entrance

Showing Vibrator Wire

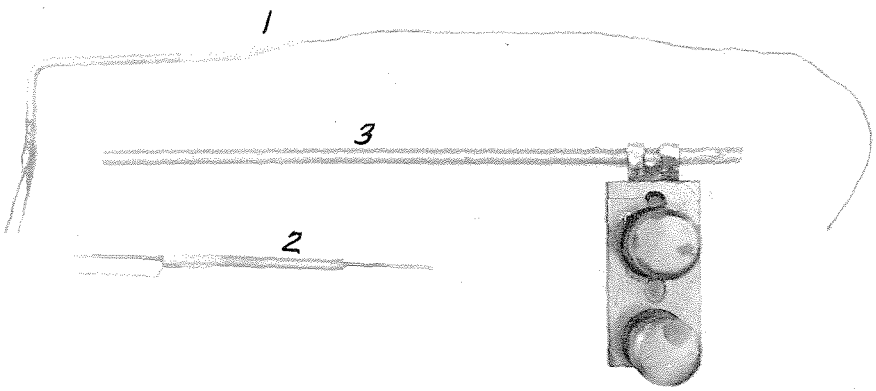

Fig. 41

Hot Wire Holder

across the channel and No. 2 for determining fluctuations very near to the wall. A fine platinum wire about 0.0005 inch in diameter was soldered across to two terminals and then mounted on the vibrator wire for calibration. After the calibration it was placed in the left end on the holder, 3, and then used to make the turbulence surveys in the roughness channel.

Method of Calibration of Hot Wire

Figs. 42 and 43 and Table VI show the readings to be taken, and necessary curves for the hot wire calibration. After the hot wire was placed on vibrator wire, the air speed in the calibrating tunnel was adjusted to some desired value. Then the vibrator was adjusted to give a specified value of amplitude and frequency. Keeping the speed constant, the compensation resistance R_c was changed in increments of 500 ohms recording the reading of the I^2 meter at each change. A curve of I-vs-R_c was then plotted for this frequency and amplitude.

A second series of I^2 readings were taken with a different frequency and amplitude, keeping the product of frequency and amplitude the same as in the first observation. Another curve was then plotted on the first graph for the second conditions. The intersection of the two curves gave the desired compensation resistance. This indicated that the lag of the hot wire was fully compensated between these two frequencies.

In using this method the amplifier must be so designed to be

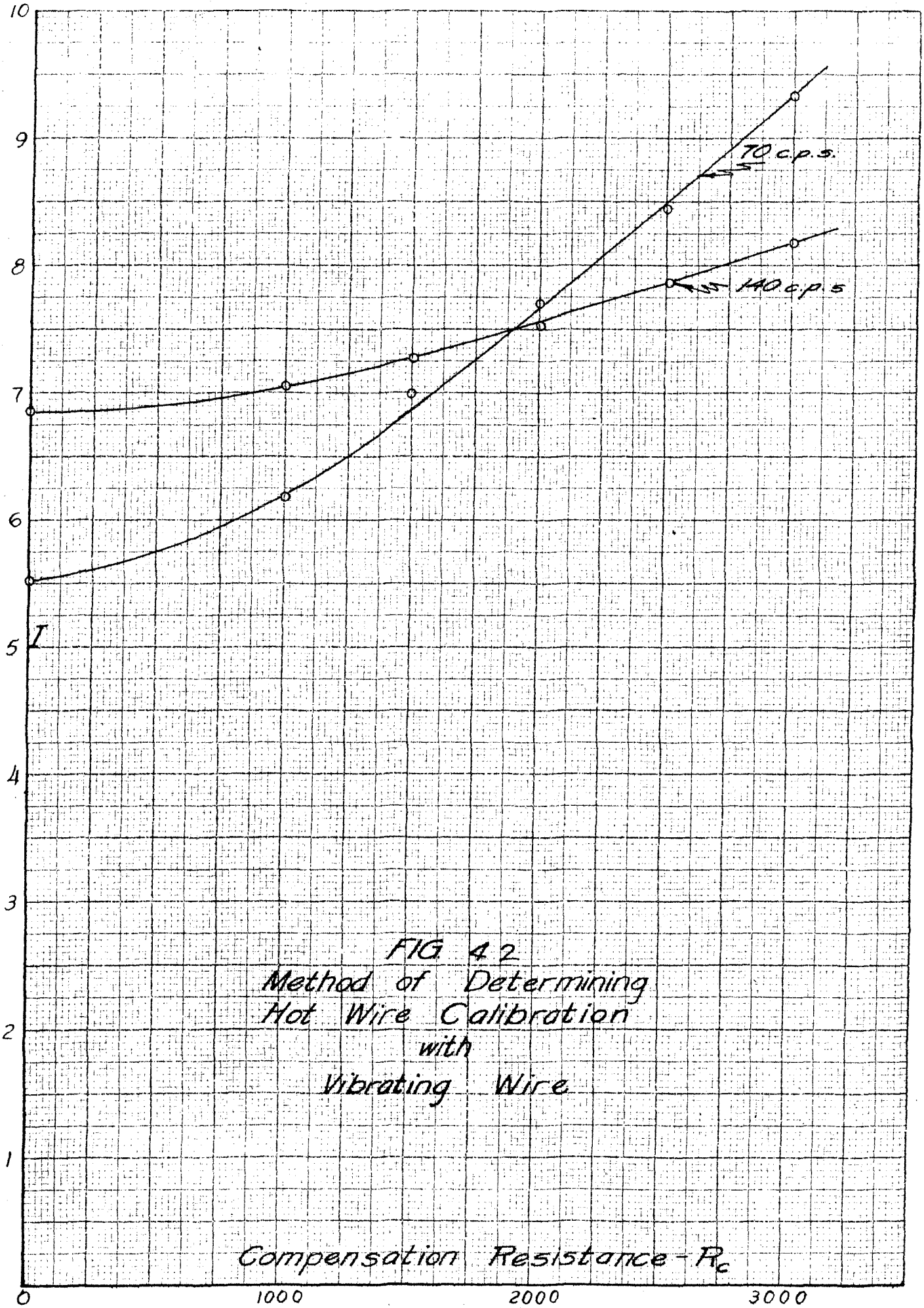

FIG 42
Method of Determining
Hot Wire Calibration
with
Vibrating Wire

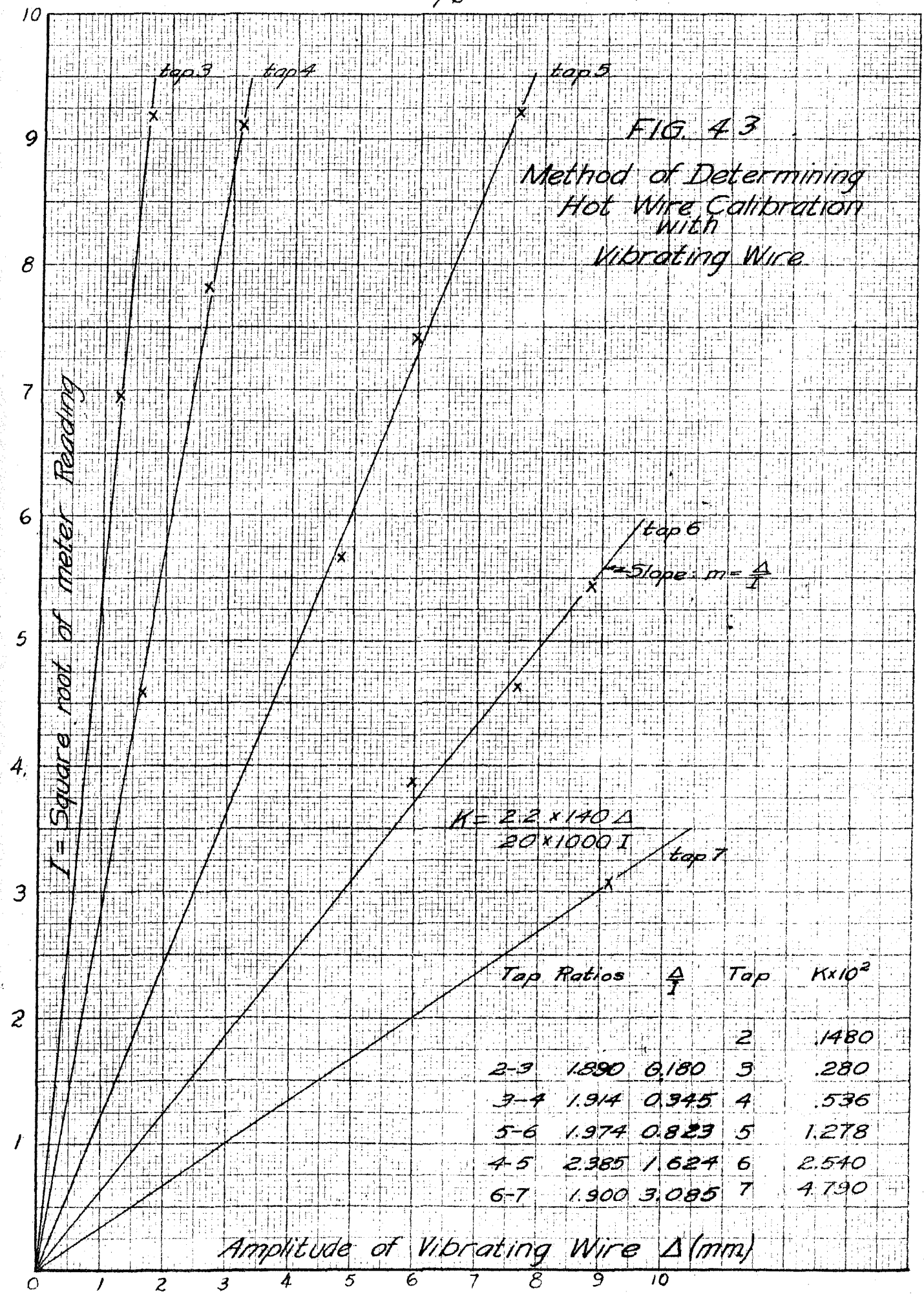

FIG. 43

Method of Determining Hot Wire Calibration with Vibrating Wire

Tap Ratios	$\frac{\Delta}{I}$	Tap	$K \times 10^2$
		2	.1480
2-3	1.890	0.180	3 .280
3-4	1.914	0.345	4 .536
5-6	1.974	0.823	5 1.278
4-5	2.385	1.624	6 2.540
6-7	1.900	3.085	7 4.790

TABLE VI

Determination of Compensation Resistance
Vibrator Tunnel
U_m = 20.00 m/sec

Amplitude of Vibrating Wire, = 12.0 mm
Frequency of " " , f = 70.0 cps

R_c	0	1000	1500	2000	2500	3000
Tap	5	5	5	5	5	5
I^2	30.5	38	49	59	71	87
I	5.52	6.16	7.0	7.68	8.43	9.33

Amplitude, = 6.0 mm
Frequency, f = 140 cps

R_c	0	1000	1500	2000	2500	3000
Tap	5	5	5	5	5	5
I^2	47	49	53	57	62	67
I	6.85	7.0	7.28	7.55	7.87	8.18

Compensation Resistance set at R_c = 1810 ohms
Frequency 140 cps

	Tap	I^2	I		Tap	I^2	I
1.22				1.22	3	48	6.93
1.64	4	21	4.58	1.64	3	84	9.17
2.62	4	61	7.81				
3.10	4	83	9.11				
4.77	5	32	5.66				
6.00	5	55	7.42	6.00	6	15	3.87
7.61	5	85	9.22	7.61	6	21.5	4.63
8.80				8.80	6	29.5	5.43
9.41	7	9.5	3.08	9.41	6	32	5.66

R_c = Compensation resistance
I^2 = meter reading
$I = I^2$
Tap = Proportional to the amplification factor.

compensating over a large range of frequencies and to be "flat" at these low values.

After obtaining the desired R_c, this value was set on the resistance box and a series of runs were made at different amplitudes, Δ, but the same frequency. This run gave a series of points for each setting of the attenuator taps of the desired range of amplification.

The plot of I-vs- Δ gave a straight line for each tap setting. The slope of this line Δ/I was used in computation of the turbulent velocity in the equation,

$$u'/u = \frac{2.22\ fmI}{1000\ u_c} \quad \text{(see appendix B)}$$

where f = the frequency, m is the slope of the lines in Fig. 43, which varies with each tap setting, u_c is the air velocity in the calibrating tunnel, and I is the square root of the I^2 meter reading in the fluctuating air stream.

For any particular calibration this equation may be reduced to $u'/u = KI$ where K has different values for each tap setting. In these tests, Δ = 2 x amplitude of vibration. This simple equation made it very much more convenient to get the final results.

The same micrometer screw and holder was used for the hot wire work as was used in the pressure drop measurements.

The hot wire amplifier, and the vibrator circuits are shown in Figs. 44 and 45 respectively.

A more complete and detailed account of this vibrator and hot wire set will be found in F. D. Knoblock's thesis.

Discussion of Curves and Results

The curves in Fig. 46 show how the turbulence level is increased by the increase in the relative roughness. For roughness R-3 the corrugations were spaced at 36.4 mm, and for this type of roughness the turbulence is quite erratic near the wall, and seems to produce a sine wave parallel with the flow.

The effect of the wide spacing is to produce a more or less restricted channel at the crest of the corrugations and produces an effect similar to a converging channel and thus has a tendency to reduce the turbulence in this region. Roughness R-4 shows this effect to a far greater extent. For this roughness the spacing is 72.8 mm.

In all of this group of curves the greatest effect of the turbulence is near the wall. As the condition of smooth walls is approached the curves flatten out more and have the appearance of an inverted velocity profile.

Fig. 47 illustrates the correlation between the velocity components as computed from the relationship that $\tau = -\rho\, u'v'$. For smooth walls we have constant correlation throughout a wide range of the channel width, and the magnitude is increased as the velocity is increased. Wattendorf's experiments at C. I. T. appear to have been conducted at a velocity near 11 meters per second.

In the upper set of curves for different roughnesses it is shown that for the two roughnesses R-1 and R-2 with the corrugations, that the correlation is not as constant, but the other two types exhibit similar characteristics to that of the smooth wall.

The curves in Fig. 48 to 52 show the effect of longitudinal position on the turbulent values, due to the position of the crest of the corrugations with respect to the hot wire position. For R-1 and R-2 the effect is not noticeable. For these two roughnesses the pressure variation across the channel showed no appreciable change either. R-3 and R-4 show very marked effect of this longitudinal position.

Scale effect is portrayed in Figs. 53 to 56. All of these roughnesses seem to exhibit a tendency for the increase in turbulence with a decrease in velocity. Smooth walls shows the greatest variation in this respect.

The effect of Reynolds Number for smooth walls is shown in Fig. 57, for different positions from the wall. At low velocities the turbulence near the wall increases very rapidly.

The velocity fluctuations in the entrance section are depicted for various roughnesses, in Figs.58 to 61. For the first two or three stations the turbulence is about the same for all roughnesses, and the wall conditions appear to have little effect in the main part of the channel until we reach about 25 cm from the entrance. After this point there is an increase in the turbulence level at the

center of the channel as the roughness of the walls is increased. The development of the boundary layer is very well shown by these curves.

Table VII gives the per cent turbulence at points across the channel for the various types of roughness, and Table VIII shows the correlation between the velocity fluctuations. The values here have been computed from points taken from the faired curves of $\frac{u'}{u}$ and $\frac{u}{U_m}$.

Conclusions

It is observed from these experiments that the roughness of the wall has a material effect on the turbulence in the channel, the turbulence increasing as the roughness is increased.

The effect on the correlation between the fluctuations appears to be dependent on the particular type of rough surface on the walls. R-6 has a larger relative roughness than R-5 but both of these roughnesses are greater than for smooth walls, but the latter shows a higher correlation coefficient. R-5 and R-6 were roughnesses of very small surface projections.

While R-1 and R-2 are very much different types of rough surfaces, R-2 has the larger relative roughness of these two types yet its correlation seems to be the least. There appears to be no definite relationship existing between the relative roughness and the correlation coefficient, except that the same general type of rough surface gives the same general type of curve for the correlation across the channel.

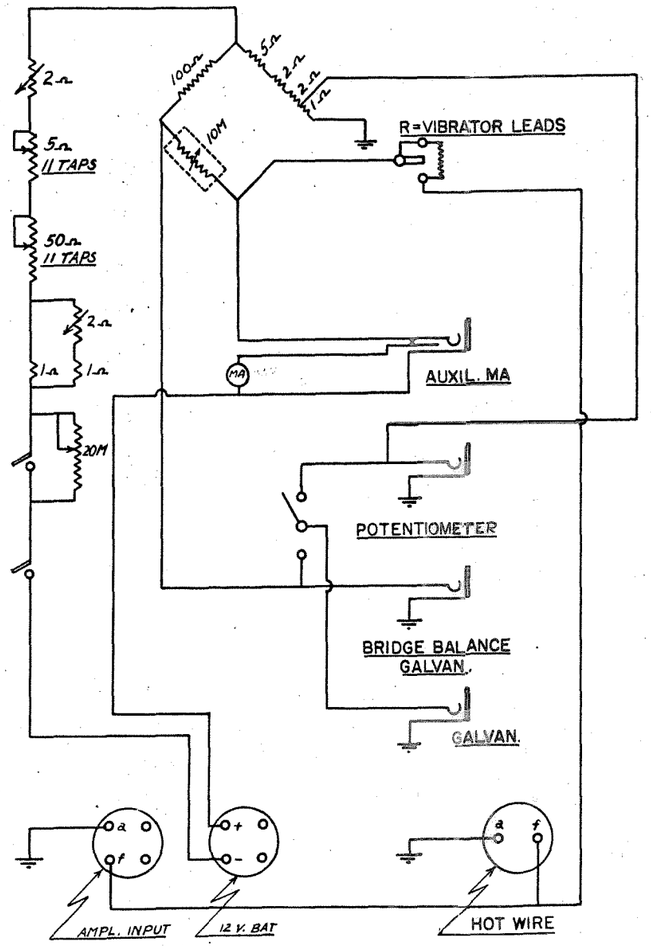

INPUT CIRCUIT

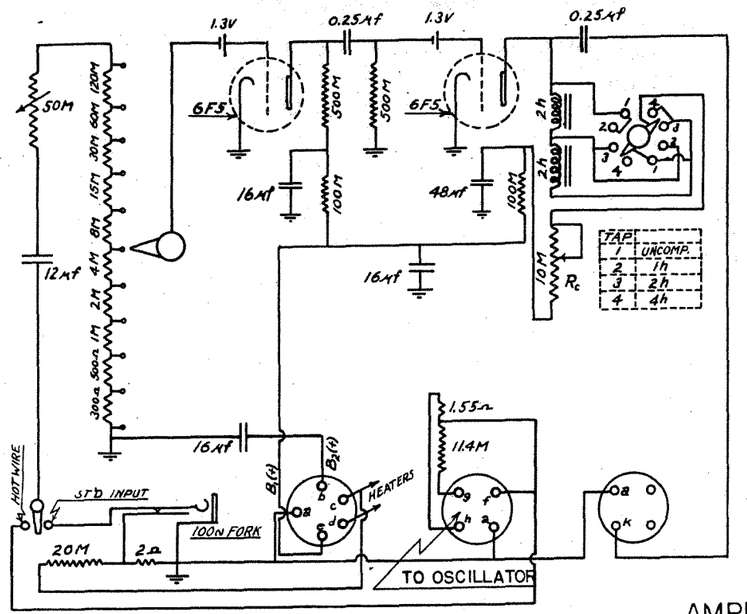

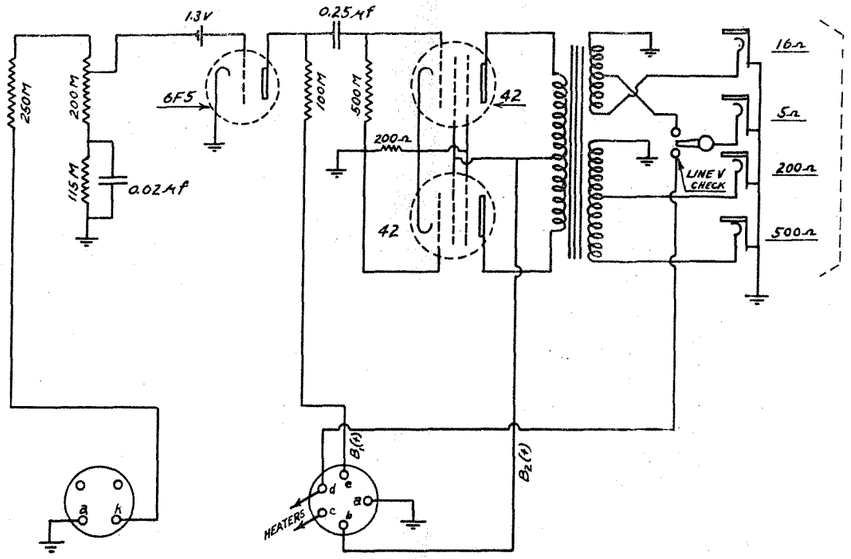

OUTPUT JACKS TO THERMO METER OSCILLOSCOPE

AMPLIFIERS

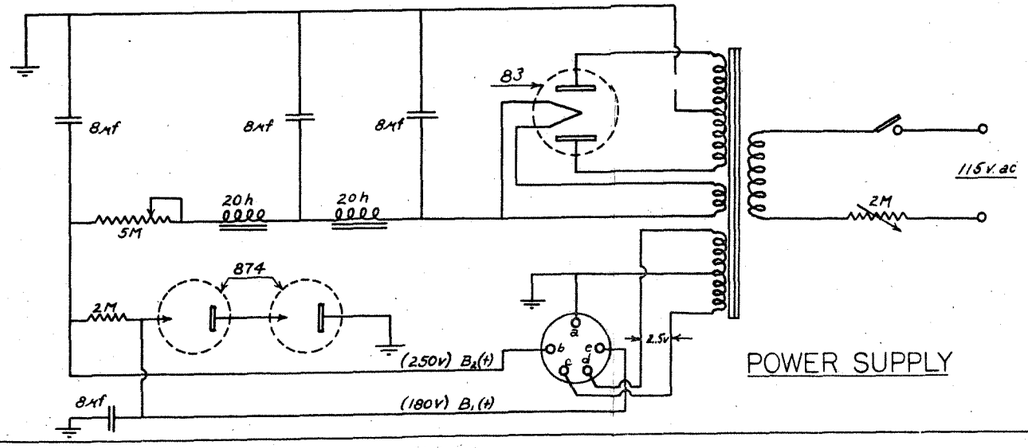

POWER SUPPLY

FIG. 44
HOT-WIRE ANEMOMETER - #1

NOTE: M = 1000Ω

MAY 1938

FIG 45

VIBRATOR CIRCUIT

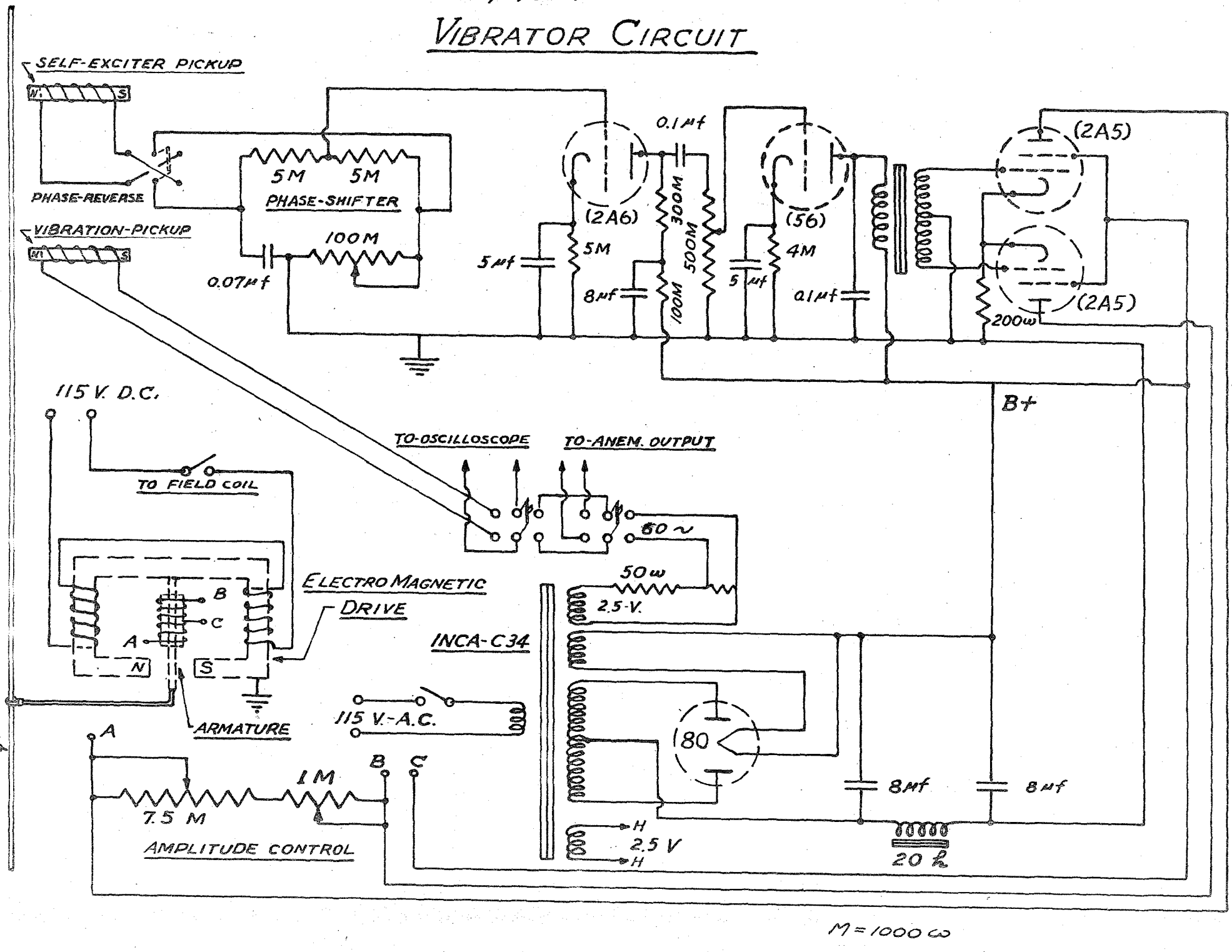

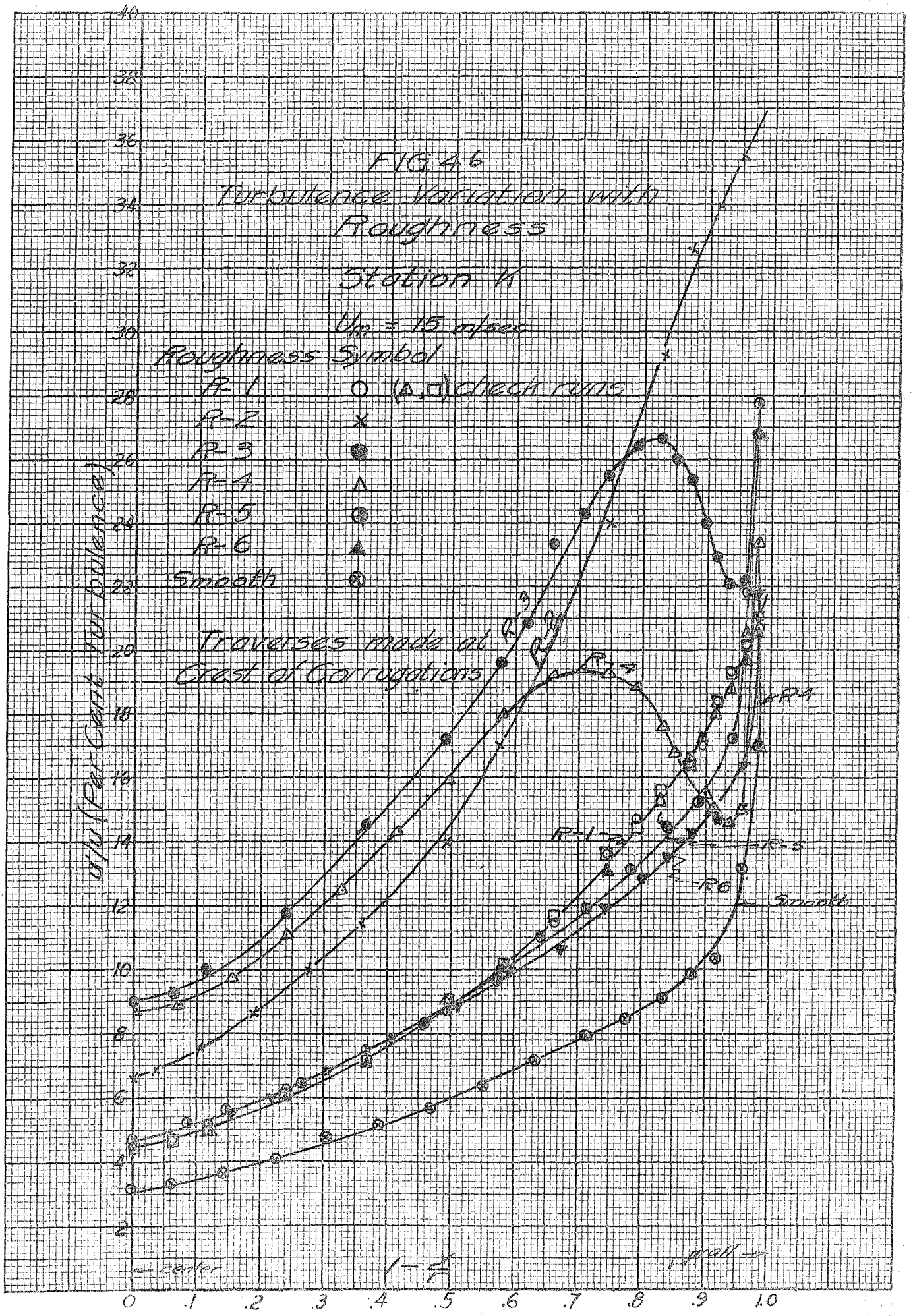
FIG 46
Turbulence Variation with Roughness
Station H
Um = 15 m/sec
Roughness Symbol
R-1 ○ (△,□) check runs
R-2 ×
R-3 ●
R-4 △
R-5 ⊙
R-6 ▲
Smooth ⊗
Traverses made at Crest of Corrugations
w/U (Per Cent Turbulence)
y = Center
y = Wall
R-1
R-4
R-5
R-6
Smooth
0 .1 .2 .3 .4 .5 .6 .7 .8 .9 1.0
2 4 6 8 10 12 14 16 18 20 22 24 26 28 30 32 34 36 38 40

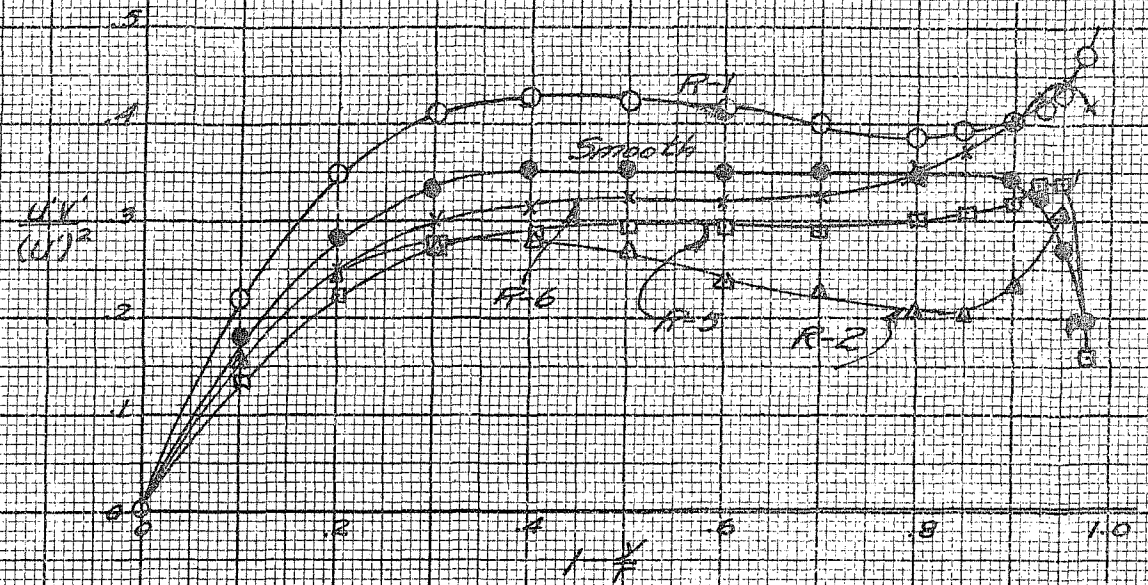

Correlation of Velocity Fluctuations
Various Types of Roughness
U_m = 15 m/sec.

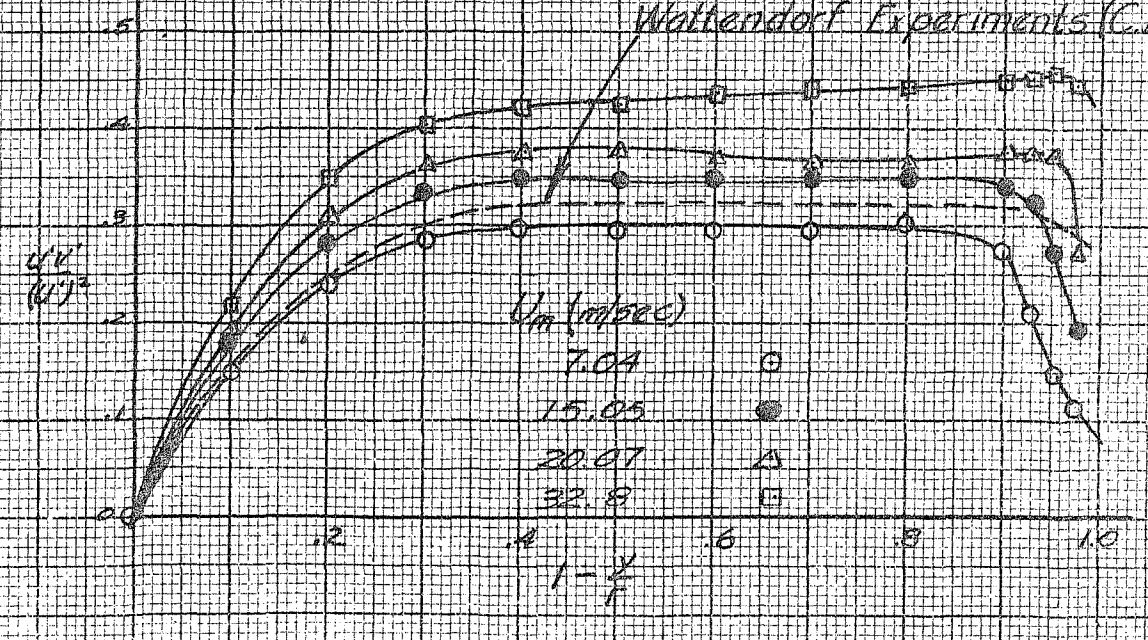

FIG. 47

Correlation of Velocity Fluctuations
Smooth Walls
Various Velocities

FIG. 48
Effect of Longitudinal Position on Turbulence
Station H
Roughness R-1
○ at crest
△ 24 mm. behind Crest
□ 455 mm. behind Crest

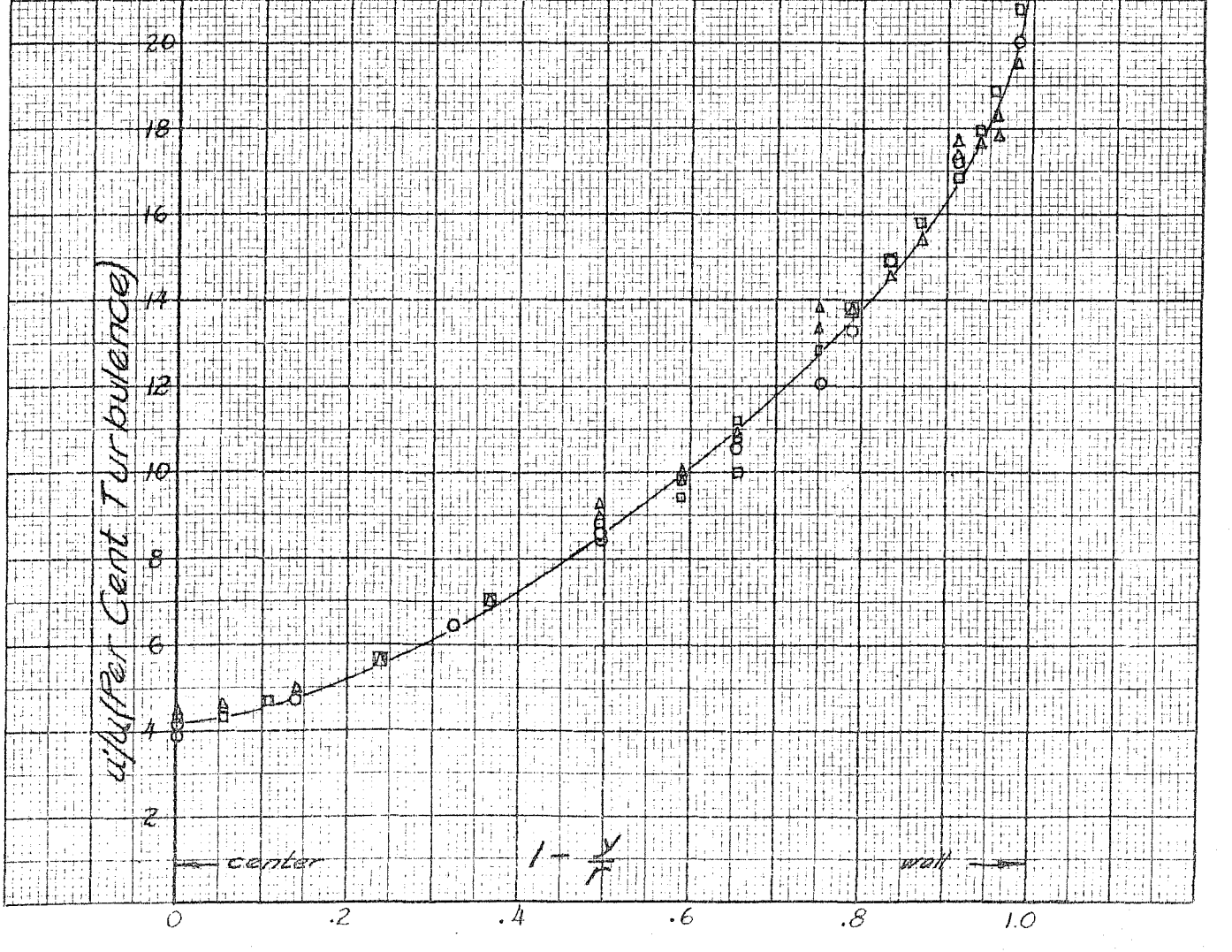

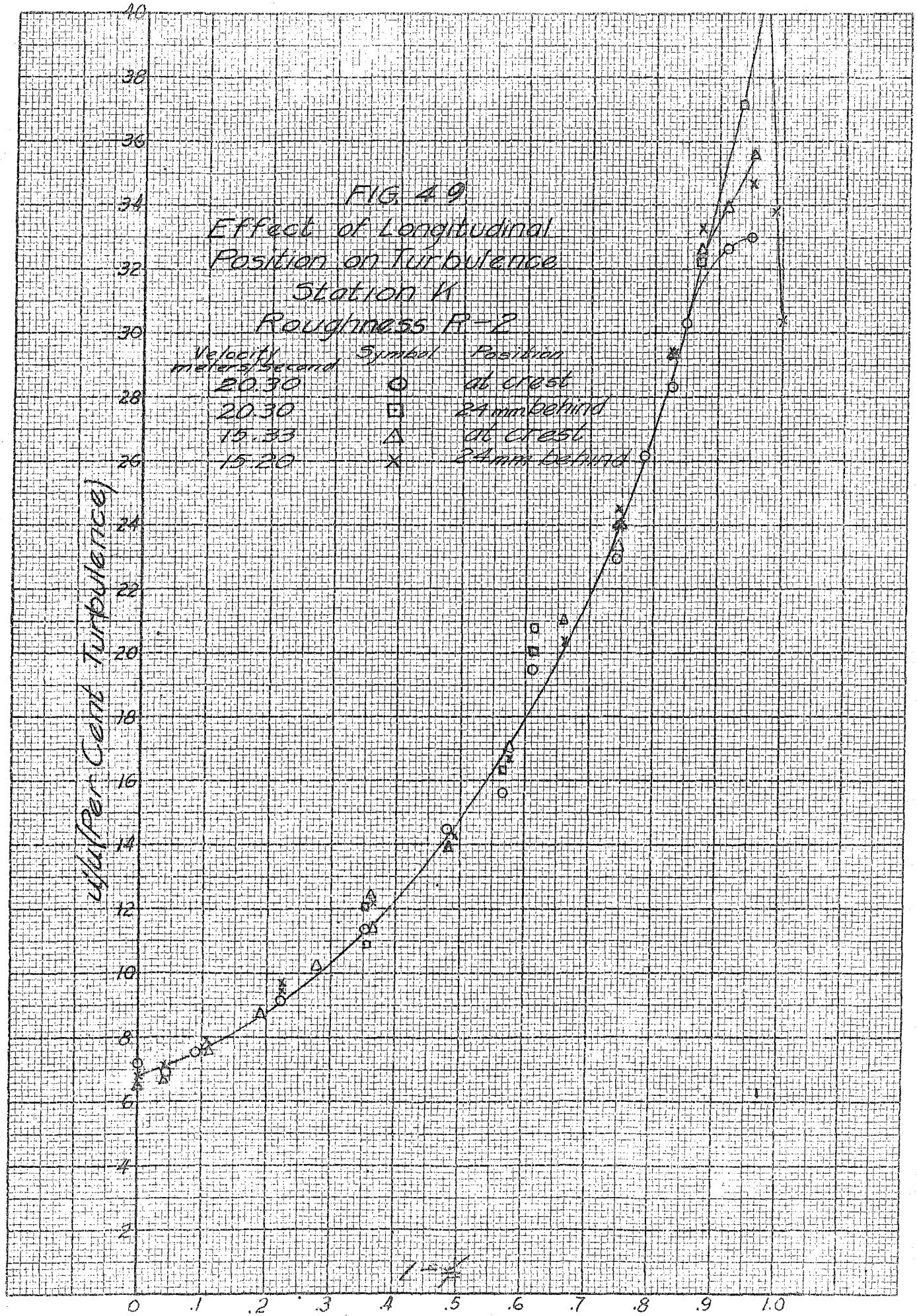
FIG. 49
Effect of Longitudinal Position on Turbulence
Station H
Roughness R-2
Velocity meters/second
20.30
20.30
15.33
15.20
Symbol
Position
at crest
24 mm behind
at crest
24 mm behind
Intensity (per Cent Turbulence)
40
38
36
34
32
30
28
26
24
22
20
18
16
14
12
10
8
6
4
2
0
.1
.2
.3
.4
.5
.6
.7
.8
.9
1.0

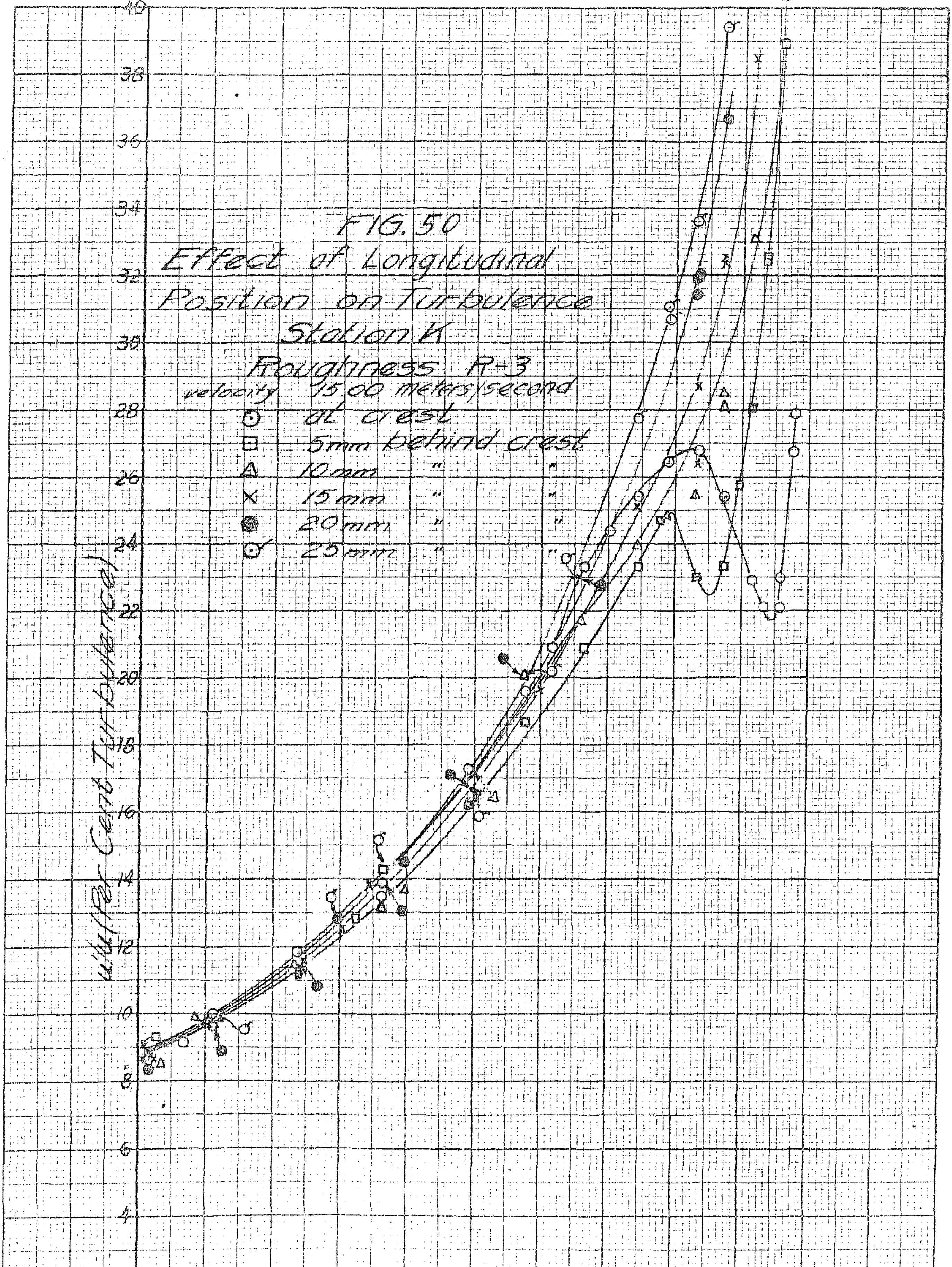
FIG. 50
Effect of Longitudinal
Position on Turbulence
Station K
Roughness R-3
velocity 15.00 meters/second
at crest
5mm behind crest
10mm " "
15mm " "
20mm " "
25mm " "
u'/U (Per Cent Turbulence)
1 − y/Y
0
.1
.2
.3
.4
.5
.6
.7
.8
.9
1.0
2
4
6
8
10
12
14
16
18
20
22
24
26
28
30
32
34
36
38
40

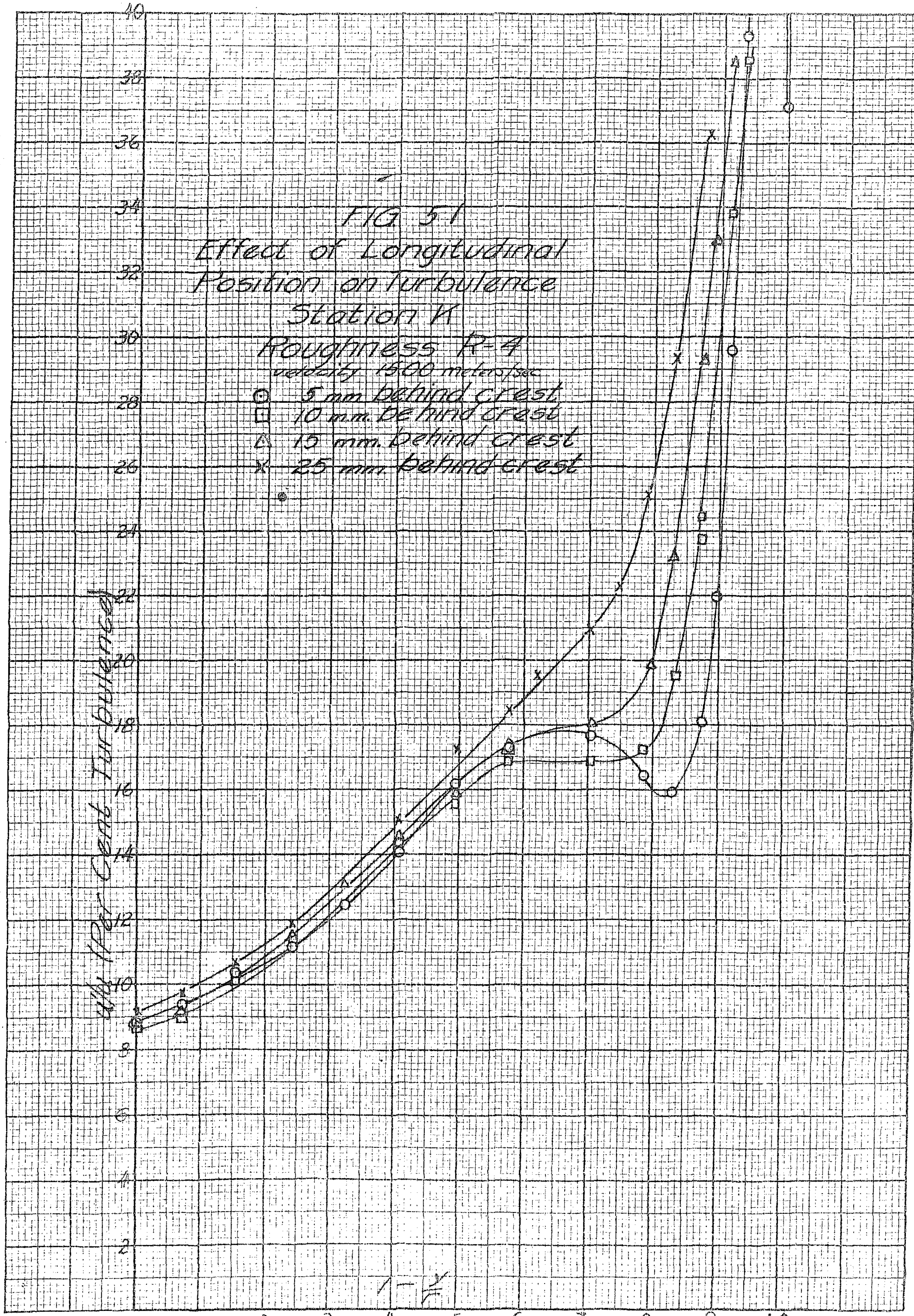
FIG. 51
Effect of Longitudinal
Position on Turbulence
Station K
Roughness R-4
velocity 15.00 meters/sec
5 mm behind crest
10 m.m. behind crest
15 mm. behind crest
25 mm. behind crest
u'/U (Per Cent Turbulence)
1 − y/r
0
.1
.2
.3
.4
.5
.6
.7
.8
.9
1.0
2
4
6
8
10
12
14
16
18
20
22
24
26
28
30
32
34
36
38
40

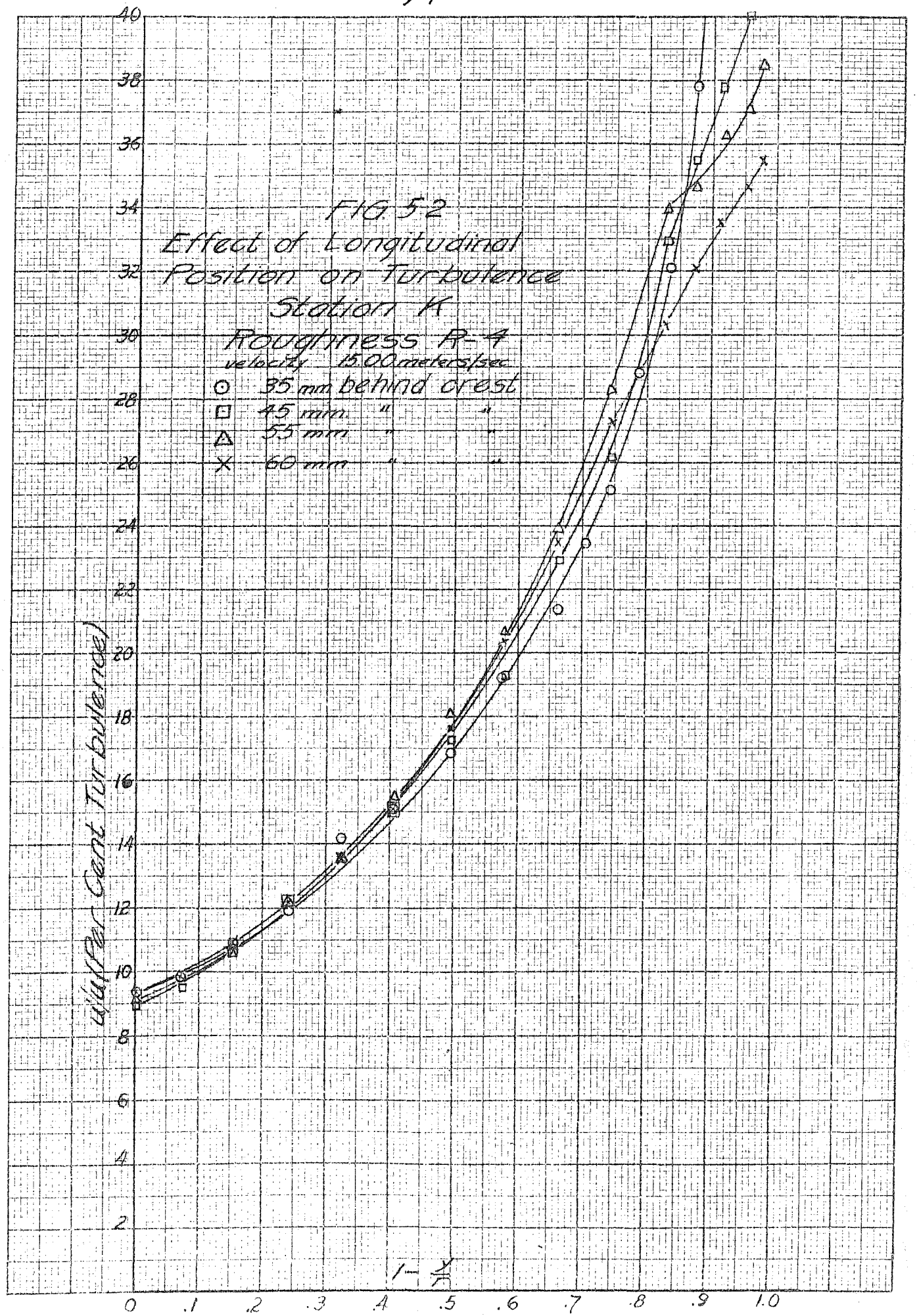
FIG 52
Effect of Longitudinal Position on Turbulence
Station A
Roughness A-4
velocity 15.00 meters/sec.
○ 35 mm behind crest
□ 45 mm " "
△ 55 mm " "
× 60 mm " "
Per Cent Turbulence
y/δ
0
.1
.2
.3
.4
.5
.6
.7
.8
.9
1.0
2
4
6
8
10
12
14
16
18
20
22
24
26
28
30
32
34
36
38
40

FIG 53

Turbulence Measurements
Showing Scale Effect
Station K
Roughness R-4

Velocity meters/second	Symbol
6.70	X
15.05	□
18.65	○

} At Crest

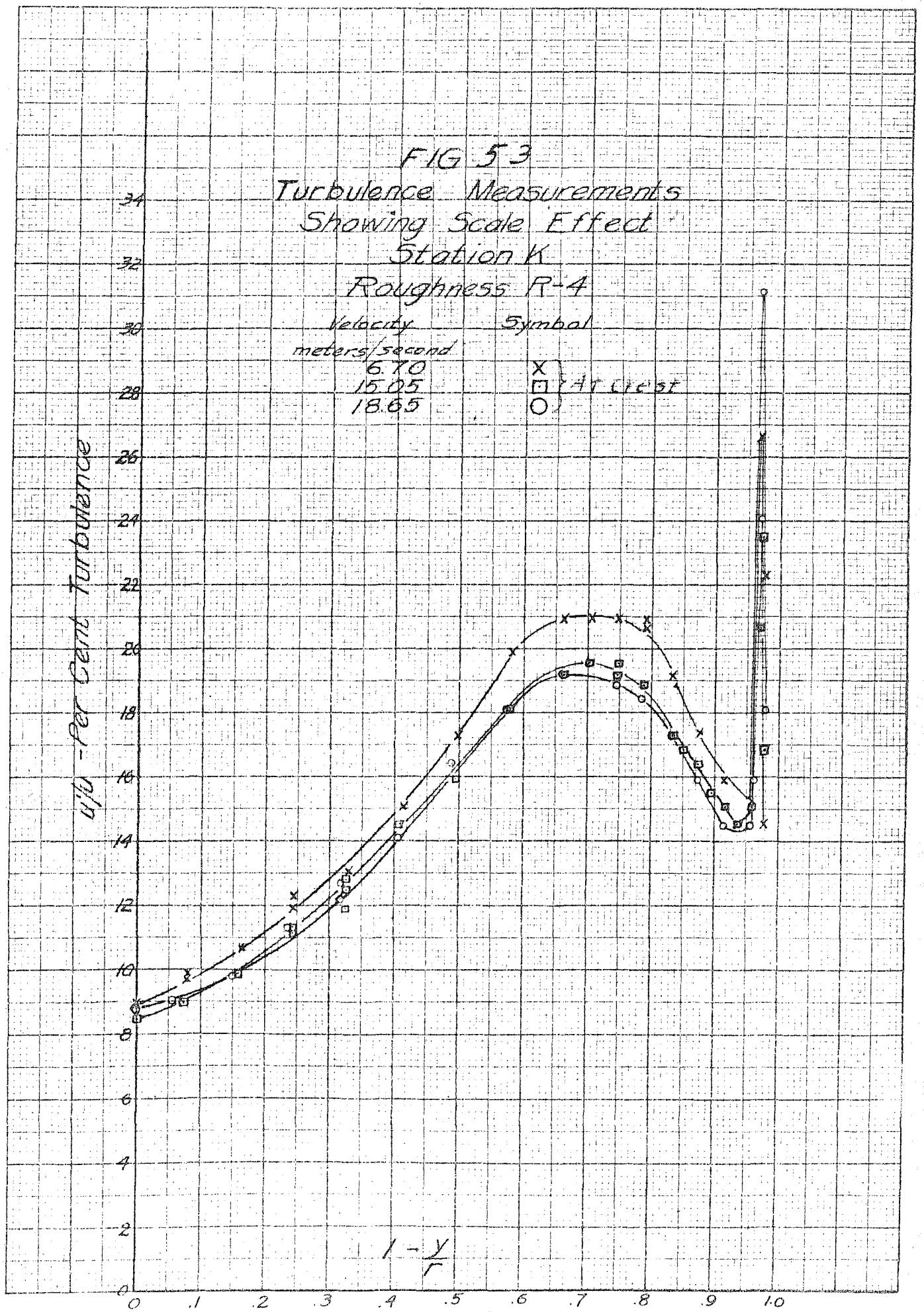

FIG 54
Turbulence Measurements
Showing Scale Effect
Station K
Roughness R-5

Velocity meters/second	Symbol
6.96	□
14.92	⊙
19.88	△
29.00	×

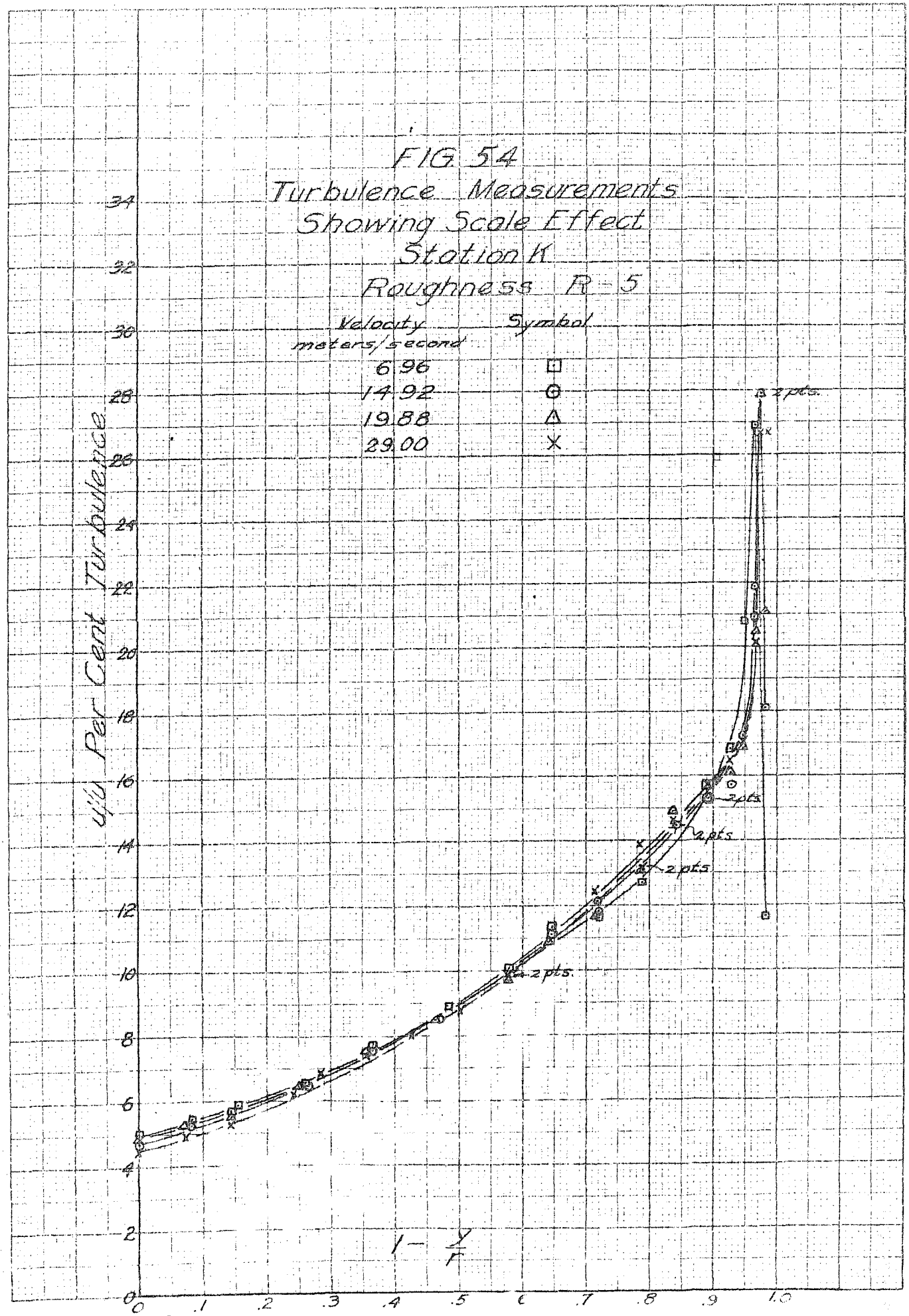

FIG. 55
Turbulence Measurements
Showing Scale Effect
Station K
Roughness R-6

velocity meters/second	symbol
6.97	△
14.94	□
20.00	⊙
24.87	×

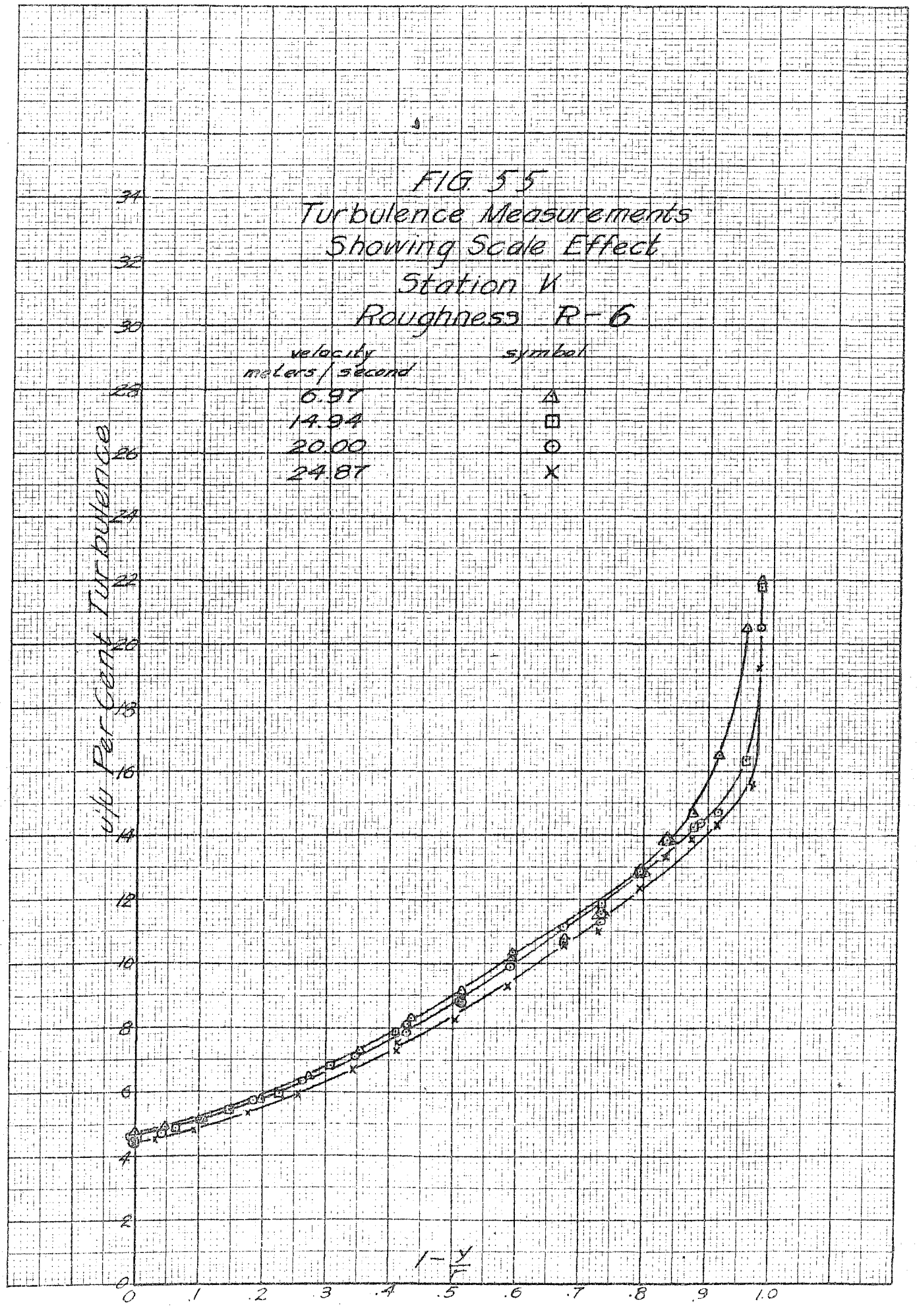

FIG 56
Turbulence Measurements
Showing Scale Effect
Station H
Smooth Walls

Velocity meters/second	Symbol
7.04	○
15.05	X
20.07	△
25.81	□
32.80	⊙

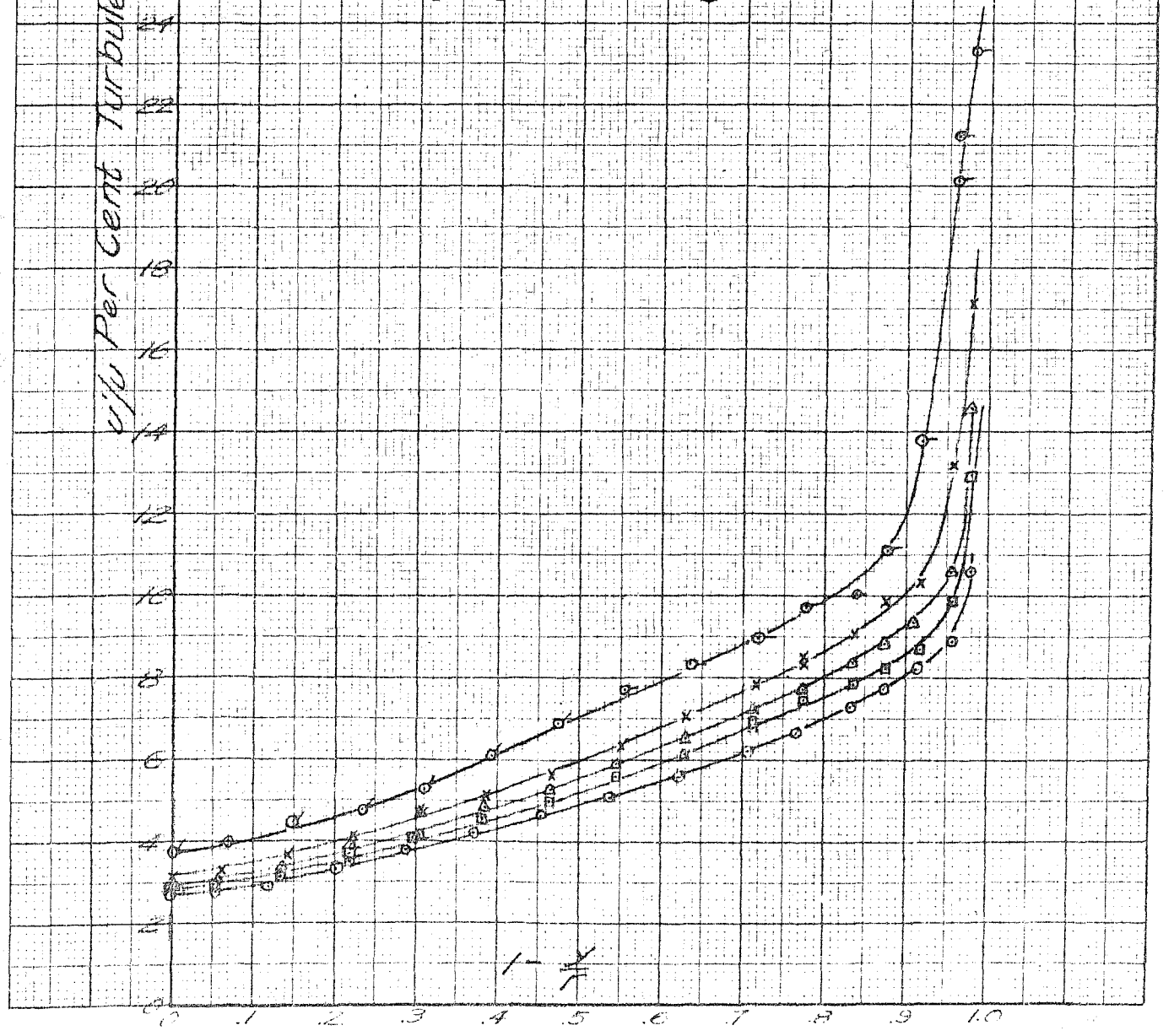

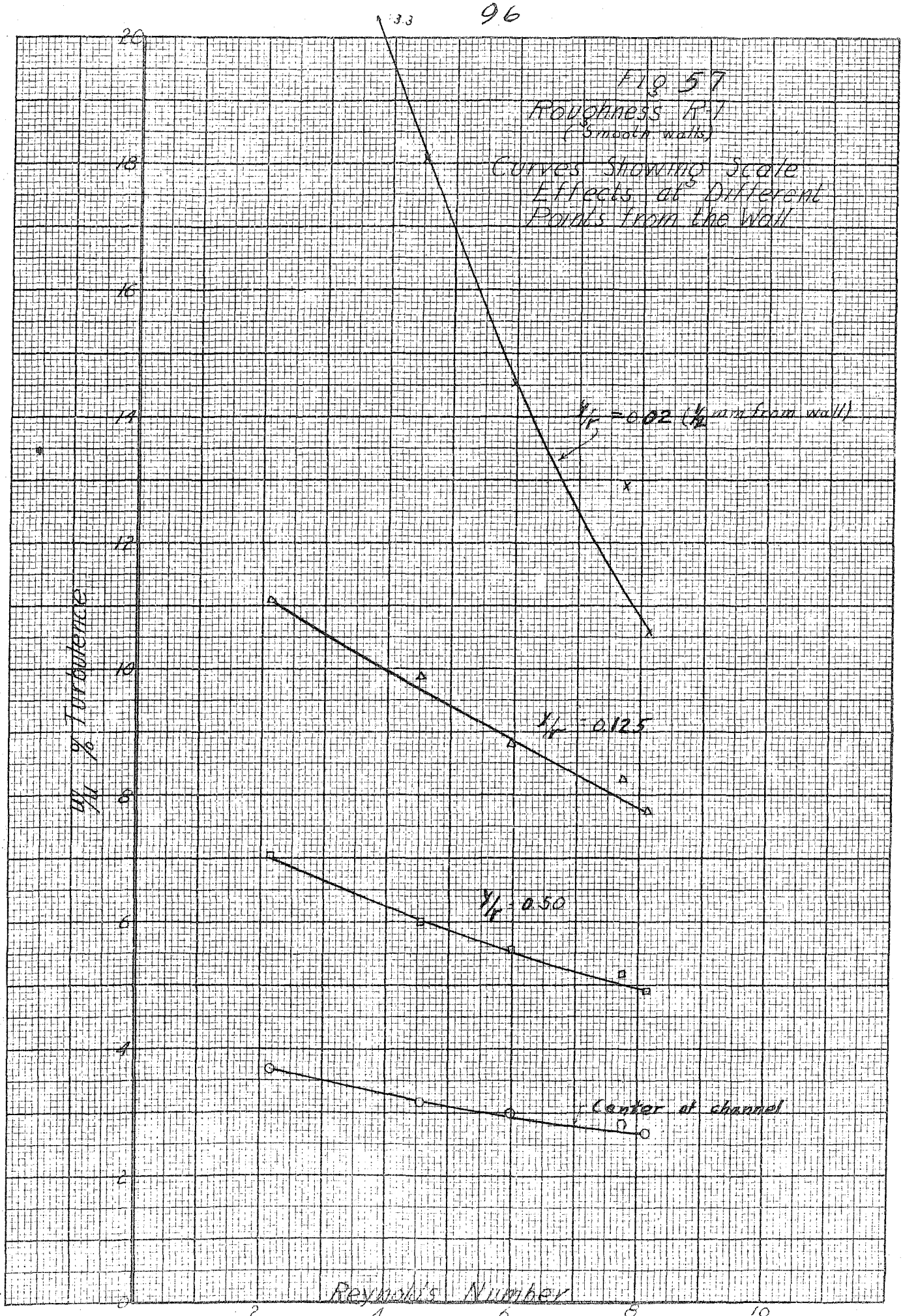
Fig 57
Roughness K=1
(Smooth walls)
Curves Showing Scale Effects at Different Points from the Wall
3.3
y/r = 0.02 (½ mm from wall)
y/r = 0.125
y/r = 0.50
Center of channel
u/v % Turbulence
Reynold's Number
20
18
16
14
12
10
8
6
4
2
0
2
4
6
8
10
R x 10⁻⁴

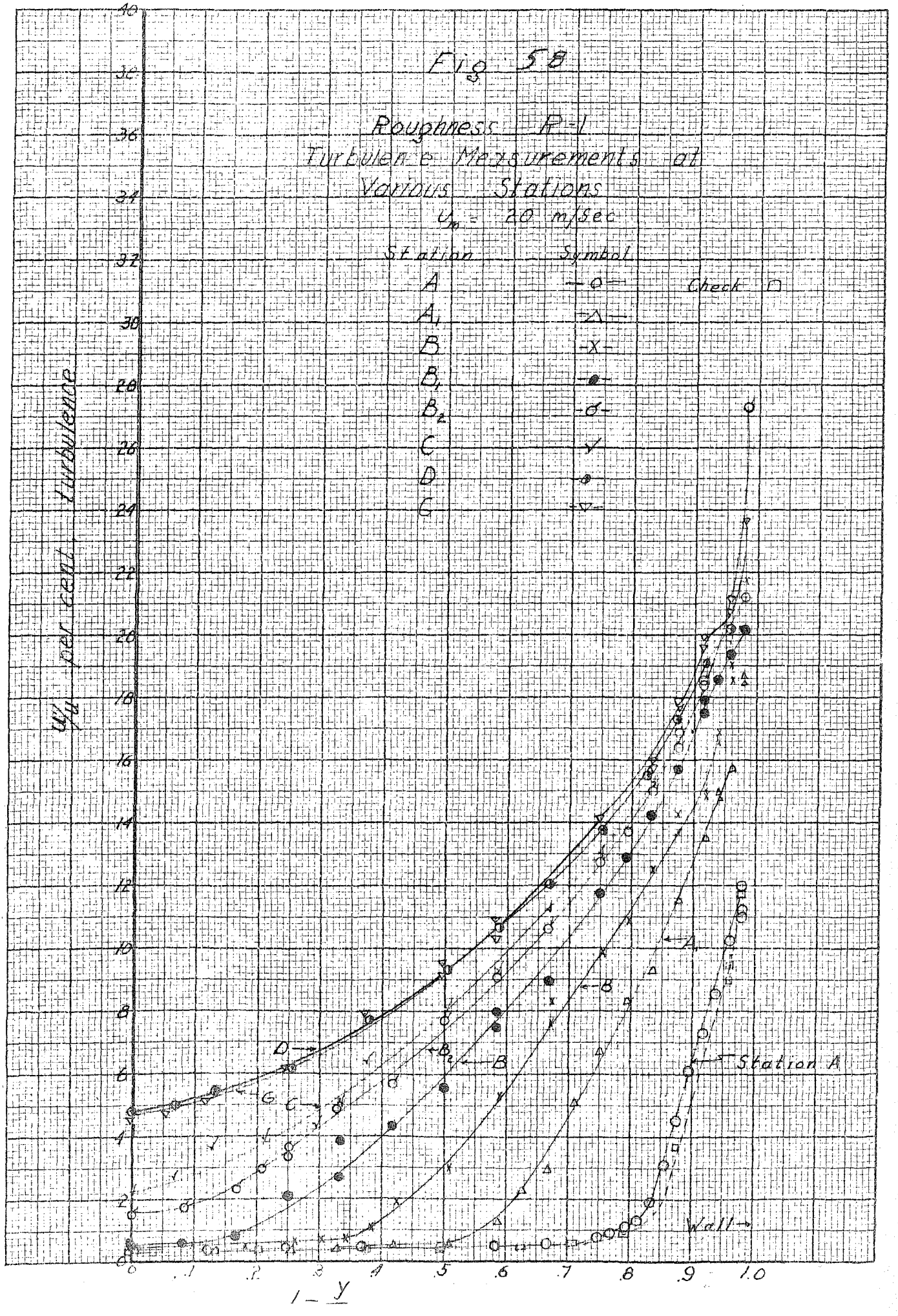
Fig. 58
Roughness R=1
Turbulence Measurements at Various Stations
U_∞ = 20 m/sec
Station
Symbol
A
A1
B
B1
B2
C
D
E
Check D
Station A
Wall
U/U_∞ per cent Turbulence
1 − y/δ

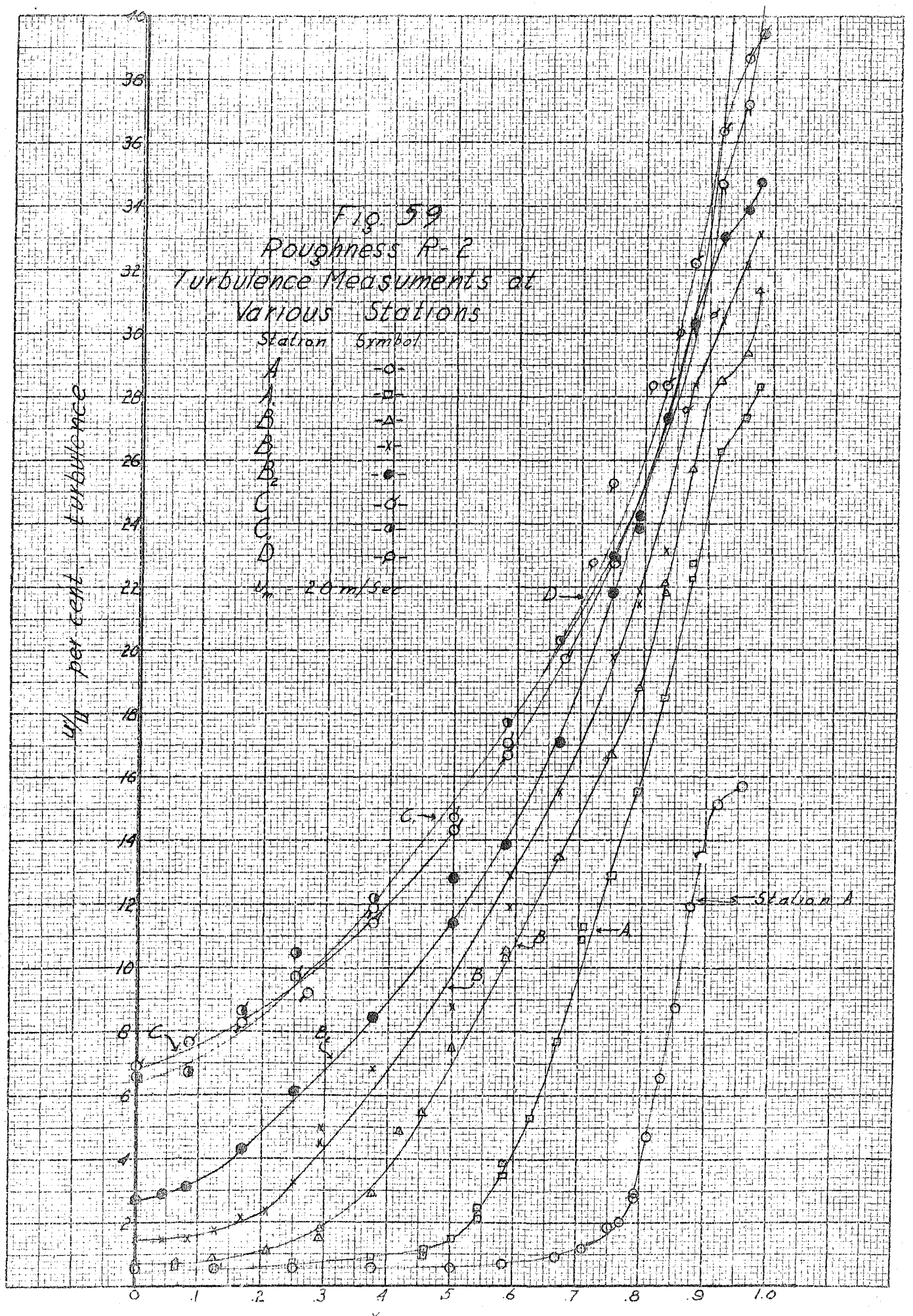
Fig 59
Roughness R-2
Turbulence Measurements at
Various Stations
Station Symbol
A -o-
A1 -□-
B -Δ-
B1 -x-
B2 -●-
C -◇-
C1 -◇-
D -p-
U1 = 20 m/sec
u/U per cent turbulence
Station A
A
B
B1
C
C1
D
0 .1 .2 .3 .4 .5 .6 .7 .8 .9 1.0
2 4 6 10 12 16 18 20 22 24 26 28 30 32 34 36

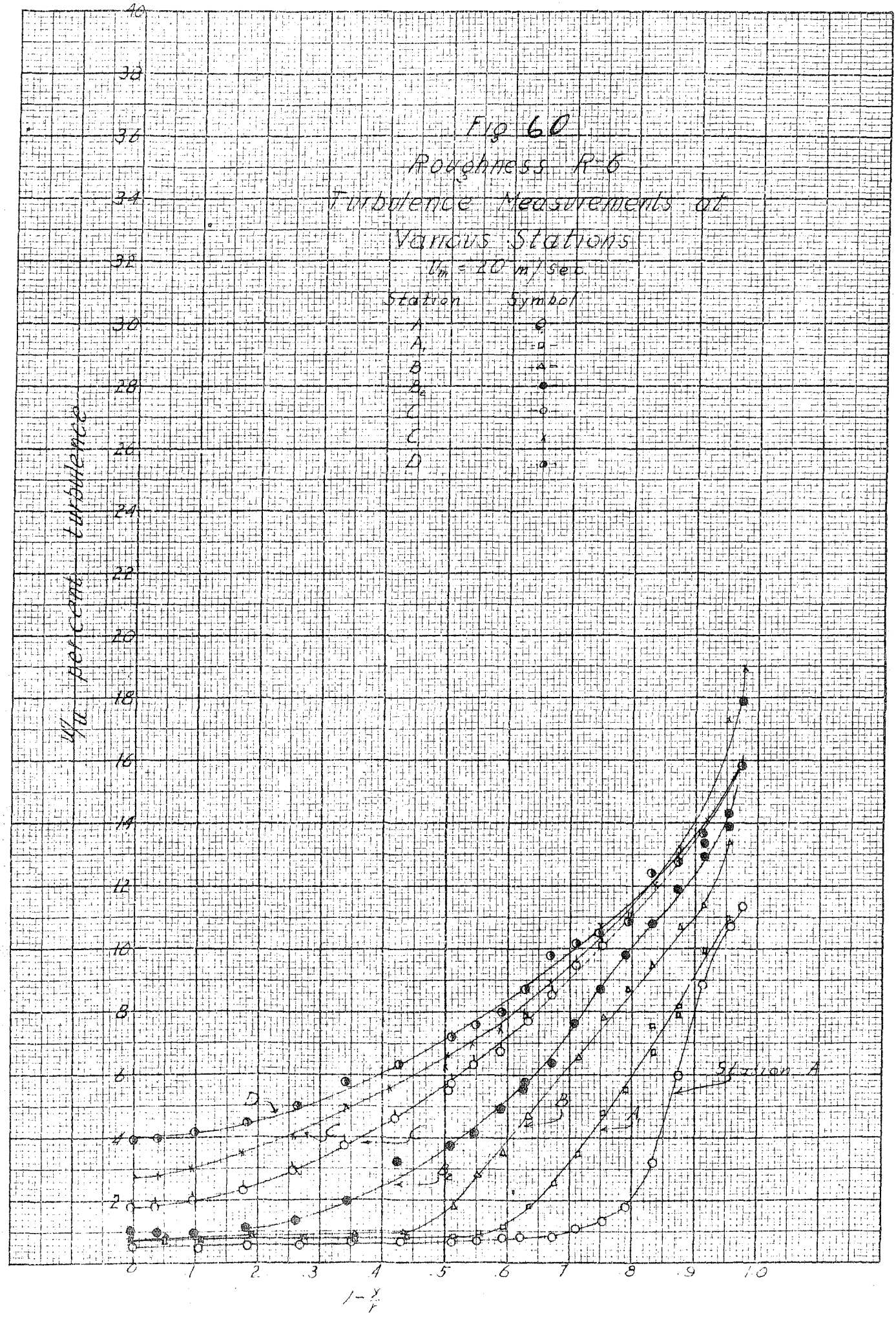
Fig 60
Roughness R-6
Turbulence Measurements at
Various Stations
U_m = 20 m/sec.
Station Symbol
A
A1
B
B2
C
C
D
u/U percent turbulence
Station A
Station B
Station C
Station D
0 1 2 3 4 5 6 7 8 9 10
1 - y/r

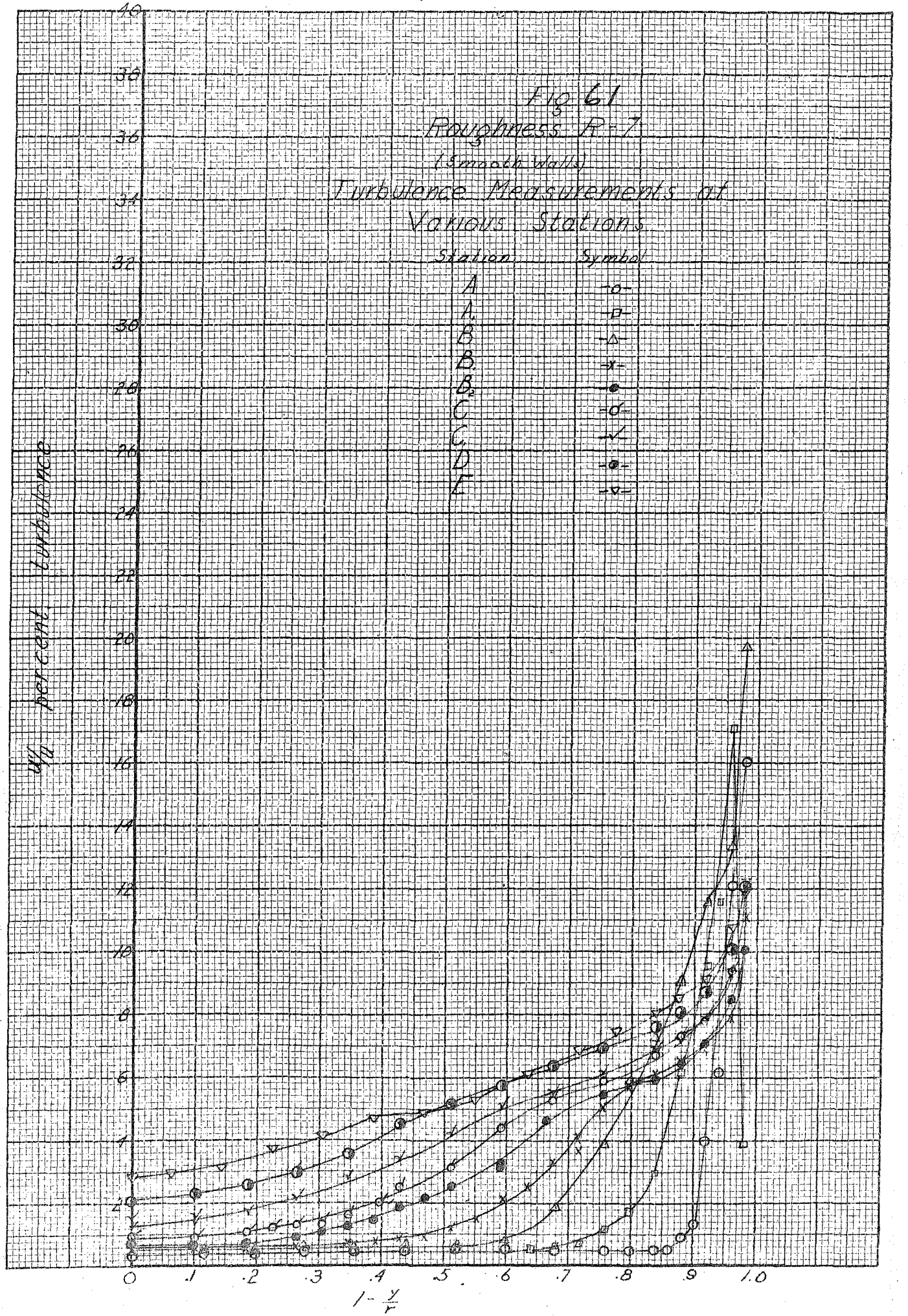
Fig. 61
Roughness R = 7
(Smooth walls)
Turbulence Measurements at
Various Stations
Station
Symbol
A
A₁
B
B₁
B₂
C
C₁
D
E
u/U, per cent turbulence
1 - y/r
40
38
36
34
32
30
28
26
24
22
20
18
16
14
12
10
8
6
4
2
0
.1
.2
.3
.4
.5
.6
.7
.8
.9
1.0

TABLE VII

Turbulence Measurements
Station K

Roughness R-1		Roughness R-2		Roughness R-3		Roughness R-4	
1-y/r	u'/u %	1-y/r	u'u %	1-y/r	u'/u %	1-y/r	u'/u %
0.979	20.58	0.951	35.55	0.979	26.75	0.979	16.82
0.958	20.16	0.915	33.88	0.958	22.10	0.973	23.40
0.937	19.30	0.872	32.59	0.936	22.10	0.969	20.62
0.916	17.94	0.830	29.33	0.915	22.90	0.958	15.05
0.894	16.97	0.745	24.00	0.894	24.00	0.937	14.56
0.873	16.37	0.660	21.01	0.873	25.40	0.916	15.05
0.831	15.62	0.574	17.07	0.852	26.10	0.895	15.50
0.789	14.70	0.489	13.87	0.831	26.75	0.873	16.40
0.747	13.56	0.362	11.40	0.788	26.40	0.851	16.82
0.662	11.49	0.277	10.24	0.746	25.40	0.831	17.64
0.578	10.00	0.191	8.79	0.703	24.37	0.789	18.81
0.494	8.72	0.106	7.66	0.661	23.30	0.747	19.19
0.367	7.48	0.043	6.80	0.619	20.90	0.705	19.56
0.240	6.32	0	6.57	0.576	19.60	0.662	19.19
0.114	5.10			0.492	17.23	0.578	18.06
		U_m = 15.33 m/sec					
0.059	4.69			0.364	14.56	0.494	15.95
0	4.47			0.237	11.83	0.409	14.56
				0.110	10.00	0.325	12.49
U_m = 14.90 m/sec							
				0.068	9.16	0.241	11.19
				0.004	8.94	0.156	9.83
						0.072	8.97
				U_m = 15.00 m/sec		0	8.79
						U_m = 15.05 m/sec	

u' = mean-root-square of the velocity fluctuations.
u = velocity at a point where u' is measured.

TABLE VII (continued)

Turbulence Measurements
Station K

Roughness R-5		Roughness R-6		Roughness R-7 (Smooth Walls)	
1-y/r	u'u %	1-y/r	u'/u %	1-y/r	u'/u %
0.982	18.05	0.980	21.71	0.980	17.09
0.973	27.84	0.960	16.36	0.959	13.20
0.964	21.92	0.919	14.71	0.918	10.32
0.946	17.21	0.879	14.28	0.878	9.90
0.928	15.70	0.838	13.82	0.837	9.10
0.893	15.32	0.797	12.89	0.776	8.39
0.840	14.47	0.735	11.85	0.714	8.55
0.787	13.14	0.675	10.71	0.633	7.93
0.717	11.91	0.594	10.06	0.551	7.09
0.645	11.11	0.512	8.80	0.469	6.34
0.574	9,72	0.410	7.90	0.388	5.73
0.468	8.47	0.309	6.80	0.306	5.14
0.362	7.57	0.228	5.97	0.224	4.68
0.265	6.45	0.147	5.45	0.143	4.16
0.149	5.67	0.065	4.82	0.061	3.65
		0	4.57	0	3.26
0.079	5.22				3.18
0	4.68	U_m = 14.94 m/sec		U_m = 15.05 m/sec	

U_m = 14.92 m/sec

u' = mean-root-square of the velocity fluctuations.
u = velocity at a point where u' is measured.

TABLE VIII

Correlation Between Turbulent
Velocity Fluctuations
Station K

1-y/r	u'/u^* %	u/U_m^*	$u'v'/(u')^2$
	Roughness R-1		
0	4.5	1.0	0
0.1	4.91	0.992	0.223
0.2	5.61	0.977	0.352
0.3	6.50	0.956	0.410
0.4	7.62	0.928	0.423
0.5	8.90	0.890	0.421
0.6	10.40	0.842	0.414
0.7	12.25	0.785	0.399
0.8	14.60	0.717	0.386
0.85	15.85	0.673	0.396
0.90	17.45	0.623	0.403
0.925	18.30	0.595	0.418
0.95	19.35	0.555	0.433
0.975	20.60	0.505	0.476

U_m = 14.70 m/sec
τ_o/ρ = 1.114 $(m/sec)^2$

u'/u^* %	u/U_m^*	$u'v'/(u')^2$
Roughness R-2		
6.80	1.0	0
7.60	0.993	0.155
8.65	0.975	0.246
10.3	0.95	0.274
12.25	0.915	0.279
14.65	0.87	0.269
17.92	0.815	0.235
21.70	0.75	0.231
27.0	0.675	0.211
30.4	0.625	0.206
32.5	0.565	0.234
33.0	0.495	0.311

U_m = 19.6 m/sec
τ_o/ρ = 3.36 $(m/sec)^2$

1-y/r	u'/u^* %	u/U_m^*	$u'v'/(u')^2$
	Roughness R-5		
0	4.7	1.0	0
0.1	5.3	0.992	0.138
0.2	6.0	0.977	0.223
0.3	6.85	0.955	0.271
0.4	7.85	0.936	0.286
0.5	9.00	0.895	0.295
0.6	10.30	0.861	0.292
0.7	11.8	0.812	0.291
0.8	13.5	0.745	0.303
0.85	14.5	0.705	0.311
0.90	15.6	0.665	0.321
0.925	16.4	0.625	0.337
0.95	17.5	0.593	0.338
0.975	27.9	0.545	0.162

U_m = 14.86 m/sec
τ_o/ρ = 0.846 $(m/sec)^2$

u'/u^* %	u/U_m^*	$u'v'/(u')^2$
Roughness R-6		
4.7	1.0	0
5.1	0.992	0.157
5.8	0.977	0.250
6.6	0.955	0.302
7.6	0.936	0.317
8.75	0.895	0.327
10.10	0.860	0.319
11.40	0.810	0.324
12.90	0.740	0.352
13.70	0.696	0.376
14.6	0.645	0.407
15.1	0.610	0.431
16.0	0.578	0.445
18.2	0.530	0.420

U_m = 15.02 m/sec
τ_o/ρ = 0.907 $(m/sec)^2$

* These values are taken from faired curves.

TABLE VIII (continued)

Correlation Between Turbulent
Velocity Fluctuations
Station K

Smooth Walls

1-y/r	u'/u* %	u/U_m*	u'v'/(u')^2	u'/u* %	u/U_m*	u'v'/(u')^2
U_m = 7.04 m/sec				U_m = 15.05 m/sec		
τ_o/ρ = 0.1198 (m/sec)^2				τ_o/ρ = 0.481 (m/sec)^2		
0	3.75	1.0	0	3.10	1.0	0
0.1	4.05	0.995	0.148	3.45	0.995	0.181
0.2	4.55	0.985	0.241	3.95	0.985	0.281
0.3	5.20	0.968	0.286	4.50	0.970	0.336
0.4	6.05	0.945	0.295	5.20	0.947	0.350
0.5	6.95	0.920	0.294	6.00	0.922	0.347
0.6	7.85	0.890	0.296	6.80	0.893	0.347
0.7	8.80	0.856	0.297	7.70	0.860	0.349
0.8	9.9	0.807	0.302	8.65	0.815	0.343
0.90	12.0	0.740	0.275	10.05	0.745	0.342
0.925	14.5	0.715	0.208	10.85	0.715	0.327
0.95	18.4	0.680	0.146	12.40	0.690	0.276
0.975	22.5	0.630	0.117	16.40	0.630	0.195
U_m = 20.07 m/sec.				U_m = 32.8 m/sec		
τ_o/ρ = 0.805 (m/sec)^2				τ_o/ρ = 1.934 (m/sec)^2		
0	2.95	1.0	0	2.70	1.0	0
0.1	3.25	0.993	0.192	2.87	0.996	0.220
0.2	3.65	0.984	0.310	3.25	0.988	0.350
0.3	4.20	0.970	0.362	3.75	0.974	0.405
0.4	4.83	0.955	0.376	4.30	0.955	0.426
0.5	5.51	0.933	0.378	4.90	0.929	0.425
0.6	6.30	0.906	0.368	5.50	0.901	0.438
0.7	7.11	0.875	0.362	6.12	0.869	0.445
0.8	8.00	0.828	0.365	6.95	0.823	0.440
0.9	9.20	0.752	0.374	8.00	0.750	0.450
0.925	9.7	0.723	0.377	8.40	0.725	0.449
0.95	10.35	0.690	0.373	8.80	0.693	0.460
0.975	13.2	0.640	0.273	9.80	0.640	0.447

* These values are taken from faired curves.

B I B L I O G R A P H Y

Bibliography

1. Karman, "The Fundamentals of the Statistical Theory of Turbulence," Journal of the Aeronautical Sciences, February 1937.

2. Taylor, "The Statistical Theory of Isotropic Turbulence," Journal of the Aeronautical Sciences, June 1937.

3. Nikuradse, "Strömungsgesetze in rauken Rohren," V.D.I., Forsch H. 361, 1933.

4. Schlichting, "Experimentelle Untersuchungen zum Rauhigkeits problem," Ingenieur-Archiv, VII Band, 1 Heft, Feburar 1936.

5. L. Hopf, Z. angew. Math. Mech. 3 (1923) S. 329.

6. K. Fromm, Z. angew. Math. Mech. 3 (1923) S. 339.

7. F. L. Wattendorf and A. M. Kuethe, "Investigations of Turbulent Flow by Means of the Hot-Wire Anemometer," Physics, Vol. 5, June 1934, pages 153-164.

8. H. L. Dryden and A. M. Kuethe, "The Measurement of Air Speed Fluctuations by means of the Hot-Wire Anemometer," N.A.C.A. Technical Report 320 (1929).

9. A. Fage, "Study of Turbulent Flow by Means of the Ultra-Microscope," Proc. Roy. Soc. A135, 828, 656 (1932).

10. L. Prandtl, Bericht über Untersuchungen zur Ausgebildeten Turbulenz, Zeits. f. Angew. Math. u Mech. 5, 136 (1925).

11. Gebelein, Turbulenz, Berlin, 1935.

12. L. V. King, Phil. Trans. Roy. Soc. (London) A214, 373 (1914).

13. O. Reynolds, "An Experimental Investigation of the Circumstances which Determine Whether the Motion of Water shall be Direct or Sinuous and of the Laws of Resistance in Parallel Channels," Phil. Trans. Roy. Soc. 174, 935 (1883).

14. Wattendorf, "A Study of the Effect of Curvature on Fully Developed Turbulent Flow," Proc. Roy. Soc. of London, Series A, No. 865, Vol. 148, February 1935.

APPENDIX

APPENDIX A

Method of Computing Pressure

Correction due to Wall Deflection

Let u_o = velocity before deflection

b_o = width of channel before deflection

p_o = static pressure before deflection

q_o = dynamic pressure before deflection.

Then for the continuity equation

$$u_o b_o = ub$$

the total head at the same station will be the same before deflection as after deflection.

From Bernoullis' theorem

$$H_o = p_o + q_o = p + q$$

$$p_o - p = q - q_o$$

Since $$q = \frac{1}{2} \rho u^2$$

then $$\frac{q_o}{q} = \frac{u_o^2}{u^2} = \left(\frac{b}{b_o}\right)^2$$

$\Delta p = p_o - p = q \left(1 - \frac{b}{b_o}\right)^2$ change in pressure due to wall deflection.

$$b^2 = (b_o - \Delta b)^2 = b_o - 2b_o \Delta b + \Delta b^2$$

$$\Delta p = q \left[1 - \frac{(b^2 - 2b_o \Delta b + \Delta b^2)}{b_o^2}\right]$$

Neglecting $\frac{\Delta b^2}{b_o^2}$ we have

$$\Delta p = 2q \frac{\Delta b}{b_o}$$

where q is the dynamic pressure measured at the station.

APPENDIX B

Method of Computing Velocity Fluctuation From Amplitude and Frequency of the Vibrator

The instantaneous velocity, U, in the channel may be represented by a mean velocity, $\bar{u}$, and fluctuating velocity, u', as represented by Fig. A.

$U = \bar{u} + u'$

$U^2 = \bar{u} + 2\bar{u}\,u' + (u')^2$

But the time average of

$\bar{u}\,u' = 0$

Therefore $U^2 = \bar{u}^2 + (u')^2$

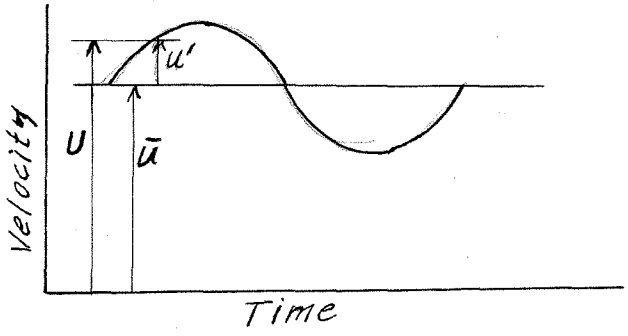

Fig. A

The vibrating wire has a motion illustrated by Fig. B.

If Δ = 2 x amplitude of vibrating wire

and f = the frequency

$\theta = \omega t$

then $\omega = 2\pi f$

and then $y = A \sin \theta = A \sin \omega t$

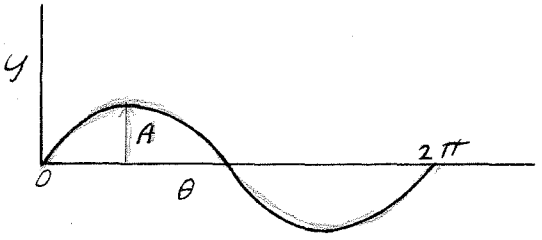

Fig. B

$$\overline{(u')^2} = \overline{\left(\frac{dy}{dx}\right)^2} = \frac{2}{2\pi}\int_{t=0}^{\frac{\pi}{\omega}} A^2\,\omega^2\cos^2\omega t\,dt$$

$$= \frac{1}{\pi}\,A^2\,\omega^2\,\frac{\pi}{2}$$

Therefore $\overline{(u')^2} = \frac{A^2\omega^2}{2}$ But $A = \frac{\Delta mm}{2x1000}$ (meters)

then

$$\overline{u'} = \frac{1}{\sqrt{2}}\,\frac{\omega\,\Delta}{2 \times 1000} = \frac{1}{\sqrt{2}}\,2\pi f\,\frac{\Delta}{2 \times 1000}$$

$$\frac{\overline{u'}}{\bar{u}} = \frac{2.221\,f\Delta}{\bar{u}\,1000}$$